



UNIVERSITY  
OF  
JOHANNESBURG

## COPYRIGHT AND CITATION CONSIDERATIONS FOR THIS THESIS/ DISSERTATION



- Attribution — You must give appropriate credit, provide a link to the license, and indicate if changes were made. You may do so in any reasonable manner, but not in any way that suggests the licensor endorses you or your use.
- NonCommercial — You may not use the material for commercial purposes.
- ShareAlike — If you remix, transform, or build upon the material, you must distribute your contributions under the same license as the original.

### How to cite this thesis

Surname, Initial(s). (2012). Title of the thesis or dissertation (Doctoral Thesis / Master's Dissertation). Johannesburg: University of Johannesburg. Available from: <http://hdl.handle.net/102000/0002> (Accessed: 22 August 2017).



**APPLICATION OF SUPPORTED PALLADIUM TOWARDS THE  
ELECTROCATALYTIC OXIDATION OF LOW MOLECULAR WEIGHT  
ALCOHOL (METHANOL)**

---

**By**

**SAMARJEET SINGH SIWAL**

**Student Number: 201464060**

**Thesis in fulfilment of the requirement for the degree**

**PHILOSOPHIAE DOCTOR**

**In**

**CHEMISTRY**

**In the**

**FACULTY OF SCIENCE**

**of the**

**UNIVERSITY OF JOHANNESBURG**

**SUPERVISOR: PROF. KAUSHIK MALLICK**

**AUGUST, 2017**

## DECLARATION

---

I hereby declare that this dissertation, which I herewith submit for the research qualification

### **DOCTOR OF PHILOSOPHY IN CHEMISTRY**

To the University of Johannesburg, Department of Chemistry, is, apart from the recognised assistance of my supervisor, my own work and has not previously been submitted by me to another institution to obtain a research diploma or degree.

SAMARJEET SINGH SIWAL on this 8 August day of 2017.

*(Candidate)*

PROF. KAUSHIK MALLICK on this 8 August day of 2017.

*(Supervisor)*



UNIVERSITY  
OF  
JOHANNESBURG

DEDICATION

---

*I dedicate this work to my  
parents*

*Smt. Rameshri Devi*

*&*

*Late Shri Ompal Singh*

*and my brother:*

*Mr. Amarjeet Singh Siwal*



UNIVERSITY  
OF  
JOHANNESBURG

## PUBLICATIONS AND PRESENTATIONS

---

The work presented in this thesis has been presented at various national and international conferences. Furthermore, results emanating from this study have also been either published or submitted to peer-reviewed journals. The list of research articles presented in conferences and published/submitted is given below-

### Conference Presentations

1. **Samarjeet Siwal**, M. Choudhary, D. Nandi, S. Matseke, S. Mpelane, K. Mallick, "Incorporation of Graphene oxide to the Polymer based palladium catalyst: Synergic performance on Electrochemical Methanol Oxidation" AEM2016: International Conference on Advanced Energy Nanomaterials, 12-14 September 2016.
2. M. Choudhary, **Samarjeet Siwal**, and K. Mallick, "Role of gold nanoparticles on the charge storage ability for the polymer-graphene composite" AEM2016: International Conference on Advanced Energy Nanomaterials, 12-14 September 2016.
3. **Samarjeet Siwal**, M. Choudhary, and K. Mallick " Single Step Synthesis of Polymer Supported Palladium (I) Composite: As a Anode Catalyst for Direct Methanol Fuel Cell Application" Unisa's BRICS International Symposium, March-2016.
4. **Samarjeet Siwal**, M. Choudhary, and K. Mallick "Improvement of graphitic carbon nitride as a catalyst for Direct Methanol Fuel Cell" Unisa's BRICS International Symposium, March-2015.

## Peer-reviewed Publications

1. M. Choudhary, **Samarjeet Siwal**, R.U Islam, M. Witcomb and K. Mallick, “Polymer stabilized silver nanoparticle: An efficient catalyst for proton-coupled electron transfer reaction and the electrochemical recognition of biomolecule”. *Chemical Physics Letters* **608** (2014) 145-151.
2. M. Choudhary, S. K. Shukla, A. Taher, **Samarjeet Siwal** and K. Mallick, “Organic–Inorganic Hybrid Supramolecular Assembly: An Efficient Platform for Nonenzymatic Glucose Sensor”. *ACS Sustainable Chemistry & Engineering* **2** (2014) 2852-2858.
3. R. U. Islam, A. Taher, M. Choudhary, **Samarjeet Siwal** and K. Mallick, “Polymer immobilized Cu(I) formation and azide-alkyne cycloaddition: A one pot reaction”. *Scientific Report* **5** (2015) 9632.
4. M. Choudhary, **Samarjeet Siwal**, A. Taher and K. Mallick, “Recognition of biomolecules using gold-polymer composites: metal nanoparticles play the role of the catalyst”. *Journal of Materials Science* **50** (2015) 6087-6095.
5. M. Choudhary, **Samarjeet Siwal** and K. Mallick. Single step synthesis of ‘silver-polymer hybrid material’ and its catalytic application. *RSC Advances* **5** (2015) 58625-58632.
6. M. Choudhary, **Samarjeet Siwal** D. Nandi and K. Mallick. Catalytic performance of the in situ synthesized palladium-polymer nanocomposite. *New Journal of Chemistry* **40** (2016) 2296-2303.
7. M. Choudhary, **Samarjeet Siwal**, D. Nandi, K. Mallick. Single step synthesis of gold–amino acid composite, with the evidence of the catalytic hydrogen atom transfer (HAT) reaction, for the electrochemical recognition of Serotonin. *Physica E: Low-dimensional Systems and Nanostructures* **77** (2016) 72-80.
8. **Samarjeet Siwal**, M. Choudhary, S. Mpelane, R. Brink and K. Mallick. Single Step Synthesis of Polymer Supported Palladium (I) Composite: An efficient Anode Catalyst for Direct Methanol Fuel Cell Application. *RSC Advances* **6** (2016) 47212-47219.
9. D. Nandi, **Samarjeet Siwal**, M. Choudhary, K. Mallick. Carbon Nitride supported Palladium nanoparticles: An active system for the reduction of aromatic nitro-compounds. *Applied Catalysis A: General* **523**(2016) 31-38.

10. D. Nandi, A. Taher, R. U. Islam, M. Choudhary, **Samarjeet Siwal** and K. Mallick, "Light effect on Click reaction: Role of photonic quantum dot catalyst". *Scientific Reports* **6** (2016) 33025.
11. M. Choudhary, R. Brink, D. Nandi, **Samarjeet Siwal** and K. Mallick, "Gold nanoparticle within the polymer chain, a multi-functional composite material, for the electrochemical detection of dopamine and the hydrogen atom-mediated reduction of Rhodamine-B, a mechanistic approach". *Journal of Materials Science* **53** (2017) 770-781.
12. D. Nandi, A. Taher, R. U. Islam, **Samarjeet Siwal**, M. Choudhary and K. Mallick, " Carbon Nitride Supported Copper Nanoparticles: Light Induced Electronic Effect of the Support for Triazole Synthesis" *Royal Society Open Science* **3**(2016)160580.
13. M. Choudhary, **Samarjeet Siwal** and K. Mallick, "Charge storage ability of the gold nanoparticles: Towards the performance of a supercapacitor". *Applied Surface Science* (2017) <http://dx.doi.org/10.1016/j.apsusc.2017.01.258>.
14. D. Nandi, **Samarjeet Siwal**, and K. Mallick, "Mono Arylation of Imidazo[1,2-a]pyridine and 1,2-dimethyl imidazole: Application of Carbon Nitride Supported Palladium Catalyst" *ChemistrySelect* **2** (2017) 1747-1752.
15. D. Nandi, **Samarjeet Siwal** and K. Mallick, "A Carbon nitride supported copper nanoparticles: A heterogeneous catalyst for the N-arylation of hetero-aromatic compounds ". *New Journal of Chemistry* **41** (2017) 3082-3088.
16. R. Brink, M. Choudhary, **Samarjeet Siwal**, D. Nandi and K. Mallick, " Silver-polymer functional-nanocomposite: A single step synthesis approach with *in-situ* optical study". *Applied Surface Science* **412** (2017) 482-488.
17. **Samarjeet Siwal**, S. Matseke, S. Mpelane, D. Nandi and K. Mallick, "Palladium-polymer nanocomposite: An anode catalyst for the electrochemical oxidation of methanol". *International Journal of Hydrogen Energy* (2017), article in press. <http://dx.doi.org/10.1016/j.ijhydene.2017.03.033>.
18. R. Barik, N. Hooda, D. Nandi, **Samarjeet Siwal**, S. K. Ghosh and K. Mallick. "Multifunctional performance of nanocrystalline tin oxide". *Journal of Alloys and Compounds* **723** (2017)201–207.

## ACKNOWLEDGEMENTS

---

I would like to express my great gratitude to the following people and institutions for all their assistance, support, insight and dedication toward the success of this project:

- All thanks to GOD, Lord Almighty on his protection and guidance throughout this research amidst a thousand of trials and challenges.
- It is my great pleasure to express most sincere thanks and profound sense of gratitude to my supervisor: **Professor Kaushik Mallick**, Department of Chemistry, University of Johannesburg, Johannesburg, for his excellent supervision, continuous support and encouragement right from the selection of the topic to the finalization of the thesis.
- I am also thankful to Dr. Sudheesh K. Shukla for proof reading this work; you are the best. Your support is highly appreciated.
- My gratitude goes to the Faculty of Science, University of Johannesburg and GES for their financial assistance.
- I am indebted to my encourager: Prof. Ankit Chaudhary, Dr. Ashish M. Gujrathi, Dr. Meenakshi Choudhary, Dr. A.S.K. Sinha, Dr. Ashish Dongre, Mr. Jaganmoy Jodder and Mr. Rahul Singh for their constant encouragement, unwavering confidence in my capabilities and effort in creating a favorable working environment.
- I was fortunate to have the constant encouragement of my parents throughout my research work. I am also indebted to my family members Smt. Sushma Ghumaan, Rekha Siwal, Praveen Beniwal, Jyoti Beniwal, Indu Dhillon, Amardeep Dhillon and my nephew Harshjeet Ghumaan and Devendra Siwal for their moral support,



encouragement and blessings. They have been always a source of inspiration for me.

- Finally, and most importantly, I would like to thank my wife Dr. Preeti Dhillon. Her support, encouragement, quiet patience and unwavering love were undeniably the bedrock upon which the past period of my life have been built.
- I am also grateful to non-teaching staffs of Chemistry Department for their constant assistance.
- I am also thankful to all my seniors, friends and well wishers for their direct or indirect help in successful completion of the thesis. My special thanks go to Dr. Sanyasi Sitha, Siyasanga Mpelane, Dr. Abu Taher, Dr. Debkumar Nandi, Dr. Rasmita Barik, Dr. Ruchika Sharma, Nishu Hooda, Dr. Sarit Ghosh, Raugme Brink and the entire UJ technical staff for their assistance and making life interesting and fun at UJ and in South Africa.
- Last but not the least, this work owes a lot to many other persons whose I have failed to incorporate here. But I solemnly remember all of their effort, encouragement and enthusiasm that were bestowed on me at different times. I offer my sincere thanks to all of them.

*Samarjeet Singh Siwal*

## ABSTRACT

---

In present scenario, direct methanol fuel cell (DMFC) becoming more familiar and promising fuel cell due to its straightforward configuration system & weight and elevated power generation efficiency.

This thesis focuses on metal nanoparticles based nanocomposite which is prepared by using *in situ* polymerization and composite formation (IPCF) technique and used for fuel cell application. The MNP-CP composite system was deposited on WE by drop and dry method. The integration of various nanomaterials is described, in order to understand the effect of different surface modifications and morphologies of various materials for electro-oxidation of low molecular weight alcohols (C1-C4). In this work, IPCF approaches are the promising methods to fabricate the key building blocks of nanocomposites system for fundamental research.

The entire work of the thesis contributes in the field of fuel cell by exploring the applicability's of conductive polymer (CP) and metallic nanoparticles (MNPs) based nanocomposite systems. In general, potentiometric and amperometric electrochemical approach were employed to model the electrochemical performance of the CP-MNP. The CP-MNP composite were used to modify the working electrode (WE) i.e. glassy carbon electrodes (GCE). The intimate contact between CP and MNP in nanocomposites system were characterize by optical microscopic techniques such as transmission electron microscopy (TEM), scanning electron microscopy (SEM), ultra-violet visible (UV) spectrophotometer, X-ray diffraction (XRD) pattern, X-ray photoelectron spectroscopy (XPS) and photoluminescence (PL).

Polymer supported ionic palladium has been synthesized using a single step, *IPCF* route from the corresponding monomer and metal salt precursors. The composite has been

characterized using various optical and microscopic and characterization techniques. The synthesized material was also successfully used as the electrocatalysts for methanol oxidation in alkaline media and recommending its potential application for methanol fuel cells, where we have achieved the highest current density value  $5.03 \text{ mA cm}^{-2}$ .

Finally, we synthesize a polymer supported palladium nanoparticles by using an IPCF method,. The resultant material was characterized by optical and surface characterization techniques, which offered the information about the chemistry of metal and polymer. The microscopic characterization showed the morphology of the composite and the orientation of the metal nanoparticles within the polymer matrix. The synthesized material was successfully used as an electrocatalysts for the methanol oxidation. Also for our palladium based nanoparticle system, a stable and higher value of  $I_F/I_B$  ratio was obtained, which evidenced as the less carbon monoxide formation, when palladium nanoparticles were used as an electro-catalyst for methanol oxidation reaction.



## TABLE OF CONTENTS

<b><u>Section</u></b>	<b><u>Page</u></b>
Declaration .....	i
Dedication .....	ii
Publications and Presentations.....	iii
Acknowledgements.....	vi
Abstract.....	viii
Table of Contents .....	x
List of Figures.....	xiv
List of Tables .....	xviii
List of Abbreviations .....	xix
<b>CHAPTER 1 INTRODUCTION.....</b>	<b>1</b>
1.1. Background.....	1
1.2 Problem Statement or Hypothesis and Results Expected .....	2
1.3 Justification of the Study Concerning Relevant and Recent Literature: .....	4
1.4 Aims and Objectives of Study:.....	5
1.4.1 Aims:.....	5
1.4.2 Objectives: .....	6
1.5 The Thesis Statement.....	6
1.6 Brief Overview of Chapters.....	6
1.7 References .....	8
<b>CHAPTER 2 LITTERATURE REVIEW.....</b>	<b>13</b>
2.1 Introduction.....	13
2.2 History of fuel cells.....	13
2.3 Overview of platinum group metal electrocatalysts .....	14
2.4 The potential of fuel cells .....	15
2.5 Types of Fuel Cells .....	16
2.5.1 Proton exchange membrane fuel cell.....	16
2.5.2 Solid oxide fuel cell .....	17
2.5.3 Alkaline fuel cell .....	18

2.5.4	Molten-carbonate fuel cell .....	18
2.5.5	Phosphoric-acid fuel cell .....	19
2.5.6	Direct-methanol fuel cell.....	19
2.6	Electro oxidation of direct alcohol fuel cells .....	19
2.6.1	Direct fuel cells.....	19
2.7	The Compact of Direct Methanol Fuel Cell .....	28
2.7.1	Advantages .....	28
2.7.2	Environmental affects.....	28
2.7.3	Potential applications .....	29
	2.7.3.2 Transportation application:.....	30
2.7.4	Transportable applications and micro-fuel cells: .....	31
2.8	Direct Methanol Fuel Cell Concept .....	32
2.8.1	Generalities.....	32
2.8.2	Reactions .....	33
2.9	Problems in DMFC .....	33
2.9.1	Steady electro-oxidation kinetics.....	33
2.9.2	Methanol Crossover .....	34
	2.9.2.1 Explanation:.....	34
	2.9.2.2 Easy solutions to counter crossover: .....	35
2.9.3	Gas management on anode side .....	35
2.10	Electrode structure.....	36
2.10.1	Catalysts .....	37
	2.10.1.1 Anode catalyst:.....	37
	2.10.1.2 Cathode catalyst: .....	39
2.10.2	Catalyst structure .....	39
2.11	Catalyst synthesis for fuel cell application.....	40
2.12	Sub-conclusion .....	41
2.13	References .....	42
<b>CHAPTER 3 EXPERIMENTAL METHODOLOGY.....</b>		<b>62</b>
3.1	Introduction.....	62
3.2	Reagents Materials, and Solvent .....	62
3.3	Research Plan .....	63

3.4	Instrumentation .....	66
3.4.1	Brunauer-Emmett-Teller (BET) N <sub>2</sub> adsorption method.....	67
3.4.1.1	Sample preparation:.....	67
3.4.2	Fourier Transform Infrared .....	67
3.5	Microscopy Techniques .....	68
3.5.1	Transmission Electron Microscopy (TEM).....	68
3.5.2	Scanning Electron Microscopy (SEM).....	69
3.6	Electrochemical Characterization .....	69
3.6.1	Electrochemical impedance spectroscopy (EIS) .....	69
3.6.2	Cyclic voltammetry .....	72
3.6.3	Chronoamperometry .....	73
3.6.3.1	Principle of chronoamperometry .....	74
3.7	Sub-conclusion .....	74
3.8	References .....	75

**CHAPTER 4 SINGLE STEP SYNTHESIS OF POLYMER SUPPORTED  
PALLADIUM COMPOSITE: A POTENTIAL ANODE CATALYST FOR THE  
APPLICATION OF METHANOL OXIDATION..... 76**

4.1	Introduction .....	76
4.2	Experimental procedure.....	78
4.2.1	Materials: .....	78
4.2.2	Material characterization: .....	78
4.2.3	Preparation of Pd-pTA composite catalyst: .....	79
4.2.4	Electrochemical Measurements: .....	80
4.3	Result and discussion:.....	80
4.3.1	Characterization of the compound .....	80
4.3.2	Performance of Pd-pTA as an electrocatalyst for methanol oxidation reaction.....	86
4.4	Sub-conclusion .....	92
4.5	References .....	93

<b>CHAPTER 5 PALLADIUM-POLYMER NANOCOMPOSITE: AN ANODE</b>	
<b>CATALYST FOR THE ELECTROCHEMICAL OXIDATION OF METHANOL...</b>	<b>100</b>
5.1 Introduction .....	100
5.2 Experiment section .....	102
5.2.1 Materials .....	102
5.2.2 Material characterization .....	102
5.2.3 Preparation of a Pd-pDAN composite catalyst .....	103
5.2.4 Electrochemical measurements .....	104
5.3 Result and discussion: .....	104
5.4 Sub-conclusion: .....	112
<b>CHAPTER 6 CONCLUSION AND PERSPECTIVES .....</b>	<b>118</b>
6.1 Summary of Findings and Conclusion .....	118
6.2 Recommendations for Future Work .....	118



## LIST OF FIGURES AND SCHEMES

---

<b><u>Figure</u></b>	<b><u>Description</u></b>	<b><u>Page</u></b>
<b>Scheme 1.1</b>	Synthesis of the metal-polymer nanocomposite.....	4
<b>Scheme 1.2</b>	Modification of GCE with nanocomposite by using “drop and dry” method and electro-oxidation of methanol. ....	4
<b>Figure 2.1</b>	DMFC principle scheme.....	33
<b>Figure 2.2</b>	Methanol crossover occurrence. ....	35
<b>Figure 2.3</b>	Catalyst model. ....	39
<b>Scheme 3.1</b>	Flow chart of entire research study. ....	64
<b>Figure 3.1</b>	Structure of a three electrode operation electrochemical cell arrangement. The experimental cell consists a glass vial including a detachable lid having an inlet place as the electrode and gas cleaning. Here, the enough carrying electrolytes (to be contained) were chosen inside a glass vial and the reference electrode (RE), working electrode (WE) and counter electrode (CE) were dipped inside the cell. ....	66
<b>Figure 3.2</b>	Schematic description of electrochemical cell equivalent circuit (left) and Nyquist plot (right) for impedance spectroscopy. ....	71
<b>Figure 3.3</b>	A Typical Cyclic Voltammogram Plot. ....	72
<b>Figure 3.4</b>	The chronoamperometric analysis. (a) The potential-time profile used through the experiment, $E_i$ is initial state and $E_1$ is the potential whither no reduction of O happens or some other potential of concern. (b) The similar response of the current because variations of the potential.....	74
<b>Figure 4.1</b>	(A) TEM and (B) SEM image of the Pd-pTA composite. (C) The XRD patterns of the Pd-pTA composite and the XPS signal (D) indicates the presence of characteristic ionic palladium species in the sample. ....	81



<b>Figure 4.2</b>	(A) The UV-visible spectra of <i>p</i> TA (a) and Pd- <i>p</i> TA (b). (B) The photoluminescence spectra for <i>p</i> TA (a) and Pd- <i>p</i> TA (b). ....	82
<b>Figure 4.3</b>	FTIR spectra of Pd- <i>p</i> TA. ....	83
<b>Figure 4.4</b>	The optical images of (a) <i>p</i> TA and (b) Pd- <i>p</i> TA. (A) Nitrogen adsorption and desorption isotherms and (B) pore size distribution of the (a) <i>p</i> TA and (b) Pd- <i>p</i> TA.....	84
<b>Figure 4.5</b>	The electrochemical impedance spectroscopy analysis for the (a) <i>p</i> TA and (b) Pd- <i>p</i> TA in 0.50M KOH within the frequency ranges from 3 MHz to 10 Hz. The electron transfer resistance values for (a) <i>p</i> TA and (b) Pd- <i>p</i> TA are 68.60 ohm and 58.30 ohm, respectively. ....	85
<b>Figure 4.6</b>	(A) Cyclic voltammogram of bare GCE (curve 'a'), <i>p</i> TA modified GCE (curve 'b') in the absence of methanol, whereas, the curve 'c' and curve 'd' represent the voltammogramme for bare GCE and <i>p</i> TA modified GCE, respectively, in the presence of 1.0 mol dm <sup>-3</sup> methanol and 0.5 mol dm <sup>-3</sup> KOH under the scan rate of 50 mVs <sup>-1</sup> . (B) Cyclic voltammogram of Pd- <i>p</i> TA modified GCE, in the absence of methanol (curve 'e') and in the presence of 1 mol dm <sup>-3</sup> methanol (curve 'f'), in 0.5 mol dm <sup>-3</sup> KOH under the scan rate of 50 mVs <sup>-1</sup> . ....	87
<b>Figure 4.7</b>	(A) Represents 10 consecutive scans (cyclic voltammograms) in the presence of 1.0 mol dm <sup>-3</sup> methanol and 0.5 mol dm <sup>-3</sup> KOH. The magnified section shows, from 'a' (first scan) to 'b' (tenth scan), the increase of current density (peak height) with the shifting of peak position towards lower potential direction. (B) Polymer stabilized palladium nanoparticles (sample collected from the working electrode at the end of the experiment). (C) The characteristic XPS peak with the binding energy value 335.23 eV for the Pd 3d5/2 line indicates the presence of metallic state of palladium.....	88
<b>Figure 4.8</b>	(A)The stability study of Pd- <i>p</i> TA catalyst on glassy carbon electrode in the presence of 1.0 mol dm <sup>-3</sup> methanol in 0.5mol	

dm<sup>-3</sup>KOH under the scan rate of 50 mV/s for 500 cycles.(B) The chronoamperometric response for the Pd-*p*TA catalyst in the presence of 1.0 mol dm<sup>-3</sup> methanol and 0.5 mol dm<sup>-3</sup> KOH at 30 °C at the fixed potential of 0.07V for the period of 3000 seconds. (C) show the linear relation between the current density (obtained from anodic peak) and the cycle number, obtained from the cyclic voltammogram data (A). (D) A fraction of the liner plot is shown by an arrow at higher magnification. (E) Current retention capability of the catalyst, which is 86.4%, has been calculated from. .... 89

**Figure 5.1** The Fourier transform infrared images for *p*DAN, spectrum (a) and Pd-*p*DAN spectrum (b)..... 105

**Figure 5.2** (A) The TEM image shows a chain like structure of Pd-*p*DAN. (B) The magnified TEM image shows the distribution of palladium nanoparticles along the core of the polymer chains. (C) The in-set TEM image shows the nanoparticulates within the polymer. (D) A typical EDX spectra indicates the presence of palladium in the sample (the copper peak is derived from the TEM support grid). .... 106

**Figure 5.3** (A) X-ray Diffraction pattern for (a) *p*DAN and (b) Pd-*p*DAN. In the spectrum (b), the peaks at 40.2°, 46.5°, 68.0°, 82.2° and 86.7° representing the (111), (200), (220), (311) and (222) Bragg reflection, respectively, indicates the crystalline nature of the palladium nanoparticles. (B) Palladium 3d X-ray photoelectron spectroscopy of Pd-*p*DAN. The peaks at binding energies at 335.20 eV and 340.05 eV for 3d<sub>5/2</sub> and 3d<sub>3/2</sub>, respectively, are indicative of metallic palladium..... 107

**Figure 5.4** (A) In the main panel, the electrochemical impedance spectra for the (a) *p*DAN and (b) Pd-*p*DAN in KOH (0.5 mol dm<sup>-3</sup>) within the frequency ranges from 7 MHz to 10 Hz. (B) The in-set image shows the magnified Z' axis, where the electron transfer resistance values for both the samples are clearly visible:(a) *p*DAN (62.26 ohm) and (b) Pd-*p*DAN (18.76 ohm).(C) The

electrochemical cell equivalent circuit for Pd-pDAN. (D) Cyclic voltammogram of bare (a) and pDAN modified (b) GCE, in KOH (0.5 mol dm<sup>-3</sup>). Cyclic voltammogram of bare (c) and pDAN modified (d) GCE in the presence of KOH (0.5 mol dm<sup>-3</sup>) and methanol (1.0 mol dm<sup>-3</sup>). (E) In the main panel, cyclic voltammetry, current vs potential graphs for Pd-pDAN modified GCE, in absence of methanol, voltammogram (e), and in the presence of methanol (1.0 mol dm<sup>-3</sup>), voltammogram (f), in KOH (0.5 mol dm<sup>-3</sup>). ..... 109

**Figure 5.5**

(A) The stability study of Pd-pDAN modified electrode in the presence of methanol (1.0 mol dm<sup>-3</sup>) and KOH (0.5 mol dm<sup>-3</sup>) under the scan rate of 50 mV/s for 100 cycles. (B) The chronoamperometric response for the Pd-pDAN modified electrode presence of methanol (1.0 mol dm<sup>-3</sup>) and KOH (0.5 mol dm<sup>-3</sup>) at 30 °C under the fixed potential of -0.05V for the period of 3000 seconds. (C) A linear relation between the current density (anodic peak during the forward scan) and the cycle number; obtained from the cyclic voltammogram data (figure 5A). (C) Current retention graph calculated from the cyclic voltammogram data (figure 5A). (D) The bar diagram shows the relation between current density and the I<sub>F</sub> / I<sub>B</sub> ratio. .... 111

## LIST OF TABLES

---

<b><u>Table</u></b>	<b><u>Description</u></b>	<b><u>Page</u></b>
<b>Table 2.1</b>	The electrocatalytic characteristics of typical anode catalysts including several combinations towards fuel cell applications	38
<b>Table 3.1</b>	Table and Origin of Materials	63
<b>Table 3.2</b>	Standard Operating Parameters for CV	73
<b>Table 4.1</b>	A comparative data on the Pd-based catalyst for the electro-oxidation of methanol	91



## LIST OF ABBREVIATIONS

---

CV	Cyclic Voltammetry
CA	Chronoamperometric
EIS	Electrochemical Impedance Spectroscopy
CP	Conductive Polymer
GCE	Glassy Carbon Electrode
PdNPs	Palladium Nanoparticles
PBS	Phosphate Buffer Saline
SEM	Scanning Electron Microscopy
TEM	Transmission Electron Microscopy
EDX	Energy Dispersive X-ray Spectroscopy
FTIR	Fourier Transform Infra-red
UV-Vis	Ultra Violet-Visible
XRD	X-ray diffraction
LMW	Low Molecular Weight
TGA	Thermogravimetric Analysis
XPS	X-Ray Photoelectron Spectroscopy
BET	Brunauer-Emmett-Teller
PGMs	Platinum Group Metals
DMFCs	Direct Methanol Fuel Cells
DEFCs	Direct Ethanol Fuel Cells
IPCF	<i>in-situ</i> Polymerization and Composite Formation

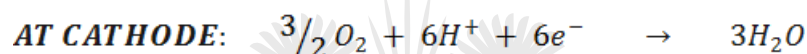
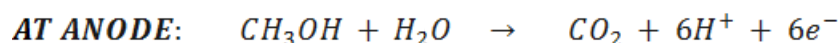
# CHAPTER 1

## INTRODUCTION

---

### 1.1. Background

In present era, direct methanol fuel cell (DMFC) become more familiar and power promising fuel cell due to uncomplicated system configuration, small range & weight and elevated power generation efficiency. DMFC comes under the category of polymeric electrolyte fuel cell and can be defined as "an electrochemical device that converts chemical energy into the electrical energy directly via oxidation-reduction reaction of methanol. The reaction mechanism of DMFC is similar to the polymer electrolyte membrane fuel cell.



DMFC can efficiently work as a primary power source in the application of motor vehicles such as car, motor cycles and other portable devices/fuel engine. In comparison with H<sub>2</sub>/air polymeric electrolyte membrane (PEM)-fuel cell DMFC is found to be an excellent substitute owing to its simple liquid fuel handling of fuel, high current density and improved safety.

A complete DMFC system contains - PEM, bipolar plates, current collector plates, gaskets, end plates and reactant (Methanol and oxygen/air). Each and every components of the DMFC plays an important role and can directly affect the performance of DMFC. Nafion, a perfluoro sulfonic acid polymer, is commonly used as a PEM in DMFC because it shows enough proton conductivity, thermal and chemical stability and oxidative stability. Bipolar plates are usually used to distribute the fuel and oxidant surrounded by the cell and split both the compartment of the stack. They also can distribute current and humidify gases such as. Gas-kits are used to avoid leaking of reactant and separate current between the current collector and end plate.

There is a huge number of parameters and factors responsible for the performance of DMFC, such as operating temperature, fuel concentration, catalyst loading, flow line plan, etc. So many study and work have done by researchers in different-different areas and on various parameters to develop the efficiency of DMFC.

Primarily, methanol and ethanol are broadly proposed hydrogen substitute fuels for mobile applications including electric vehicles [1, 2]. There are numerous advantages to using methanol as a fuel in comparison to hydrogen; these advantages are i) an economical liquid fuel, ii) directly handled, iii) transported, and iv) stored and with a high energy density value [3, 4]. In addition, ethanol also presents a striking substitute as a fuel at low-temperature because it can be produced from agriculture products in bulk and is one of the most valuable renewable biofuel from the agitation of biomass. Some other low molecular weight alcohols, includes propanol and ethylene glycol have also been tested as fuel, but particularly for alkaline fuel cells [5].

Over the past few decades, the electro-oxidation of alcohol in fuel cell application has attracted growing attention. Fuel cells offer excellent benefits over conventional power origin systems. A fuel cell is a tool in which a chemical reaction with the help of a number of oxidizing agents can exchanges the chemical energy into a fuel [6]. The use of existing gasoline infrastructures with an alcohol based fuel cell is striking due to liquid organic fuels can be simply stored and transported.

## **1.2 Problem Statement or Hypothesis and Results Expected**

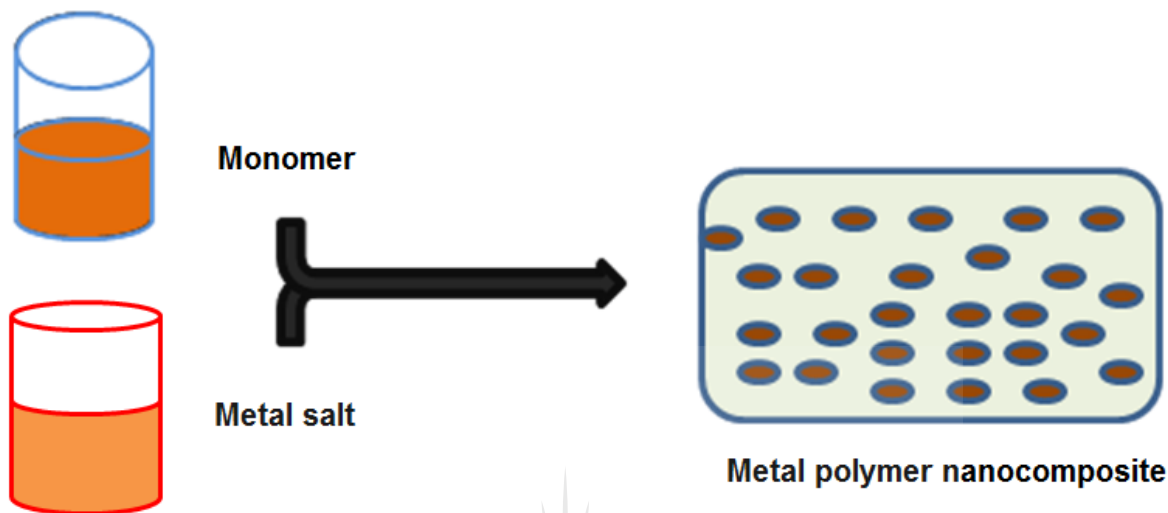
The exhaustive literature review has been carried out based on fuel cell technology, and we came to know that it mainly depends on two critical materials; (i) the membrane [7] and (ii) the electro-catalyst. Both of the key materials are also directly linked to the main obstacles faced in fuel cells, such as (a) fuel crossover [8] which can only prevail over by developing new membranes; and (b) time-consuming anode kinetics which can only be conquered by

developing new anodic catalysts. There are two major obstacles in respect to new anode catalysts, specifically, the performance, including activity, consistency, stability and cost reduction.

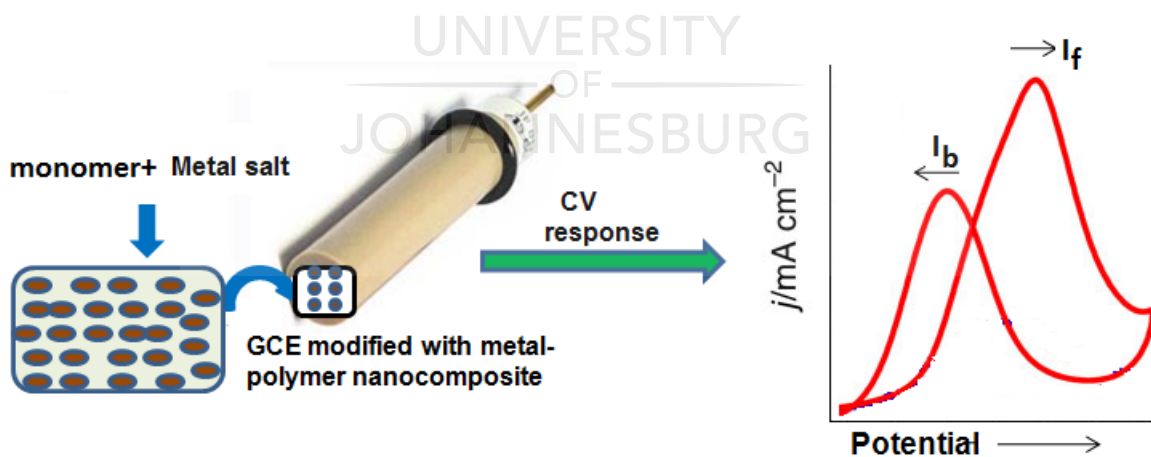
The progress in the field of fuel cell catalyst has attracted widespread consideration to exploring substitute energy sources [9]. The rapid development of nanotechnology creates highly stable and dynamic supported catalysts. In general, the platinum group metal nanoparticles used as a promising fuel cell catalyst; increased surface area, resulting enhanced catalytic performances [10]. On the other hand, nanoparticles have an intrinsic affinity to minimize their energy through cluster [10] and to prevent that particle are usually capped with different stabilizers which include surfactant [11], polymer [12], dendrimers [13] and ligands [14]. The benefit of polymers as a stabilizer is owing to its dynamic nature which could give the metal particles an additional stability [15]. The synthesized composite architectures for polymers and metal nanoparticles gives the mutually useful functionality along with mechanical integrity. Metal nanoparticles united with an appropriately conjugated polymer can form an exclusive composite with interesting physical properties and potential applications. These type of composites have been shown to demonstrate different properties directly applicable to dielectrics, energy storage and catalytic activity [16]. To improvement of the incorporation of metal nanoparticles into a polymer matrix, a number of research has been carried out [17-21]. On the contrary, some polymers also strictly bound the catalytic performance by lowering the accessibility of surface metal atoms. To prevail over the existing problems to synthesize the catalyst, platinum group nanometals dispersed on various solid supports (metal oxides and carbon) that can boost up the accessibility and also stabilize the nanoparticles onto the surface of the respective particles [22-25].



The following schematic diagram showing the synthesis of metal-polymer nanocomposite (**Scheme 1**) and fabrication of glassy carbon electrode (GCE) (**Scheme 2**) for the electro-oxidation of a fuel cell.



**Scheme 1.1** Synthesis of the metal-polymer nanocomposite.



**Scheme 1.2** Modification of GCE with nanocomposite by using “drop and dry” method and electro-oxidation of methanol.

### 1.3 Justification of the Study Concerning Relevant and Recent Literature:

Development of a high-performance fuel cell catalyst has been attracted extensive attention to exploring the alternative green energy resources [9]. During the last decade, there has been

considerable interest in the design and testing of molecular electrocatalysts for the interconversion of renewable energy and chemical fuels [26-30]. To become a competitive energy sources with available electrocatalytic energy conversion technologies, finding a new catalysts with robust in nature, fast in activation and with high energy-efficiency, is very essential. Pt-group metal-based nanoparticles used as a most efficient fuel cell catalyst, and it is now well known that a small particle size with a high surface area and the accessible metal surface can significantly improve catalytic performances [10, 31-33]. Pt-group metal nanoparticles such as palladium, ruthenium and platinum are particularly interesting owing to their size-dependent electrical, optical and catalytic properties. Pt nanoparticles (Pt-NPs) had a progressing and promising role in the field electrocatalytic sensors for alcohol oxidation [34, 35]. The integration of Pt-NPs with conducting polymers has a significant impact in the field of electrocatalytic sensors. Pt-NPs hybrid nanocomposites have a potential role for the electrocatalytic oxidation of methanol and ethanol, due to their respective electrocatalytic behavior [36]. The Pt-NPs is a redox active metal which has the potential to fabricate electrochemical sensors for methanol oxidation at the nanoscopic scale [37]. Palladium-based catalyst (such as Pd/Ni/Si-micro channel-plate) has also reported as an electrochemical sensor for ethanol detection [38]. Electro-deposition of hexahedral Pd nano crystals shows high order sensing ability when it combined with multi-walled carbon nanofibers and used for the electro-oxidation of ethanol [39]. Electrode modified with polyaniline based metal nanoparticles (Pt, Pt-Pd and Pt-Ru) showed the promising electro-oxidation of glycerol [40]. In another study, Pt-Sn/C-Rh and Pt-Sn/C-CeO<sub>2</sub> modified electrode used as an electrochemical sensor for the ethanol oxidation [41].

## **1.4 Aims and Objectives of Study:**

### **1.4.1 Aims:**

The aim of the study to develop the platinum group metals based catalyst for the electro-chemical oxidation low molecular weight alcohols (C1-C4).

### 1.4.2 Objectives:

The objectives of the research are as follows:

[1] **Design and synthesis** of the catalysts based on platinum group nano metals supported on the polymer matrix.

[2] **Characterize** the synthesized nano-structured materials.

[3] **Investigate** the electro-catalytic responses of the alcohols regarding selectivity and specificity towards the catalysts.

[4] **Develop** the platinum group nano-metal based electro-catalysts suitable for fuel cell application.

### 1.5 The Thesis Statement

The goal of this thesis is to examine the fuel cell applications in platinum group nanometal based electro-catalysts. Determine the performance, whether or PGM based electrode material is better towards the electro catalytic oxidation of direct alcohol fuel cell in the alkaline medium.

### 1.6 Brief Overview of Chapters

The overall structure of the thesis proceeds by the following six chapters:

- ❖ **Chapter 1** presents a general introduction, motivation, justification, thesis statement, aim and objectives of PhD work.
- ❖ **Chapter 2** describe the background of review on electro-oxidation of alcohols, history of fuel cells and metal nanoparticles-polymer based nanocomposites and their role in the fabrication of anode catalyst.
- ❖ **Chapter 3** focuses the list of materials used, methodology followed, design and apparatus used for this research project. The used analytical technique is also described in this chapter. This chapter consists of a general section which explains common procedure used to perform the PhD work in general, and those peculiar to achieve each milestone of this study.

- ❖ **Chapter 4** reports the single step synthesis of polymer supported palladium composite:  
A potential candidate for the electro-oxidation of methanol under alkaline condition
- ❖ **Chapter 5** reports the palladium-polymer nanocomposite: An anode catalyst for the electrochemical oxidation of methanol.
- ❖ **Chapter 6** presents the general conclusion and future prospective of this work based on the result obtained.



## 1.7 References

1. Lamy, C., E.M. Belgsir, and J.M. Léger, Electrocatalytic oxidation of aliphatic alcohols: Application to the direct alcohol fuel cell (DAFC). *Journal of Applied Electrochemistry*, 2001. 31(7): p. 799-809.
2. Peled, E., et al., New Fuels as Alternatives to Methanol for Direct Oxidation Fuel Cells. *Electrochemical and Solid-State Letters*, 2001. 4(4): p. A38-A41.
3. Hamnett, A., Fuel Cells and Catalysis mechanism and electrocatalysis in the direct methanol fuel cell. *Catalysis Today*, 1997. 38(4): p. 445-457.
4. Reddington, E., et al., Combinatorial Electrochemistry: A Highly Parallel, Optical Screening Method for Discovery of Better Electrocatalysts. *Science*, 1998. 280(5370): p. 1735-1737.
5. Antolini, E., Palladium in fuel cell catalysis. *Energy & Environmental Science*, 2009. 2(9): p. 915-931.
6. W. Vielstich, A.L., H. Gasteiger,, *Handbook of Fuel Cells, Fundamental, technology and application*. 2003: Wiley.
7. Amphlett, J.C., et al., A model predicting transient responses of proton exchange membrane fuel cells. *Journal of Power Sources*, 1996. 61(1): p. 183-188.
8. Ravikumar, M.K. and A.K. Shukla, Effect of methanol crossover in a liquid-feed polymer-electrolyte direct methanol fuel cell. *Journal of The Electrochemical Society*, 1996. 143(8): p. 2601-2606.
9. Gasteiger, H.A., et al., Activity benchmarks and requirements for Pt, Pt-alloy, and non-Pt oxygen reduction catalysts for PEMFCs. *Applied Catalysis B: Environmental*, 2005. 56(1-2): p. 9-35.

10. Guo, S., et al., Platinum Nanoparticle Ensemble-on-Graphene Hybrid Nanosheet: One-Pot, Rapid Synthesis, and Used as New Electrode Material for Electrochemical Sensing. *ACS Nano*, 2010. 4(7): p. 3959-3968.
11. Mallik, K., et al., Seed Mediated Formation of Bimetallic Nanoparticles by UV Irradiation: A Photochemical Approach for the Preparation of “Core–Shell” Type Structures. *Nano Letters*, 2001. 1(6): p. 319-322.
12. Mahato, S.K., et al., Polymer-Stabilized Palladium Nanoparticles for the Chemoselective Transfer Hydrogenation of  $\alpha,\beta$ -Unsaturated Carbonyls: Single-Step Bottom-Up Approach. *ChemCatChem*, 2014. 6(5): p. 1419-1426.
13. Myers, V.S., et al., Dendrimer-encapsulated nanoparticles: New synthetic and characterization methods and catalytic applications. *Chemical Science*, 2011. 2(9): p. 1632-1646.
14. Son, S.U., et al., Facile Synthesis of Various Phosphine-Stabilized Monodisperse Palladium Nanoparticles through the Understanding of Coordination Chemistry of the Nanoparticles. *Nano Letters*, 2004. 4(6): p. 1147-1151.
15. Dong, H., et al., One-Pot Synthesis of Robust Core/Shell Gold Nanoparticles. *Journal of the American Chemical Society*, 2008. 130(39): p. 12852-12853.
16. Gangopadhyay, R. and A. De, Conducting Polymer Nanocomposites: A Brief Overview. *Chemistry of Materials*, 2000. 12(3): p. 608-622.
17. Stefania, S., et al., Polymer-encapsulated metal nanoparticles: optical, structural, micro-analytical and hydrogenation studies of a composite material. *Nanotechnology*, 2008. 19(7): p. 075708.
18. Islam, R.U., et al., In situ synthesis of a Pd–poly (1,8-diaminonaphthalene) nanocomposite: An efficient catalyst for Heck reactions under phosphine-free conditions. *Catalysis Communications*, 2010. 12(2): p. 116-121.

19. Islam, R.U., et al., In-situ synthesis of a palladium-polyaniline hybrid catalyst for a Suzuki coupling reaction. *Journal of Organometallic Chemistry*, 2011. 696(10): p. 2206-2210.
20. Islam, R.U., et al., Conjugated polymer stabilized palladium nanoparticles as a versatile catalyst for Suzuki cross-coupling reactions for both aryl and heteroaryl bromide systems. *Catalysis Science & Technology*, 2011. 1(2): p. 308-315.
21. Ul Islam, R., et al., Palladium–Poly(3-aminoquinoline) Hollow-Sphere Composite: Application in Sonogashira Coupling Reactions. *ChemCatChem*, 2013. 5(8): p. 2453-2461.
22. Mallick, K., M.J. Witcomb, and M.S. Scurrell, Supported gold catalysts prepared by in situ reduction technique: preparation, characterization and catalytic activity measurements. *Applied Catalysis A: General*, 2004. 259(2): p. 163-168.
23. Mallick, K., M.J. Witcomb, and M.S. Scurrell, Simplified single-step synthetic route for the preparation of a highly active gold-based catalyst for CO oxidation. *Journal of Molecular Catalysis A: Chemical*, 2004. 215(1–2): p. 103-106.
24. Mallick, K. and M.S. Scurrell, CO oxidation over gold nanoparticles supported on TiO<sub>2</sub> and TiO<sub>2</sub>-ZnO: catalytic activity effects due to surface modification of TiO<sub>2</sub> with ZnO. *Applied Catalysis A: General*, 2003. 253(2): p. 527-536.
25. Mondal, A. and N.R. Jana, Surfactant-Free, Stable Noble Metal–Graphene Nanocomposite as High Performance Electrocatalyst. *ACS Catalysis*, 2014. 4(2): p. 593-599.
26. Thoi, V.S., et al., Complexes of earth-abundant metals for catalytic electrochemical hydrogen generation under aqueous conditions. *Chemical Society Reviews*, 2013. 42(6): p. 2388-2400.

27. Young, K.J., et al., Light-driven water oxidation for solar fuels. *Coordination chemistry reviews*, 2012. 256(21-22): p. 2503-2520.
28. Cook, T.R., et al., Solar Energy Supply and Storage for the Legacy and Nonlegacy Worlds. *Chemical Reviews*, 2010. 110(11): p. 6474-6502.
29. Benson, E.E., et al., Electrocatalytic and homogeneous approaches to conversion of CO<sub>2</sub> to liquid fuels. *Chemical Society Reviews*, 2009. 38(1): p. 89-99.
30. Savéant, J.-M., *Molecular Catalysis of Electrochemical Reactions. Mechanistic Aspects*. *Chemical Reviews*, 2008. 108(7): p. 2348-2378.
31. Zhang, S., et al., Graphene Decorated with PtAu Alloy Nanoparticles: Facile Synthesis and Promising Application for Formic Acid Oxidation. *Chemistry of Materials*, 2011. 23(5): p. 1079-1081.
32. Huang, X., et al., Amine-Assisted Synthesis of Concave Polyhedral Platinum Nanocrystals Having {411} High-Index Facets. *Journal of the American Chemical Society*, 2011. 133(13): p. 4718-4721.
33. Ma, L., et al., Control Over the Branched Structures of Platinum Nanocrystals for Electrocatalytic Applications. *ACS Nano*, 2012. 6(11): p. 9797-9806.
34. Li, Y., L. Tang, and J. Li, Preparation and electrochemical performance for methanol oxidation of pt/graphene nanocomposites. *Electrochemistry Communications*, 2009. 11(4): p. 846-849.
35. Jiang, L., et al., Structure and chemical composition of supported Pt–Sn electrocatalysts for ethanol oxidation. *Electrochimica Acta*, 2005. 50(27): p. 5384-5389.
36. Dong, L., et al., Graphene-supported platinum and platinum–ruthenium nanoparticles with high electrocatalytic activity for methanol and ethanol oxidation. *Carbon*, 2010. 48(3): p. 781-787.



37. Guo, D.-J. and H.-L. Li, High dispersion and electrocatalytic properties of Pt nanoparticles on SWNT bundles. *Journal of Electroanalytical Chemistry*, 2004. 573(1): p. 197-202.
38. Shi, J., et al., Pd/Ni/Si-microchannel-plate-based amperometric sensor for ethanol detection. *Electrochimica Acta*, 2011. 56(11): p. 4197-4202.
39. Tian, N., et al., Direct Electrodeposition of Tetrahedral Pd Nanocrystals with High-Index Facets and High Catalytic Activity for Ethanol Electrooxidation. *Journal of the American Chemical Society*, 2010. 132(22): p. 7580-7581.
40. Nirmala Grace, A. and K. Pandian, Pt, Pt–Pd and Pt–Pd/Ru nanoparticles entrapped polyaniline electrodes – A potent electrocatalyst towards the oxidation of glycerol. *Electrochemistry Communications*, 2006. 8(8): p. 1340-1348.
41. Souza, B.D., et al., Preparation of PtSn/C-Rh and PtSn/C-CeO<sub>2</sub> for Ethanol Electro-Oxidation. *International Journal of Electrochemical Science*, 2010. 5(6): p. 895-902.

## **CHAPTER 2**

### **LITTERATURE REVIEW**

---

#### **2.1 Introduction**

The literature review presented in this chapter informed and in particular, electro-oxidation of alcohol developed on polymer/metal nanoparticles. This chapter presented a short review of fuel cells and defined the thesis topic and main perspective, rationale and motivation, research tasks and objectives of study as well as the delimitation of the study.

The outline of this literature review can be summarised as follows:

- ❖ Brief review on history of fuel cells.
- ❖ Overview of platinum group metal electrocatalysts.
- ❖ The potential of fuel cells.
- ❖ Types of fuel cells.
- ❖ Electro-oxidation of direct alcohol fuel cells.
- ❖ The compact of direct methanol fuel cell.
- ❖ Direct methanol fuel cell concept
- ❖ Problems in direct methanol fuel cell.
- ❖ Electrode structure in the application of fuel cell.
- ❖ Catalyst synthesis for fuel cell application.

#### **2.2 History of fuel cells**

Firstly in 1839, Sir William Grove (generally referred to as the "Ancestor of the Fuel Cell") exposed that by inverting the electrolysis of water it may be likely to produce electricity. Later in 1889 the two scientists, Mond and Langer [1], cast the expression of the fuel cell as they were seeking to a designer the primary realistic fuel cell using air and coal gas. Although additional efforts were made in the early on the 1900s to expand fuel

cells that might alter carbon into electricity, the initiation of the internal ignition engine temporarily repealed any hopes of additional growth of the fledgling technology.

In 1932, Francis expanded the primarily victorious fuel cell tool, with a hydrogen-oxygen cell using nickel electrodes and alkaline electrolytes, low-cost substitutes to the catalysts handled by Mond and Langer. Later, National Aeronautics and Space Administration (NASA) [2] started to construct a small current engine to use for space missions. NASA releasing the research fund for those are involving fuel cell technology. After supplying electricity to numerous space missions, fuel cells have now had an established role in the space program.

Currently, some companies, such as major automobile industries - and different agencies are supporting the continuing research in the field of fuel cell mechanics development for purpose in fuel cell vehicles and other applications. Fuel cell energy is soon demanded to substitute regular potential sources in growing years, of micro level fuel cells to be utilised in mobile phones to high-potential fuel cells for hoard car competition [3].

Pt-group metal nanoparticles such as palladium, ruthenium and platinum are particularly interesting due to their size-dependent electrical, optical and catalytic properties. Pt nanoparticles (Pt-NPs) had a progressing and promising role in the field electrocatalytic sensors for alcohol oxidation [4, 5].

### **2.3 Overview of platinum group metal electrocatalysts**

Recently, the platinum group metals based nanoparticles with different support materials, are growing in fuel cells application field and they have excellent catalytic performance towards hydrogen evolution reaction [6]. The mixtures of elements to produce intermetallic compounds and alloys using, the series of properties of metallic systems can significantly extend in materials science. In several cases, there is an improvement in distinct properties against alloying it due to the synergistic influences and the wide range of configurations,

structures and properties of metallic alloys has conducted to broad applications in microelectronics, engineering, and catalysis. The need to make materials with well-defined, controllable features and structures on the nanometer level coupled with the elasticity supported by intermetallic materials has formed concern in bimetallic and trimetallic nanocluster [7]. To improve catalytic performance and reduce operational costs of platinum electrocatalysts, advanced electro catalysts design relying on the bi-functional mechanism has proposed. Platinum-group-metal-based nanostructures have great potential in the design of multifunctional catalysts for the electro-oxidation of fuel cells [8].

#### **2.4 The potential of fuel cells**

Fuels cells do not accumulate electricity but produce it straight from fuel. Additionally, they just require being stock with combustible and oxygen to working. So the reason; they have some benefits over regular batteries such as increased running time, compact load and efficiency of recharging. Further, the world's power arrives from combusting fossil fuels in low-efficiency method [9]. The large utilisation extent of fuel cells may possibly also offer an option to these methods both for motionless and moving applications.

Fossil fuels are not an effective long-term source of energy anymore due to the exponential energy demands and the growing environmental concerns. Efforts and research have been redirected to renewable power generation and/or power sources [10]. While, a reliable and renewable power source, fuel cells have fascinated recognition for mobile accessories, electric transports and on-site energy production operations in which they have great energy productivity and low exhaust level. Due to cost and endurance concerns, there is a hindrance for commercialization at larger scale [11]. A fuel cell mainly made up of an anode where traditional hydrogen was supply and a cathode where oxygen were provided, while these electrode separated by an electrolyte. The gaseous hydrogen as oxidant has recently replaced by liquid oxidants (fuels) which have higher voltage, mass, warehouse,

handling and processing [12-14]. There is a range of variables that can be adjusted within a fuel cell to ensure its sustainability and efficiency. Of these include, the pH of the electrolyte, nature of the oxidant and the respective materials of the anode along with its relative surface modifications played an important role for its successful fabrication.

The nature of the design fuel cells was based on the proton exchange membranes (PEM). The PEM fuel cells are the extremely capable of fuel cells and exhibit outstanding achievement [15], while supplied hydrogen. Throughout the generation, storehouse and worth of hydrogen are quietun-explanation while its production is strictly influenced by the contaminating varieties of hydrogen.

## **2.5 Types of Fuel Cells**

The fuel cell have several applications in the field of gas turbine energy manufacturing, gasoline motor in car and laptop battery. Flaming engines is similar to the turbine and the gas generator flame fuels where applied pressure generated by the growth of the gases contents for the mechanical operations. Batteries alter the synthesized power back into electrical voltage, when demanded fuel cells assigned powerfully [16]. Fuel cell affords a direct current (DC) voltage that may apply toward power engines, lights and electrical devices [17].

Fuel cells typically distinguished with their consecutive temperature and the category of electrolyte. Several kinds of fuel cells serve as an application in fixed power production. Another type of cells may be valuable for small transportable importance or horsepower cars. The primary examples regarding the fuel cells such are ;

### **2.5.1 Proton exchange membrane fuel cell**

Proton exchange membrane fuel cell (PEMFCs) are becoming an encouraging technique as neat and economic power formation during the twenty-first era. PEMFCs are the essential elements within fuel cell method. The scientists concentrated on the influence to the proton

exchange membrane including proton conductivity, under electric conductivity, permeability toward fuel, which results with the price value should be cheap along with good chemical/thermal resistance and mechanical advancement. It works simply below hydrated states in modern PEMFC method which is supported upon valuable perfluorinated PEMFCs. PEMFC operation complexity could be decreased with the growth of water-less electrolytes without hydration[18]. The PEMFC as the mainly suitable nominee for transportation purposes. The PEMFC has an excellent energy density at comparatively low working temperature (ranging from 60 to 80 °C). That low running temperature indicates that it does not get much high as for the fuel cell to heat the upward and start producing the electricity [19].

### **2.5.2 Solid oxide fuel cell**

The life span of energy through regular, productive and eco-friendly use is the main difficulties and challenges for the researchers to designers and investigators. Furthermore, fuel cells become the implied approach as an improvement on an enough volume for uses as industrial electricity production. Mahato *et al.* [20] describe in a recent work that serious global society majority and the increasing demand and worth about energy and its inferable environmental results. During the special, recognition to performed on the configuration and development regarding solid oxide fuel cell (SOFCs), remarking the limitations based on materials demands and fuel specifications [21].

Individual fuel cells have great impact to satisfy for the wide-range of fixed power generators that could produce electricity for commercialization. SOFC works at very high temperatures (between 700-1000 °C) [22]. Here, the high temperature plays consistency puzzle because components of the fuel cell can split down back sequencing on and off constantly. Though, solid oxide fuel cells are extremely durable while unbroken performance. In particular, the SOFC has confirmed continues service for the living of any

fuel cell below specific working circumstances. The raised temperature likewise has a benefit: the fumes generated via the fuel cell may be channeled toward turbines to produce further electricity.

### 2.5.3 Alkaline fuel cell

Alkaline fuel cell (AFC) is one of the earliest studies of fuel cells while the United States space plan has adopted them from the early 1960s. The AFC is liable to infection; therefore it needs to be purified the hydrogen and oxygen accordingly. It may be quite costly; therefore this kind of fuel cell is strange to be marketed [23].

AFCs held the greatest effective, engaged fuel cell coming to the pioneering operation regarding Bacon *et al.* [24]. AFCs may accomplish a great role to overall higher electrical ability in compare to another fuel cell classes. AFCs propose the possible as low price, mass manufacture fuel cells and without the dependence on platinum-supported catalysts and (presently) costly membrane electrolytes. AFC works comparatively economically electrolytes based on basic principles as potassium hydroxide [25].

### 2.5.4 Molten-carbonate fuel cell

Molten-carbonate fuel cell (MCFCs) are a quite recognized competitor as the production of absolute power originating from a description concerning probable fuels, covering natural gas, biogas and synthesis gases. MCFC runs by carrying oxygen of the cathode and moving it mutually including  $\text{CO}_2$  being a carbonate ion ( $\text{CO}_3^{2-}$ ) that penetrates by the electrolyte, oxygen is when issued and recombines by hydrogen on the anodic. Hydrogen may be formed with an inherent reforming method that gets place inside the chimney; therefore heat discharged with the fuel cell supports the endothermic improving effects [26]. Similar the SOFC, this type of fuel cells too finest filled for large stable power generators. Dicksreported in his work at 600 °C; therefore it can produce fumes which may be utilized to generate extra energy [27]. The MCFC have a lower working temperature than SOFCs; indicates that they don't require such striking materials.

### **2.5.5 Phosphoric-acid fuel cell**

Phosphoric-acid fuel cell (PAFC) described mainly the fuel cell applications which should be exhibited in several countries throughout the world and as various purposes. The primary PAFC power factories were established during the 1970s, and momentarily further 500 systems have been placed throughout the world [28]. The PAFC has the possible for utilize in small fixed power-generation methods. It works at a slightly high temperature than PEMFCs, so it has a greater warm-up time [29]. This gives it inappropriate for performance in cars.

### **2.5.6 Direct-methanol fuel cell**

Direct-methanol fuel cell (DMFC) worked at low and transitional temperatures (vary up to 150 °C) and supplied by a dilute aqueous solution of methanol. Cells process in gas phase further provides an excellent performance [30]. Many researchers are working in the field of the direct alcohol fuel cell. First, let's hold an attention where a direct alcohol fuel cell converted and this the main focus of the researchers in present scenario.

## **2.6 Electro oxidation of direct alcohol fuel cells**

### **2.6.1 Direct fuel cells**

In current years, as we know that one of the optimistic prospect competitors for the substitute of the combustion-based power origins, direct fuel cells (DFCs) have been getting growing alertness because of their cleanness and high effectiveness. All along with the various kinds of DFCs, direct ethanol fuel cells (DEFCs), particularly DEFCs working in alkaline states, are particular fascinating consideration because of their numerous exclusive benefits [31].

In direct methanol fuel cells (DMFCs), methanol fuel at the fuel cell anode instantly converted into electrical energy. Unlike in DMFCs, in other types of fuel cells such as the normal hydrogen powered cells, there is a large dependence on an external hydrogen generation system, which at most times are unresponsive. Though, certain limitations



hinder the commercialization of DMFCs including its poor performance compared with hydrogen/air systems. It has found that the primary cause of this poor performance is the requirement of a highly efficient methanol oxidation catalyst. Catalytic performance investigations on various methanol oxidation catalysts have undertaken, and it has found that only platinum-based materials exhibit excellent activity and better stability [30, 32].

Recently, most scientists have been investigating the performance of direct ethanol fuel cells (DEFCs) as alternative energy resources. Although important outcomes expected from DEFCs, there are still some improvements that need to be done to enhance their chances of future use. Recently, most scientists have been investigating the act of direct ethanol fuel cells (DEFCs) as alternative energy resources. Although important outcomes expected from DEFCs, there are still some improvements that need to be done to enhance their chances of future use [33]. Compared to methanol, ethanol is also environmentally favourable, and simple production methods may be employed to produce his high amounts directly from agricultural products or biomass. That is one of the reasons why DEFCs have recently received considerable attention. Since this is a new technology, there are some drawbacks, which needs to be dealt with before DEFCs can be commercialized. Many scientists have made several improvements on DEFCs to enhance their performance, and it believed that they could be of great potential for application as energy resources. DEFCs classified into two types depend on the kind of electrolyte membrane used, i.e. acid- and alkaline-membrane DEFCs [34].

Lin *et al.*[35] carried out their work on the oxidation of methanol on electrodes arranged by dispersing Pt straight onto a nafion membrane and then they preceding the methanol each in the gas supplied method or immediately from the electrolyte in the electrolyte provided method. Based on their study they proposed the mechanism of the methanol oxidation reaction depends on the environment of the enclosing and the introduction of the methanol

on the electrode exterior. Gootzen *et al.*, [36] studied the irreversible adsorption of various C3 alcohols, ethene, and 1-butanol on platinized platinum with electrochemical mass spectrometry and fourier transform infrared spectroscopy (FTIR) in the perchloric acid electrolyte. They have concluded in their study that ethene and 2-propanol is a small volume of oxygen association happens at the C<sub>1</sub> region, supported by decarbonylation to produce CO.

Hai and Gang [37] studied the electrooxidation of C4 alcohol on Pt electrodes by employing cyclic voltammetry (CV) and *in situ* FTIR spectroscopy. They proposed dual path mechanism for the electrooxidation of 1-butanol in perchloric solution. Lamy and co-workers [13] discussed the reaction mechanism and catalytic activity of the anode material based on the electrooxidation of several low molecular weight alcohols, including ethanol, n-propanol and ethylene glycol. They demonstrated their results with the various example of a particular cell, employing a proton exchange membrane (PEM) as an electrolyte, particularly for the direct electrooxidation of ethanol. Patra and Munichandraiah [38] carried out their study on platinum nanoparticles based conductive polymer, poly(3,4-ethylenedioxythiophene) (PEDOT), reveal a high catalytic motion for electro-oxidation of methanol. They examined the impacts of the concentration of the electrolyte, the weight of Pt, and the amount of PEDOT on mass-specific movement. As the electrochemical oxidation of methanol on Pt-supported catalysts, to obtain a high catalytic change, catalyst shreds should have nanometric dimensions with a similar pattern in a shielding matrix. The shielding pattern for the scattering of Pt particles performs a significant function in the production of the electrocatalyst. Carbon materials usually applied for carrying catalyst particles [39-41]. The carbon support gives electrical connectivity between the separated particles.

Solla-Gullon *et al.* [42] were analysed and evaluated with the performance of particular crystal electrodes with basal adjustments reactivity in respect to methanol and formic acid electrooxidation on Pt nanoparticles beside well-identified exteriors. The results pointed out regarding the importance of the facade formation/shape of well-defined Pt nanoparticles on methanol and formic acid electrooxidation effects. The surface composition of the electrodes performs a significant task on the reactivity of both oxidation processes, and thus the electrocatalytic characteristics powerfully depend on the cover arrangement/shape of the nanoparticles, in exacting on the appearance of positions with (111) agreement. Certain conclusions present the opportunity of inventing innovative and sound electrocatalytic materials applying polished shape-controlled Pt nanoparticles as formerly explained with Pt unique crystal electrodes.

E. Antolini [43] low-temperature fuel cells, carbon strengthened platinum, is usually applied as anode and cathode electro catalysts with hydrogen or low molecular weight alcohols. Furthermore, platinum utilized as the anode material willingly poisoned by carbon monoxide, being in the reformat gas work as an H<sub>2</sub> transmitter in the state of polymer electrolyte fuel cells, and a by-product of alcohol oxidation in the state of direct alcohol fuel cells. Moreover, the oxygen reduction effect when applied as the cathode material on Pt individual does not give an acceptable activity. There are some articles confers a survey on Pt and non-Pt-based catalysts for electrode materials examined both as anode and cathode materials for low-temperature fuel cells [44-46]. Palladium and platinum have many parallel effects due to both belong to the same groups in the periodic table. The act of Pd is slightly economical than such of Pt, for the oxygen reduction reaction (ORR). By the addition of a suitable metal, the ORR movement of Pd can succeed that of Pt. On the other hand, the performance of Pd is significantly cheaper than the Pt, for the hydrogen oxidation reaction (HOR). However, by attaching a little quantity of Pt, the

HOR performance of Pd achieves that of absolute Pt. Here, it's a summary of Pd and Pd-based catalysts, examined both primarily anode and cathode materials as low-temperature fuel cells [47]. Ferrin and Mavrikakis [48] have examined the formation consciousness of methanol electrooxidation on eight transition metals (Cu, Au, Ag, Pd, Pt, Ir, Ni, and Rh), self-steady density functional theory (DFT). Doing the adsorption powers of 16 central on two several facets of particular eight face-centered-cubic transition metals, blended with an easy electrochemical design, they deal with the reaction mechanism within these two metals facets (111) and (100). They also examine different two methods for methanol electro-oxidation: one going through an intermediate product CO\* and the second, oxidizes methanol directly to CO<sub>2</sub> without CO\* as a transitional.

Guo, *et al.* [49] proposed a clear chemical strategy for the synthesis of high-feature three-dimensional of Pt-on-Pd bimetallic nanodendrites based on graphene and applied as an exceptional nanoelectrocatalyst for methanol oxidation. It obtained that little single-crystal Pt nano-branches sustained on PdNCs with a permeable arrangement and fine distribution was straight form onto the facade of graphene nanosheets; that shows significant electrochemical working area. Besides, a class of chemical protocols established for obtaining biased control of NC patterns in a cube, [50, 51] tube, [52] wire, [53] tetrahedral Pt, [54] mesoporous nanostructure, [55, 56] as well as dendrite, [57] between that Pt nanodentrites are of appropriate concern in catalysis owing to their porous formation, large surface area, and significant catalytic activity. Kowal, *et al.* [58] were successfully synthesized the nanoclusters of Pt, Pt-Rh, Pt-SnO<sub>2</sub> and Pt-Rh-SnO<sub>2</sub> by polyol process and dropped on large-area carbon for electrocatalytic oxidation of ethanol. Its full oxidation to CO<sub>2</sub> yields twelve electrons per particle, but the reaction on Pt is quiet, and the main output is not CO<sub>2</sub> but acetic acid and acetaldehyde[59, 60]. Guo *et al.* [61] proposed one-pot, rapid synthesis of platinum nanoparticle ensemble-at-graphene hybrid nanosheet

and worked as a novel electrode material as the electrochemical sensing. Umeda *et al.* [62] explained a novel electrode that exhibits sensitized methanol electrooxidation in an oxygen ambience. They developed a binary Pt-C electrode for use as the anode catalyst of a direct methanol fuel cell using a co-sputtering technique. Pt and Pt-based alloy-loading carbon catalysts used as an anode catalysts for the methanol oxidation reaction [63-66]. Also, the hydrogen-fueling for polymer electrolyte membrane fuel cells (PEMFCs) have the great potential density and power density with the DMFCs. The anode catalysts do not initiate the methanol oxidation being effective as they start the hydrogen oxidation reaction. So, to improve the power production features of DMFCs, at the anode catalyst is necessary to endorse the methanol oxidation reaction. Pt- and Pt-supported alloy priming have lately described improving the activation of methanol oxidation, of carbon materials on Pt- and Pt-supported alloy packing have newly published [39, 67-69].

Van Doorslaer and co-workers [70] introduced a methodology to split final reaction outputs from ionic liquids without the requirement for organic solvent removal and also investigate the importance in Pd-catalyzed aliphatic alcohol oxidation. Ionic liquids (ILs) get growing attention as green substitutes for the traditional gaseous organic mechanisms due to their different solvent characteristics [71, 72]. In recent times, several transition metal catalyzed methods in ILs for alcohol oxidations proposed [73-75]. In various examples, the IL even worked as solvent and catalyst, e.g. including a catalytic metal class's member of the IL's anion [76, 77]. Although such catalytic methods implemented correctly for allylic or benzylic alcohols, they were not quite energetic for non-initiated aliphatic alcohols. Furthermore, the expected requirement for a removal step to distribute the reagent/outcome from the IL appearance begins this come up to less engaging [78]. Maiyalagan *et al.* [79] synthesized extremely durable Pt-Ru nanoparticles carried on three-dimensional cubic patterned mesoporous carbon (Pt-Ru/CMK-8) as electrooxidation of

methanol. They also discussed the price of the catalysts, and largely the Pt-Ru bimetallic composite applied to the direct methanol fuel cell causes a significant hurdle to its extensive utilize as a power resourceful and atmosphere-favorable fuel growth technology. Singh and Awasthi [80] developed graphite oxide and used as a base of palladium nanoparticles catalyst for the electrooxidation of methanol and ethanol. They recognized that Pd nanoparticles homogeneously scattered on graphene nanosheets (GNS) are high performance with comparison to those are distributed on nanocarbon particles (NC) or multiwall carbon nanotubes (MWCNTs) for methanol and ethanol electrooxidation below the same experimental circumstances. The GNS support on Pd nanoparticles improved the electrochemical activity of Pd/GNS through alcohol oxidation can be attributed to the significantly improved electrochemical active surface area. Yin *et al.* [81] studied CO poisoning with different surface compositions of PtAu alloys during methanol electrooxidation. They concluded by results that the CO generation could be decreased slowly increasing with the surface of Au sections in PtAu compounds and CO poisoning can roughly eliminate by adapting to a usual surface Au section.

Gao *et al.*[82] successfully synthesized Pd-graphene and Pt-graphene catalysts by a fabricated electroless plating technique electrodes for direct alcohol fuel cells, with a trace of SnO<sub>2</sub>. The exterior of graphene oxide initially modified by Sn<sup>2+</sup> ions, and eventually, at the facade of graphene oxide Pd or Pt nanoparticles are stored and then they reduced graphene oxide. In the Comparison study, they found that the carbon-based Pd and Pt, the resultant graphene-Pd and Pt catalysts show improved electrocatalytic action and long-term durability to alcohol electrooxidation. Pt and Pt-supported paired combination (e.g., Pt-Ni) broadly applied as anodes in DMFCs owing to their significant catalytic activity for the methanol oxidation [83-85]. Though, the realistic application of Pt anodes is inadequate as they are quite costly and quickly infected by carbon monoxide. Pd and Pd-supported

composites considered being one of the significant replacements for Pt composites due to their great plenty and exceptional protection against CO poisoning [86, 87].

Li *et al.* [88] studied the act of incorporation of methanol and ethylene glycol oxidation toward both Pt and Pd electrodes in alkaline evidence. They found that the performance of EG oxidation enhanced than the methanol oxidation and the durability of EG oxidation improved than such of methanol and ethanol oxidation toward the Pd electrode. They concluded from their results that the mixture of methanol and EG is an encouraging applicant being fuel in direct alcohol fuel cells. Amongst all the various potential alcohols, methanol is the most promising fuel due to its usage as a fuel has numerous improvements in aqueous electrolytes, liquid fuel accessible at economical cost, easy to handle, carried, and stocked, great general density of energy equivalent to that of gasoline [88, 90]. As we know, many researchers have already done lot of work to investigate the electrooxidation of alcohol on Pt-supported composites in alkaline evidence and the DAFCs including alkaline membrane exhibit sensible performance durability [91-93]. Now the researchers are focusing toward the improvement the without Pt electrocatalysts for alcohol oxidation on Pd-supported composites, and the outcomes exhibited that Pd is a suitable electrocatalyst for ethanol as well as C3-alcohols oxidation in alkaline evidence [86, 94].

Liu *et al.* [95] introduced his study toward methanol electrooxidation into tetrahedral Pt nanocrystals (THH Pt NCs) electrodes and investigated by an aggregate of electrochemical procedures and *in situ* FTIR spectroscopy. The adornment of the tread surfaces by Ru atoms improves the susceptibility to poisoning and thus decreases the opening potential toward methanol oxidation. When they examined PtRu metal nanoparticle composite, the Ru fabricated THH Pt NCs show significantly better catalytic currents and CO<sub>2</sub> production at smallest possible scale. Meher and Rao [96] synthesized a single shuttle-shaped CeO<sub>2</sub> in gram range by an uncomplicated polymer-assisted uniform

precipitation technique. In this work, first time they reported and confirmed that CeO<sub>2</sub> with an appropriate microstructure could recover the electrocatalytic movement of Pt/C as for methanol oxidation, and also can be used for inventing different electrocatalysts for fuel cell employment.

Li *et al.* [97] reported a simple method to prepare Pt nanoparticles supported on non-covalent functionalized graphene nanosheets during solvent-shedding extended graphite with the assistance of supercritical CO<sub>2</sub> and 1-pyrenamine. After that, they applied as shielding materials as platinum to examine the possible utilization of the acquired nanocomposite in DMFCs. Researchers also showed that graphene could be scaled and functionalized of graphite including the help of the syngenic outcome of pyrene derivatives as well as supercritical CO<sub>2</sub> [98, 99]. Many researchers have reported different support catalyst such as: Yang *et al.* [100] reported an easy procedure for fabricating mesoporous chromium nitride (CrN) by the ammonolysis of a substance ternary oxide (K<sub>2</sub>Cr<sub>2</sub>O<sub>7</sub>) as high-performance catalyst aid for methanol electrooxidation. Though, in requisites of fuel cell application, some research articles trafficking including metal nitrides as catalyst supports. The activity of a tungsten nitride held on carbon black (W<sub>2</sub>N/C) being a non-noble electrocatalyst for oxygen reduction reaction (ORR) in PEMFCs has been accounted. Here the article summarized that the performance of the W<sub>2</sub>N/C catalyst approaching the ORR was lower to that of commercially accessible Pt/C catalysts previously broadly used in PEMFCs [101]. Most of the researchers done their study on titanium nitride (TiN), but it goes through from loss and corrosion in acidic conditions [102-104]. On the other hand, chromium nitride (CrN) has elevated immunity to fatigue and corrosion [105, 106]. CrN has applied as a covering material for bipolar plates in fuel cells that is a significant part of PEMFC heaps [107, 108]. Habibi and co-workers [109] were carried out proper investigations of methanol, ethanol, propanol and butanol



electrooxidation on a carbon-ceramic electrode (CCE) potentiostatically mitigated by Pd nanoparticles.

Huang and Wang [110] reported currently progressed on carbon-root aid materials for electrocatalysts of direct methanol fuel cells. They summarize the current growth in the scheme and modification of novel carbon-root anode catalysts through different approaches and their uses toward methanol oxidation reaction.

## **2.7 The Compact of Direct Methanol Fuel Cell**

### **2.7.1 Advantages**

During methanol oxidation it rescues six protons and electrons per atom. Its tremendous energy density begins of methanol a becoming fuel as fuel cells [111]. DMFC worked on low and transitional temperatures (increase up to 150°C) and supplied by a dilute aqueous solution of methanol. In fact, the extraordinary temperature improves kinetics and methanol crossover dropped beside a gas phase supplies. Despite, the demand for vaporization may be a restriction for some purposes [112, 113].

Alkaline alcohol fuel cells (AAFCs) showed the quite significant improvements when it analysed by proton exchange membrane fuel cells (PEMFCs). (i) the kinetics of the couple alcohol oxidation and oxygen reduction in an alkaline medium as an alternative to an acidic one are advanced appreciably [114, 115], (ii) in alkaline evidence, less-Pt or also non-Pt catalysts positioned on Au [116] and Pd [117, 118] with anode, Ag [119] as well as perovskite-kind oxides [120] in the cathode may be employed including excellent electrocatalytic capability so the commercialization possibility of DAFC can increase. (iii) in AFCs the fuel crossover is bypassed as of the convey of hydroxyl groups of the cathode surface to the anode side via electro-osmosis.

### **2.7.2 Environmental affects**

Fuel Cells recognised as environmentally favourable because they do not generate toxic by-products. Though, they did not discharge-free. However, they generate carbon dioxide

that is a greenhouse gas. It is additionally perfect for hydrogen that gives CO<sub>2</sub> obliquely during resolving level during the water-gas shift effect. Methanol and different alcohols too generate any other by-products similar ketones, aldehydes and carboxylic acids still within small concentrations. It originated from the biomass; the CO<sub>2</sub> appeared through cell process would yet be restored via CO<sub>2</sub> used during photosynthesis. Subsequently, this kind concerning energy would add no further to the greenhouse influence and would be sustainable. Additional, the tremendous performance of fuel cells offers that limited CO<sub>2</sub>/kW generated as related towards standard route.

In the present scenario, the energy crunch and environmental contamination are both critical hurdles encountered by human culture as of quickly rising power require and extensive ignition of fossil fuels. It extensively supposed that the traditional assumptions of energy production and regeneration are not appropriate for the world's sustainable growth [121-124]. Consequently, an enormous opportunity for research has been moved out to create clean and sustainable energy roots as well as their tools [125-128]. Amongst these various energy methods, direct methanol fuel cells (DMFCs) hold widely investigated as excellent power transforms that exchange chemical energy regarding methanol immediately toward electrical energy [129].

### **2.7.3 Potential applications**

There are fundamentally three major classes regarding applications as fuel cells. Fuel cells are quite familiar for holding a substitute toward the enclosed combustion engines but further acknowledged for transportation and stationary purposes.

#### **2.7.3.1 Stationary applications:**

During the previous decade, enormous progress has achieved in fuel cell science and technology, particularly in some employment fields such as movable, transportation, and stable power roots [130].

Fuel cells can generate electricity immediately from fuel including an excellent performance. For stationary purposes, they will change the combustion supported electric-generating systems where energy failures take place in the hot engine including while the electric dynamo. They may be used to domestic, trade and manufacturing divisions for electricity also as heat generation [131]. As you know, DMFC does not require any regenerating of methanol; there are no failures while the agitator. Apart from the medium/low working temperature get the appropriate as household-class water heating.

### **2.7.3.2 Transportation application:**

Direct methanol fuel cell technology proposes a resolution for transportation purposes in the change close to a zero discharge prospect. By applying methanol being a fuel avoids one of the significant obstacles troubling PEMFC technology, so, the evolution of an economical and secure hydrogen transportation to substitute the gasoline/diesel fuel circulation channels. It has enough recognized so the transportation for methanol shipping and storehouse can directly modify from the contemporary gasoline exhaustive transportation. An additional disadvantage in accepting PEMFC system is the need to store hydrogen (at quite excessive pressures) or take a great fuel worker to change the liquid fuel within hydrogen toward keeping the transportation. Methanol is a delightful fuel as its power density is approximately half of that of gasoline, and it's a liquid under atmospheric conditions [132]. In spite of the gripping benefits of working DMFCs in transport purposes, biggest barriers to their debut remain.

Certain obstacles incorporate the essential costs of materials utilized in forming DMFCs (mainly the huge price of platinum electrocatalysts), the crossover of methanol within the electrolyte film from the anode to the cathode and, the lower efficiency and power density representation of DMFCs in corresponding to PEMFCs. Despite certain hindrances, some

organizations (especially in the previous five years) have grown actively involved in the evolution of DMFCs for transportation purposes [133].

Even though a new cars produce an economic volume of poisonous gases than their forerunners, transport is yet a significant cause of infection. Substituting an important part with fuel cells would've a considerable impact on the atmosphere. Methanol fuel cells become delicately examined for transport purposes. The principal convenience is that storehouse and container refilling is simple for the fluid methanol [130]. Furthermore, Dillon and co-workers they did not require any rebel or humidification operation; this would spend as much of the accessible place inside a car. In fact, their scheme is compressed too whenever some water is necessary to reduce methanol.

#### **2.7.4 Transportable applications and micro-fuel cells:**

There are some organizations energetically involved in the improvement of low energy DMFCs for mobile phones, laptops, transportable camera and electronic game purposes [134, 135]. The fundamental aim of that investigation is to build up evidence of theory DMFCs proficient of substituting good-performance rechargeable batteries in the 6-billion US\$ transportable electronic accessories business. Hypothetically, methanol has a better definite energy density in corresponding with the greatest rechargeable battery, lithium polymer and lithium ion polymer arrangements.

The most significant characteristic of a transportable or micro fuel cell is just a small object. A lessened dimension and weight of the cell ought to operate at atmospheric temperature. The low function temperature concerning the PEM fuel cell is a significant benefit for transportable purposes. In fact, it is the unique fuel cell competent on operating at atmospheric temperature [136]. Since the objects parallel to conveying purpose, it performs on obviously that DMFC is also an appropriate comparison to the hydrogen fuel

cells. The fuel cells system are yet a growing and require enhancement in both technological achievement and price.

## **2.8 Direct Methanol Fuel Cell Concept**

### **2.8.1 Generalities**

Fundamentally, a proton exchange fuel cell called direct methanol fuel cell that supported through an aqueous suspension of methanol. Here the both catalytic electrodes that will be the  $\text{CH}_3\text{OH}$  oxidation and the reduction of oxygen happen parted by an electrolyte film that conducts protons from anode to cathode, whereas another compounds dissipation prevented [137]. The aggregate of electrodes and films is described film membrane assembly. Every electrode composed of a gas diffusion sheet and a catalytic sheet.

The aqueous solution of methanol supported by the anode side, that will spreads within the dispersion layer towards the catalytic layer which will be electrochemically oxidized inside mostly  $\text{CO}_2$  protons and electrons [138]. Protons appeared while the reaction scatters within the Nafion film near the cathode catalytic zone. All contribute to oxygen reduction headed for produce the water at the cathode surface. Oxygen can be absolute but it can further get from the air. The electrons have recovered via graphite bipolar plates that have the two sticks of the cell. The composition of this cell has explained in given Figure 2.1.

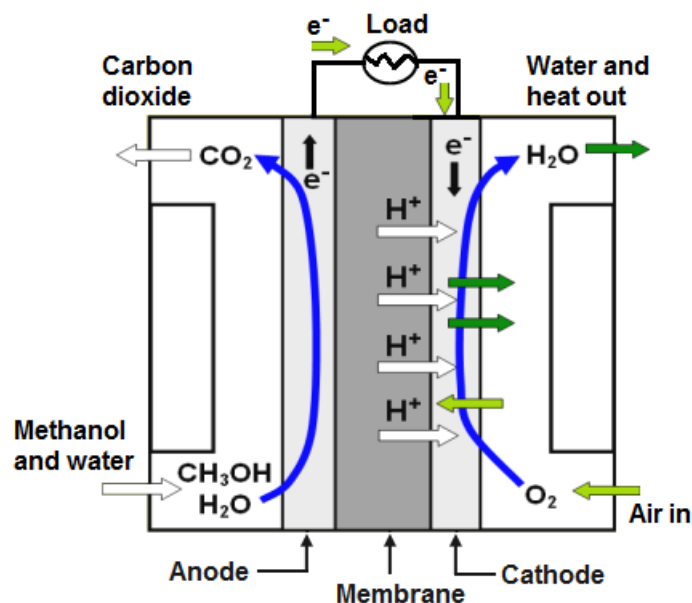
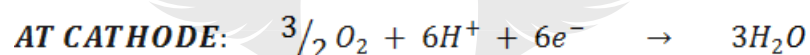
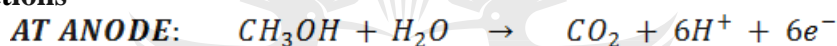


**Figure 2.1** DMFC principle scheme.

### 2.8.2 Reactions



At the anode side, the  $\text{CH}_3\text{OH}$  has oxidized in  $\text{CO}_2$  and six protons and electrons. Further, all protons developed counter at the cathode side including oxygen to reach water. The finally reaction seems similar a combustion reaction and hence occasionally pointed because of cold combustion [139-141]. In fact, the cell is expected to manage this reaction and apply it to generate current instantly.

## 2.9 Problems in DMFC

### 2.9.1 Steady electro-oxidation kinetics

Numerous exterior intermediates developed while methanol electro-oxidation. Here, methanol has largely converted to  $\text{CO}$  that is additionally oxidized to  $\text{CO}_2$ . Another  $\text{CO}$  corresponding classes further appeared:  $\text{COH}_{\text{ads}}$ ,  $\text{HCO}_{\text{ads}}$  and  $\text{HCOO}_{\text{ads}}$  [15, 142]. Few of certain intermediates are not easily oxidizable and stay powerfully adsorbed to the catalyst

exterior. Accordingly, others avoid new methanol units of adsorbing and supporting new reaction. Therefore electrooxidation of intermediates is the rate restricting level.

Here, the poisoning of the catalyst exterior severely reduces under the oxidation reaction. Also, an exact percentage of the intermediates adsorbs in advanced from oxidized into CO<sub>2</sub> and thus decrease fuel performance but bearing within full oxidation. Consequently, a highly significant hurdle is to expand further electrocatalysts which slow down the contaminating and improve the reaction. At the same period, also improved movement approaching carbon dioxide production.

## **2.9.2 Methanol Crossover**

### **2.9.2.1 Explanation:**

During PEM fuel cells, to strike the electrode approaching the different side and support non-electrochemical oxidation is the main object of the membrane to prevent fuel and oxygen. Though, during DMFC, the fuel scatters within the electrolyte membrane [143]. Owing to the hydroxyl group and their hydrophilic characteristics, methanol communicates including the ion swap positions and is pulled through hydronium ions within the extension toward diffusion essentially a decision of the concentration gradient within both electrode anode and cathode. Methanol which passes overhead reacts straightly with oxygen on the cathode surface (Figure 2.2).

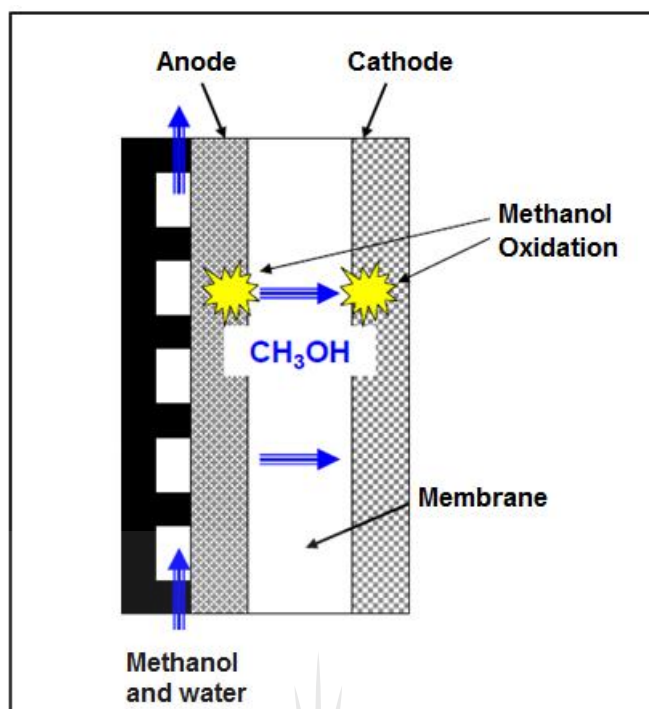


**Figure 2.2** Methanol crossover occurrence.

### 2.9.2.2 Easy solutions to counter crossover:

Crossover can be improved by adjusting the concentration of electrolyte and pressure gradient among working and counter electrode. It may be quickly restricted through applying a low methanol absorption within the anode supplies solvent and by improving cathode pressure toward a particular size. It should be scanty sufficient to decrease crossover as it potential but further, deliver the anode catalytic zone by sufficient methanol toward generating an admissible current density.

### 2.9.3 Gas management on anode side

Gas supervision toward the anode surface is an essential matter in DMFC scheme. However, toward the anode surface,  $\text{CO}_2$  conceived being a result of electrochemical methanol oxidation. If  $\text{CO}_2$  droplets cannot remove efficiently, the anode tubes will be prevented, leading to insufficient mass transport. Argyropoulos *et al.* [144] recognized the two-phase flow model in the anode tube under several working states. That flow visualization toward the anode surface generate a relevant recognition of droplet dynamics in DMFC.



Maximum of the carbon dioxide produced in methanol oxidation within the gas state and had becoming extracted by the supplies neck. CO<sub>2</sub> is accumulated at the working electrode, catalytic film and scatters through the tip like the gas dissipation film. Wherever, CO<sub>2</sub> droplets produce on the exit of the holes. The measurement depends upon the extent of the holes and the wet capability of the electrode support. Next, they enter an exact volume, these droplets delivered in the methanol solution [145]. Here is hence a two-state flow in the supplies carriers, and that is not externally outcomes at cell enforcement. The leading concentration concerning droplets gives them to combine and grow slugs. Subsequently, the amount of methanol cannot be enough to preserve a coveted current density. The current density converts bounded by methanol dissipation.

This phenomenon is mainly a matter at unusual current densities wherever a significant volume of carbon dioxide is produced. Two procedures are measured to handle of this obstacle. It is required to developed and applied concurrently. Firstly, the designs of the supplies carriers can be adjusted to support a rapid elimination of CO<sub>2</sub>. Secondly, Lu and Wang[145] also investigated the composition of the diffusion film and arrangement of droplets on the tip. According to the results, short and consistently expanded holes would form small diameter droplets quite comparison to slugs. It may produce a foamy flow preferably than a laggard flow.

### **2.10 Electrode structure**

The gasoline dissipation film concerning an electrode is typically carbon fabric. Also, carbon paper must be worked but has explained a larger conflict to methanol dissipation [146]. As well CO<sub>2</sub> droplets configuration administration was not being exceptional as including carbon fabric.

### 2.10.1 Catalysts

The catalyst film is formed of catalytic particles used over the dissipation sheet or straight at the membrane. The reaction initiative agent for both working and counter electrode are several.

#### 2.10.1.1 Anode catalyst:

In all the work in this thesis, we synthesised the anode catalyst, so our primary focus is on the anode material. Liu *et al.* [65] reported a review article on anode catalysis during the direct methanol fuel cell and clarified two main obstacles related to new DMFC anode catalysts, that is, the enforcement, covering activity, dependability and endurance, and cost mitigation.

It has established that in rate discovering levels of methanol oxidation an adsorbed hydroxyl group is essential [111]. That group develops from water separation at the catalyst exterior that takes place just on large electrode potential at Pt. This forms electro-oxidation of methanol complicated toward an absolute Pt catalyst. On the other hand, water removing happens on greatly lowering potential upon ruthenium. This the reason that a bimetallic reaction initiative agent holding Pt and Ru both usually applied on anode electrode. The chemisorption method for methanol is recommend support at Pt positions. Therefore, the levels involved with the hydroxyl groups may totally take place upon near Pt and Ru sites. It should be noted in number through the catalyst formation [146]. The optimized junction region among both catalysts is required. There has been a lot of work done on anode catalyst, reviewed some work as given in below table:

**Table 2.1** The electrocatalytic characteristics of typical anode catalysts including several combinations towards fuel cell applications.

Catalyst Composition	Experimental Conditions	Specific/mass activity	$I_F/I_R$	Ref.
PtNi/C	1 M NaOH and 1 M CH <sub>3</sub> OH	48.5 mA/cm <sup>2</sup>	-	[147]
Pt/C	0.5 M H <sub>2</sub> SO <sub>4</sub> and 1 M CH <sub>3</sub> OH	575 mA/mg	-	[89]
Pt/MC	0.5 M H <sub>2</sub> SO <sub>4</sub> and 0.5 M CH <sub>3</sub> OH	250 mA/mg	-	[148]
PtRu/MC	0.5 M H <sub>2</sub> SO <sub>4</sub> and 1 M CH <sub>3</sub> OH	487.9 mA/mg	3.3	[149]
Pt/graphene	0.5 M H <sub>2</sub> SO <sub>4</sub> and 1 M CH <sub>3</sub> OH	-	0.83	[150]
PtRu/graphene	0.5 M H <sub>2</sub> SO <sub>4</sub> and 1 M CH <sub>3</sub> OH	205.7 mA/mg	4.7	[151]
PtPd/graphene	0.1 M HClO <sub>4</sub> and 1 M CH <sub>3</sub> OH	198 mA/mg	1.61	[152]
Pd/graphene	0.5 M NaOH and 1 M CH <sub>3</sub> OH	61.6 mA/cm <sup>2</sup>	-	[153]
Pd/MnO <sub>2</sub> /CNT	0.5 M NaOH and 1 M CH <sub>3</sub> OH	432.02 mA/mg	18.3	[154]
Pd/MnO <sub>2</sub> /graphene	0.5 M KOH and 1 M CH <sub>3</sub> OH	20.4 mA/cm <sup>2</sup>	4.3	[155]
Pd/MnO <sub>2</sub> /graphene	0.5 M NaOH and 1 M CH <sub>3</sub> OH	838 mA/mg	-	[156]
Pt/TiO <sub>2</sub> /graphene	0.5 M H <sub>2</sub> SO <sub>4</sub> and 1 M CH <sub>3</sub> OH	83.1 mA/cm <sup>2</sup>	-	[157]
Pt/TiO <sub>2</sub> /C	0.5 M H <sub>2</sub> SO <sub>4</sub> and 0.5 M CH <sub>3</sub> OH	102.8 mA/mg	-	[158]
Pd/PPY/graphene	0.5 M NaOH and 1 M CH <sub>3</sub> OH	359.8 mA/mg	7.30	[159]
Pt/PDDA/graphene	1 M H <sub>2</sub> SO <sub>4</sub> and 2 M CH <sub>3</sub> OH	2.53 mA/cm <sup>2</sup>	1.9	[160]
Pt/PDDA/GO	1 M H <sub>2</sub> SO <sub>4</sub> and 2 M CH <sub>3</sub> OH	3.82 mA/cm <sup>2</sup>	3.32	[161]
Pd/C	0.5 M NaOH and 1 M CH <sub>3</sub> OH	0.36 mA/cm <sup>2</sup>	-	[162]
Pd/rGO	0.5 M NaOH and 1 M CH <sub>3</sub> OH	1.6 mA/cm <sup>2</sup>	-	[163]
Pd/PANI	1 M NaOH and 1 M CH <sub>3</sub> OH	0.82 mA/cm <sup>2</sup>	2.1	[164]
Pd(I)/pT3A	0.5 M KOH and 1 M CH <sub>3</sub> OH	5.03 mA/cm <sup>2</sup>	2.48	[165]

### 2.10.1.2 Cathode catalyst:

Absolute platinum approximately utilized being a cathodic catalyst. The catalytic particles applied as on DMFC are each metal black or sustained catalyst upon carbon powders on different fillings [166, 167]. Here, both of them extensively worked. Further, the platinum composites as cathode catalysts have dragged broad recognition as a candidate to obtain high achievement, to improve power density, and to decrease an ingredient price of PEMFCs [168].

### 2.10.2 Catalyst structure

The catalytic film has catalyst powder although including Nafion units [145, 169]. Nafion is attached on the catalyst for assist positive carrier species elimination (Figure 2.3). A little link to the Nafion system required as a successful carrier of protons toward the film. It decreases the electrical shield of the catalytic zone. Though, an extremely elevated Nafion packing would wrap the catalyst atoms and decreases the effective region.

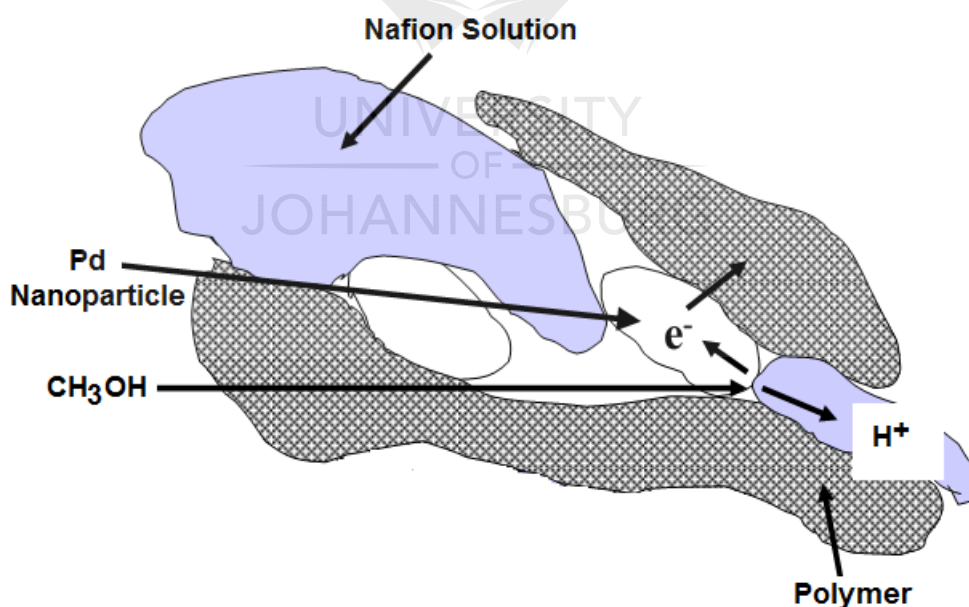


Figure 2.3 Catalyst model.

## 2.11 Catalyst synthesis for fuel cell application

In all papers in this thesis, we synthesized the anode catalyst via *in situ* polymerization and composite formation (IPCF) route. If we compare individually, metal nanoparticle (MN) and conductive polymer (CP) have the excellent properties, but when they combined to each other, the resulting nanocomposite has connection of the both the properties. MNs have a high surface area that consequential aggregation and poor colloidal stability. To overcome this issue, polymers have frequently been used as an outer shell coating of the metal nanoparticles and provide a steric barrier for aggregation. Unique synthetic approaches can play a significant role to locate the MNs over the polymer web to avoid collection of them. In this way, the polymer also collaborates with the catalytic properties of the MNs and enhances the catalytic activity. In this respect, lots of physical and chemical approaches accounted to synthesize the metal-polymer composites. Out of them, the IPCF technique [170] is more promising and performed an important role during the synthesis of metal nanoparticle-polymer composite with increased catalytic response. Composite synthesized by IPCF approach, the metal nanoparticles-polymer is formed together and come to in an intimate contact with each other. In this method, metal salt act as an oxidizing agent that initiates the oxidative polymerization of monomer while beside it, the direct reduction of metal salt generated the metal nanoparticles. There lots of work have been done to describing the IPCF method and also support the reduction of different dye as well as the synthesis of metal nanoparticle-polymer composite [171, 172]. It found that the synthesized metal nanoparticle encapsulated polymer by IPCF methods shows the excellent electro-oxidation of methanol [165].

## 2.12 Sub-conclusion

The literature review in this chapter has focused mainly on fuel cell applications. This is due to the patent operational advantages the system can deliver regarding new anode catalysts, specifically, the performance, including activity, consistency, stability and cost reduction. The progress in the field of fuel cell catalyst has attracted widespread consideration to exploring substitute energy sources. The rapid development of nanotechnology creates highly stable and dynamic supported catalysts. This thesis aims to address the highlighted research gaps through experimental study.



### 2.13 References

1. Mond, L., C. Langer, and F. Quincke, L.-Action of carbon monoxide on nickel. *Journal of the Chemical Society, Transactions*, 1890. 57(0): p. 749-753.
2. Austin, L.G., *Fuel Cells: A Review of Government-Sponsored Research 1950-1964*. NASA SP-120. 1967: p. 439.
3. <http://www.sae.org/fuelcells/fuelcells-history.htm> [Accessed on 11-10-2016].
4. Li, Y., L. Tang, and J. Li, Preparation and electrochemical performance for methanol oxidation of pt/graphene nanocomposites. *Electrochemistry Communications*, 2009. 11(4): p. 846-849.
5. Jiang, L., et al., Structure and chemical composition of supported Pt–Sn electrocatalysts for ethanol oxidation. *Electrochimica Acta*, 2005. 50(27): p. 5384-5389.
6. Bao, X., et al., Ni/nitrogen-doped graphene nanotubes acted as a valuable tailor for remarkably enhanced hydrogen evolution performance of platinum-based catalysts. *Journal of Materials Chemistry A*, 2017.
7. Rao, C.R.K. and D.C. Trivedi, Chemical and electrochemical depositions of platinum group metals and their applications. *Coordination chemistry reviews*, 2005. 249(5–6): p. 613-631.
8. Yang, H., *Platinum-Based Electrocatalysts with Core–Shell Nanostructures*. *Angewandte Chemie International Edition*, 2011. 50(12): p. 2674-2676.
9. Carrette, L., K.A. Friedrich, and U. Stimming, *Fuel Cells – Fundamentals and Applications*. *Fuel Cells*, 2001. 1(1): p. 5-39.
10. Cui, Y., et al., Synthesis of bulk and nanoporous carbon nitride polymers from ammonium thiocyanate for photocatalytic hydrogen evolution. *Journal of Materials Chemistry*, 2011. 21(34): p. 13032-13039.

11. Li, X., et al., Carbon nanotubes/tin oxide nanocomposite-supported Pt catalysts for methanol electro-oxidation. *Journal of Colloid and Interface Science*, 2015. 450: p. 74-81.
12. Datta, S.S.M.a.J., Characterization of Pt-Pd/C Electrocatalyst for Methanol Oxidation in Alkaline Medium. *International Journal of Electrochemistry*, 2011. 2011: p. 16.
13. Lamy, C., E.M. Belgsir, and J.M. Léger, Electrocatalytic oxidation of aliphatic alcohols: Application to the direct alcohol fuel cell (DAFC). *Journal of Applied Electrochemistry*, 2001. 31(7): p. 799-809.
14. Hu, C. and X. Wang, Highly dispersed palladium nanoparticles on commercial carbon black with significantly high electro-catalytic activity for methanol and ethanol oxidation. *International Journal of Hydrogen Energy*, 2015. 40(36): p. 12382-12391.
15. Sundmacher, K., et al., Dynamics of the direct methanol fuel cell (DMFC): experiments and model-based analysis. *Chemical Engineering Science*, 2001. 56(2): p. 333-341.
16. Chalk, S.G. and J.F. Miller, Key challenges and recent progress in batteries, fuel cells, and hydrogen storage for clean energy systems. *Journal of Power Sources*, 2006. 159(1): p. 73-80.
17. Kamarudin, S.K., F. Achmad, and W.R.W. Daud, Overview on the application of direct methanol fuel cell (DMFC) for portable electronic devices. *International Journal of Hydrogen Energy*, 2009. 34(16): p. 6902-6916.
18. Peighambardoust, S.J., S. Rowshanzamir, and M. Amjadi, Review of the proton exchange membranes for fuel cell applications. *International Journal of Hydrogen Energy*, 2010. 35(17): p. 9349-9384.



19. Vishnyakov, V.M., Proton exchange membrane fuel cells. *Vacuum*, 2006. 80(10): p. 1053-1065.
20. Mahato, N., et al., Progress in material selection for solid oxide fuel cell technology: A review. *Progress in Materials Science*, 2015. 72: p. 141-337.
21. Stambouli, A.B. and E. Traversa, Solid oxide fuel cells (SOFCs): a review of an environmentally clean and efficient source of energy. *Renewable and Sustainable Energy Reviews*, 2002. 6(5): p. 433-455.
22. Ormerod, R.M., Solid oxide fuel cells. *Chemical Society Reviews*, 2003. 32(1): p. 17-28.
23. Lee, J.Y., et al., Alkaline fuel cell. 1997, Google Patents.
24. Fuller, M.L.P.a.T.F., A Historical Perspective of Fuel Cell Technology in the 20th Century *Journal of The Electrochemical Society*, 2002. 149(7): p. S59-S67.
25. Bidault, F., et al., Review of gas diffusion cathodes for alkaline fuel cells. *Journal of Power Sources*, 2009. 187(1): p. 39-48.
26. Spinelli, M., et al., Application of Molten Carbonate Fuel Cells in Cement Plants for CO<sub>2</sub> Capture and Clean Power Generation. *Energy Procedia*, 2014. 63: p. 6517-6526.
27. Dicks, A.L., Molten carbonate fuel cells. *Current Opinion in Solid State and Materials Science*, 2004. 8(5): p. 379-383.
28. Sammes, N., R. Bove, and K. Stahl, Phosphoric acid fuel cells: Fundamentals and applications. *Current Opinion in Solid State and Materials Science*, 2004. 8(5): p. 372-378.
29. Bagotsky, V.S., Phosphoric Acid Fuel Cells, in *Fuel Cells*. 2012, John Wiley & Sons, Inc. p. 99-106.

30. Hogarth, M.P. and G.A. Hards, Direct Methanol Fuel Cells. *Platinum Metals Review*, 1996. 40(4): p. 150-159.
31. Hong, W., J. Wang, and E. Wang, Facile Synthesis of Highly Active PdAu Nanowire Networks as Self-Supported Electrocatalyst for Ethanol Electrooxidation. *ACS Applied Materials & Interfaces*, 2014. 6(12): p. 9481-9487.
32. Cameron, D.S., et al., Direct Methanol Fuel Cells. *Platinum Metals Review*, 1987. 31(4): p. 173-181.
33. Kamarudin, M.Z.F., et al., Review: Direct ethanol fuel cells. *International Journal of Hydrogen Energy*, 2013. 38(22): p. 9438-9453.
34. Li, Y.S., T.S. Zhao, and Z.X. Liang, Performance of alkaline electrolyte-membrane-based direct ethanol fuel cells. *Journal of Power Sources*, 2009. 187(2): p. 387-392.
35. Lin, A.S., A.D. Kowalak, and W.E. O'Grady, Studies of the role of water in the electrocatalysis of methanol oxidation. *Journal of Power Sources*, 1996. 58(1): p. 67-72.
36. Gootzen, J.F.E., et al., Adsorption of C3 Alcohols, 1-Butanol, and Ethene on Platinized Platinum As Studied with FTIRS and DEMS. *Langmuir*, 1997. 13(6): p. 1659-1667.
37. Nan-Hai, L. and S. Shi-Gang, In situ FTIR spectroscopic studies of the electrooxidation of C4 alcohol on a platinum electrode in acid solutions Part I. Reaction mechanism of 1-butanol oxidation. *Journal of Electroanalytical Chemistry*, 1997. 436(1-2): p. 65-72.
38. Patra, S. and N. Munichandraiah, Electrooxidation of Methanol on Pt-Modified Conductive Polymer PEDOT. *Langmuir*, 2008. 25(3): p. 1732-1738.

39. Wu, G., Y.-S. Chen, and B.-Q. Xu, Remarkable support effect of SWNTs in Pt catalyst for methanol electrooxidation. *Electrochemistry Communications*, 2005. 7(12): p. 1237-1243.
40. Lee, J.S., et al., Performance and impedance under various catalyst layer thicknesses in DMFC. *Electrochimica Acta*, 2004. 50(2-3): p. 807-810.
41. Uchida, M., et al., Influences of Both Carbon Supports and Heat-Treatment of Supported Catalyst on Electrochemical Oxidation of Methanol. *Journal of The Electrochemical Society*, 1995. 142(8): p. 2572-2576.
42. Solla-Gullon, J., et al., Shape-dependent electrocatalysis: methanol and formic acid electrooxidation on preferentially oriented Pt nanoparticles. *Physical Chemistry Chemical Physics*, 2008. 10(25): p. 3689-3698.
43. Antolini, E., Palladium in fuel cell catalysis. *Energy & Environmental Science*, 2009. 2(9): p. 915-931.
44. Götz, M. and H. Wendt, Binary and ternary anode catalyst formulations including the elements W, Sn and Mo for PEMFCs operated on methanol or reformat gas. *Electrochimica Acta*, 1998. 43(24): p. 3637-3644.
45. Zhou, W., et al., Pt based anode catalysts for direct ethanol fuel cells. *Applied Catalysis B: Environmental*, 2003. 46(2): p. 273-285.
46. Mukerjee, S., et al., Role of Structural and Electronic Properties of Pt and Pt Alloys on Electrocatalysis of Oxygen Reduction: An In Situ XANES and EXAFS Investigation. *Journal of The Electrochemical Society*, 1995. 142(5): p. 1409-1422.
47. Antolini, E., Formation of carbon-supported PtM alloys for low temperature fuel cells: a review. *Materials Chemistry and Physics*, 2003. 78(3): p. 563-573.

48. Ferrin, P. and M. Mavrikakis, Structure Sensitivity of Methanol Electrooxidation on Transition Metals. *Journal of the American Chemical Society*, 2009. 131(40): p. 14381-14389.
49. Guo, S., S. Dong, and E. Wang, Three-Dimensional Pt-on-Pd Bimetallic Nanodendrites Supported on Graphene Nanosheet: Facile Synthesis and Used as an Advanced Nanoelectrocatalyst for Methanol Oxidation. *ACS Nano*, 2009. 4(1): p. 547-555.
50. Wang, C., et al., Synthesis of Monodisperse Pt Nanocubes and Their Enhanced Catalysis for Oxygen Reduction. *Journal of the American Chemical Society*, 2007. 129(22): p. 6974-6975.
51. Wang, C., et al., A General Approach to the Size- and Shape-Controlled Synthesis of Platinum Nanoparticles and Their Catalytic Reduction of Oxygen. *Angewandte Chemie International Edition*, 2008. 47(19): p. 3588-3591.
52. Chen, Z., et al., Supportless Pt and PtPd Nanotubes as Electrocatalysts for Oxygen-Reduction Reactions. *Angewandte Chemie International Edition*, 2007. 46(22): p. 4060-4063.
53. Chen, J., et al., Single-Crystal Nanowires of Platinum Can Be Synthesized by Controlling the Reaction Rate of a Polyol Process. *Journal of the American Chemical Society*, 2004. 126(35): p. 10854-10855.
54. Tian N, Z.Z., Sun SG, Ding Y, Wang ZL, Synthesis of tetrahedral platinum nanocrystals with high-index facets and high electro-oxidation activity. *Science*, 2007. 316: p. 4.
55. Yamauchi, Y., et al., Mesoporous Platinum with Giant Mesocages Templated from Lyotropic Liquid Crystals Consisting of Diblock Copolymers. *Angewandte Chemie International Edition*, 2008. 47(29): p. 5371-5373.

56. Yamauchi, Y., et al., Pt Fibers with Stacked Donut-Like Mesospace by Assembling Pt Nanoparticles: Guided Deposition in Physically Confined Self-Assembly of Surfactants. *Journal of the American Chemical Society*, 2008. 130(16): p. 5426-5427.
57. Mahmoud, et al., A New Catalytically Active Colloidal Platinum Nanocatalyst: The Multiarmed Nanostar Single Crystal. *Journal of the American Chemical Society*, 2008. 130(14): p. 4590-4591.
58. Kowal, A., et al., Synthesis, characterization and electrocatalytic activity for ethanol oxidation of carbon supported Pt, Pt–Rh, Pt–SnO<sub>2</sub> and Pt–Rh–SnO<sub>2</sub> nanoclusters. *Electrochemistry Communications*, 2009. 11(4): p. 724-727.
59. Wang, H., Z. Jusys, and R.J. Behm, Ethanol Electrooxidation on a Carbon-Supported Pt Catalyst: Reaction Kinetics and Product Yields. *The Journal of Physical Chemistry B*, 2004. 108(50): p. 19413-19424.
60. Camara, G.A. and T. Iwasita, Parallel pathways of ethanol oxidation: The effect of ethanol concentration. *Journal of Electroanalytical Chemistry*, 2005. 578(2): p. 315-321.
61. Guo, S., et al., Platinum Nanoparticle Ensemble-on-Graphene Hybrid Nanosheet: One-Pot, Rapid Synthesis, and Used as New Electrode Material for Electrochemical Sensing. *ACS Nano*, 2010. 4(7): p. 3959-3968.
62. Umeda, M., et al., Methanol oxidation enhanced by the presence of O<sub>2</sub> at novel Pt-C co-sputtered electrode. *Physical Chemistry Chemical Physics*, 2010. 12(26): p. 7041-7049.
63. Moore, J.T., et al., Synthesis and Characterization of a Pt<sub>3</sub>Ru<sub>1</sub>/Vulcan Carbon Powder Nanocomposite and Reactivity as a Methanol Electrooxidation Catalyst. *Chemistry of Materials*, 2003. 15(17): p. 3320-3325.

64. Xue, X., et al., Synthesis and Characterization of Pt/C Nanocatalysts Using Room Temperature Ionic Liquids for Fuel Cell Applications. *Fuel Cells*, 2006. 6(5): p. 347-355.
65. Liu, H., et al., A review of anode catalysis in the direct methanol fuel cell. *Journal of Power Sources*, 2006. 155(2): p. 95-110.
66. Antolini, E., J.R.C. Salgado, and E.R. Gonzalez, The methanol oxidation reaction on platinum alloys with the first row transition metals: The case of Pt–Co and –Ni alloy electrocatalysts for DMFCs: A short review. *Applied Catalysis B: Environmental*, 2006. 63(1–2): p. 137-149.
67. Rao, V., et al., The influence of carbon support porosity on the activity of PtRu/Sibunit anode catalysts for methanol oxidation. *Journal of Power Sources*, 2005. 145(2): p. 178-187.
68. Mu, Y., et al., Controllable Pt Nanoparticle Deposition on Carbon Nanotubes as an Anode Catalyst for Direct Methanol Fuel Cells. *The Journal of Physical Chemistry B*, 2005. 109(47): p. 22212-22216.
69. Han, K., J. Lee, and H. Kim, Preparation and characterization of high metal content Pt–Ru alloy catalysts on various carbon blacks for DMFCs. *Electrochimica Acta*, 2006. 52(4): p. 1697-1702.
70. Van Doorslaer, C., et al., Spontaneous product segregation from reactions in ionic liquids: application in Pd-catalyzed aliphatic alcohol oxidation. *Physical Chemistry Chemical Physics*, 2010. 12(8): p. 1741-1749.
71. Plechkova, N.V. and K.R. Seddon, Applications of ionic liquids in the chemical industry. *Chemical Society Reviews*, 2008. 37(1): p. 123-150.
72. Welton, T., Ionic liquids in catalysis. *Coordination chemistry reviews*, 2004. 248(21–24): p. 2459-2477.

73. Seddon, K.R. and A. Stark, Selective catalytic oxidation of benzyl alcohol and alkylbenzenes in ionic liquids. *Green Chemistry*, 2002. 4(2): p. 119-123.
74. Souza, R.F.d., J. Dupont, and J.E.d.L. Dullius, Aerobic, catalytic oxidation of alcohols in ionic liquids. *Journal of the Brazilian Chemical Society*, 2006. 17: p. 48-52.
75. Rong, M., et al., Catalytic oxidation of alcohols by a double functional ionic liquid [bmim]BF<sub>4</sub>. *Catalysis Communications*, 2009. 10(4): p. 362-364.
76. Chhikara, B.S., R. Chandra, and V. Tandon, Oxidation of alcohols with hydrogen peroxide catalyzed by a new imidazolium ion based phosphotungstate complex in ionic liquid. *Journal of Catalysis*, 2005. 230(2): p. 436-439.
77. Qian, W., et al., Clean and Highly Selective Oxidation of Alcohols in an Ionic Liquid by Using an Ion-Supported Hypervalent Iodine(III) Reagent. *Angewandte Chemie International Edition*, 2005. 44(6): p. 952-955.
78. Xie, H., S. Zhang, and H. Duan, An ionic liquid based on a cyclic guanidinium cation is an efficient medium for the selective oxidation of benzyl alcohols. *Tetrahedron Letters*, 2004. 45(9): p. 2013-2015.
79. Maiyalagan, T., T.O. Alaje, and K. Scott, Highly Stable Pt–Ru Nanoparticles Supported on Three-Dimensional Cubic Ordered Mesoporous Carbon (Pt–Ru/CMK-8) as Promising Electrocatalysts for Methanol Oxidation. *The Journal of Physical Chemistry C*, 2011. 116(3): p. 2630-2638.
80. Singh, R.N. and R. Awasthi, Graphene support for enhanced electrocatalytic activity of Pd for alcohol oxidation. *Catalysis Science & Technology*, 2011. 1(5): p. 778-783.

81. Yin, M., et al., Inhibiting CO formation by adjusting surface composition in PtAu alloys for methanol electrooxidation. *Chemical Communications*, 2011. 47(28): p. 8172-8174.
82. Gao, L., et al., Novel Strategy for Preparation of Graphene-Pd, Pt Composite, and Its Enhanced Electrocatalytic Activity for Alcohol Oxidation. *Langmuir*, 2012. 29(3): p. 957-964.
83. Wen, Z., J. Liu, and J. Li, Core/Shell Pt/C Nanoparticles Embedded in Mesoporous Carbon as a Methanol-Tolerant Cathode Catalyst in Direct Methanol Fuel Cells. *Advanced Materials*, 2008. 20(4): p. 743-747.
84. Zhang, X., et al., Porous platinum nanowire arrays for direct ethanol fuel cell applications. *Chemical Communications*, 2009(2): p. 195-197.
85. Yamauchi, Y., et al., Electrochemical Synthesis of Mesoporous Pt–Au Binary Alloys with Tunable Compositions for Enhancement of Electrochemical Performance. *Journal of the American Chemical Society*, 2012. 134(11): p. 5100-5109.
86. Xu, C.W., et al., Highly Ordered Pd Nanowire Arrays as Effective Electrocatalysts for Ethanol Oxidation in Direct Alcohol Fuel Cells. *Advanced Materials*, 2007. 19(23): p. 4256-4259.
87. Ksar, F., et al., Bimetallic Palladium–Gold Nanostructures: Application in Ethanol Oxidation. *Chemistry of Materials*, 2009. 21(15): p. 3677-3683.
88. Li, Z.Y., et al., Electrooxidation of Methanol and Ethylene Glycol Mixture on Platinum and Palladium in Alkaline Medium. *Fuel Cells*, 2012. 12(4): p. 677-682.
89. Yuan, D., et al., Pt supported on highly graphitized lace-like carbon for methanol electrooxidation. *Carbon*, 2008. 46(3): p. 531-536.



90. Wang, L., et al., Mass Production of Graphene via an in Situ Self-Generating Template Route and Its Promoted Activity as Electrocatalytic Support for Methanol Electrooxidation. *The Journal of Physical Chemistry C*, 2010. 114(19): p. 8727-8733.
91. Zhiani, M., et al., Comparative study between platinum supported on carbon and non-noble metal cathode catalyst in alkaline direct ethanol fuel cell (ADEFC). *International Journal of Hydrogen Energy*, 2011. 36(8): p. 5110-5116.
92. Spendelow, J.S., et al., Methanol Dehydrogenation and Oxidation on Pt(111) in Alkaline Solutions. *Langmuir*, 2006. 22(25): p. 10457-10464.
93. Switzer, E.E., et al., Templated Pt–Sn electrocatalysts for ethanol, methanol and CO oxidation in alkaline media. *Electrochimica Acta*, 2009. 54(3): p. 989-995.
94. Xu, C., et al., Oxide (CeO<sub>2</sub>, NiO, Co<sub>3</sub>O<sub>4</sub> and Mn<sub>3</sub>O<sub>4</sub>)-promoted Pd/C electrocatalysts for alcohol electrooxidation in alkaline media. *Electrochimica Acta*, 2008. 53(5): p. 2610-2618.
95. Liu, H.-X., et al., Tetrahedral Pt Nanocrystal Catalysts Decorated with Ru Adatoms and Their Enhanced Activity in Methanol Electrooxidation. *ACS Catalysis*, 2012. 2(5): p. 708-715.
96. Meher, S.K. and G.R. Rao, Polymer-Assisted Hydrothermal Synthesis of Highly Reducible Shuttle-Shaped CeO<sub>2</sub>: Microstructural Effect on Promoting Pt/C for Methanol Electrooxidation. *ACS Catalysis*, 2012. 2(12): p. 2795-2809.
97. Li, L., et al., Facile Fabrication of Pt Nanoparticles on 1-Pyrenamine Functionalized Graphene Nanosheets for Methanol Electrooxidation. *ACS Sustainable Chemistry & Engineering*, 2013. 1(5): p. 527-533.

98. Zheng, X., et al., High-throughput, direct exfoliation of graphite to graphene via a cooperation of supercritical CO<sub>2</sub> and pyrene-polymers. *RSC Advances*, 2012. 2(28): p. 10632-10638.
99. Li, L., et al., Solvent-Exfoliated and Functionalized Graphene with Assistance of Supercritical Carbon Dioxide. *ACS Sustainable Chemistry & Engineering*, 2013. 1(1): p. 144-151.
100. Yang, M., R. Guarecuco, and F.J. DiSalvo, Mesoporous Chromium Nitride as High Performance Catalyst Support for Methanol Electrooxidation. *Chemistry of Materials*, 2013. 25(9): p. 1783-1787.
101. Zhong, H., et al., A novel non-noble electrocatalyst for oxygen reduction in proton exchange membrane fuel cells. *Journal of Power Sources*, 2007. 164(2): p. 572-577.
102. Wang, Y.-J., D.P. Wilkinson, and J. Zhang, Noncarbon Support Materials for Polymer Electrolyte Membrane Fuel Cell Electrocatalysts. *Chemical Reviews*, 2011. 111(12): p. 7625-7651.
103. Avasarala, B. and P. Haldar, On the stability of TiN-based electrocatalysts for fuel cell applications. *International Journal of Hydrogen Energy*, 2011. 36(6): p. 3965-3974.
104. Avasarala, B., et al., Titanium nitride nanoparticles based electrocatalysts for proton exchange membrane fuel cells. *Journal of Materials Chemistry*, 2009. 19(13): p. 1803-1805.
105. Nam, N.D., et al., Corrosion protection of CrN/TiN multi-coating for bipolar plate of polymer electrolyte membrane fuel cell. *Thin Solid Films*, 2011. 519(20): p. 6787-6791.

106. Paulauskas, I.E., et al., Corrosion behavior of CrN, Cr<sub>2</sub>N and  $\pi$  phase surfaces on nitrated Ni–50Cr for proton exchange membrane fuel cell bipolar plates. *Corrosion Science*, 2006. 48(10): p. 3157-3171.
107. Park, Y.-C., et al., Corrosion properties and cell performance of CrN/Cr-coated stainless steel 316L as a metal bipolar plate for a direct methanol fuel cell. *Electrochimica Acta*, 2011. 56(22): p. 7602-7609.
108. Dur, E., Ö.N. Cora, and M. Koç, Experimental investigations on the corrosion resistance characteristics of coated metallic bipolar plates for PEMFC. *International Journal of Hydrogen Energy*, 2011. 36(12): p. 7162-7173.
109. Habibi, E., et al., Comparative electrooxidation of C1–C4 alcohols on Pd|CC nanoparticle anode catalyst in alkaline medium. *International Journal of Hydrogen Energy*, 2014. 39(32): p. 18416-18423.
110. Huang, H. and X. Wang, Recent progress on carbon-based support materials for electrocatalysts of direct methanol fuel cells. *Journal of Materials Chemistry A*, 2014. 2(18): p. 6266-6291.
111. Arico, A., S. Srinivasan, and V. Antonucci, DMFCs: From Fundamental Aspects to Technology Development. *Fuel Cells*, 2001. 1(2): p. 133-161.
112. Aricò, A.S., et al., Optimization of operating parameters of a direct methanol fuel cell and physico-chemical investigation of catalyst–electrolyte interface. *Electrochimica Acta*, 1998. 43(24): p. 3719-3729.
113. Chu, D. and R. Jiang, Novel electrocatalysts for direct methanol fuel cells. *Solid State Ionics*, 2002. 148(3–4): p. 591-599.
114. Shen, P.K. and C. Xu, Alcohol oxidation on nanocrystalline oxide Pd/C promoted electrocatalysts. *Electrochemistry Communications*, 2006. 8(1): p. 184-188.

115. Xu, C., P.k. Shen, and Y. Liu, Ethanol electrooxidation on Pt/C and Pd/C catalysts promoted with oxide. *Journal of Power Sources*, 2007. 164(2): p. 527-531.
116. Habibi, E. and H. Razmi, Glycerol electrooxidation on Pd, Pt and Au nanoparticles supported on carbon ceramic electrode in alkaline media. *International Journal of Hydrogen Energy*, 2012. 37(22): p. 16800-16809.
117. Pattabiraman, R., Electrochemical investigations on carbon supported palladium catalysts. *Applied Catalysis A: General*, 1997. 153(1): p. 9-20.
118. Hu, F., et al., Pd electrocatalyst supported on carbonized TiO<sub>2</sub> nanotube for ethanol oxidation. *Journal of Power Sources*, 2006. 163(1): p. 415-419.
119. Jouanneau, A. and M.C. Petit, Etude du degagement d'oxygene sur une electrode de nickel. *Electrochimica Acta*, 1970. 15(8): p. 1325-1335.
120. Yeung, K.L.K. and A.C.C. Tseung, The Reduction of Oxygen on Teflon-Bonded Perovskite Oxide Electrodes. *Journal of The Electrochemical Society*, 1978. 125(6): p. 878-882.
121. Chu, S. and A. Majumdar, Opportunities and challenges for a sustainable energy future. *Nature*, 2012. 488(7411): p. 294-303.
122. Sahoo, N.G., et al., Graphene-Based Materials for Energy Conversion. *Advanced Materials*, 2012. 24(30): p. 4203-4210.
123. Reddy, A.L.M., et al., Hybrid Nanostructures for Energy Storage Applications. *Advanced Materials*, 2012. 24(37): p. 5045-5064.
124. Wang, H. and H. Dai, Strongly coupled inorganic-nano-carbon hybrid materials for energy storage. *Chemical Society Reviews*, 2013. 42(7): p. 3088-3113.
125. Steele, B.C.H. and A. Heinzl, Materials for fuel-cell technologies. *Nature*, 2001. 414(6861): p. 345-352.

126. Winter, M. and R.J. Brodd, What Are Batteries, Fuel Cells, and Supercapacitors? *Chemical Reviews*, 2004. 104(10): p. 4245-4270.
127. Guo, Y.-G., J.-S. Hu, and L.-J. Wan, Nanostructured Materials for Electrochemical Energy Conversion and Storage Devices. *Advanced Materials*, 2008. 20(15): p. 2878-2887.
128. Choi, N.-S., et al., Challenges Facing Lithium Batteries and Electrical Double-Layer Capacitors. *Angewandte Chemie International Edition*, 2012. 51(40): p. 9994-10024.
129. Paik, Y., S.-S. Kim, and O.H. Han, Methanol Behavior in Direct Methanol Fuel Cells. *Angewandte Chemie International Edition*, 2008. 47(1): p. 94-96.
130. Dillon, R., et al., International activities in DMFC R&D: status of technologies and potential applications. *Journal of Power Sources*, 2004. 127(1-2): p. 112-126.
131. Elliott, A.M.S.a.R.N., Stationary Fuel Cells: Future Promise, Current Hype. 2004.
132. Zhang, J., K.M. Colbow, and D.P. Wilkinson, Ionomer impregnation of electrode substrates for improved fuel cell performance. 2001, Google Patents.
133. Qian, W., et al., Architecture for portable direct liquid fuel cells. *Journal of Power Sources*, 2006. 154(1): p. 202-213.
134. Kelley, S.C., G.A. Deluga, and W.H. Smyrl, A Miniature Methanol/Air Polymer Electrolyte Fuel Cell. *Electrochemical and Solid-State Letters*, 2000. 3(9): p. 407-409.
135. Ren, X., et al., Recent advances in direct methanol fuel cells at Los Alamos National Laboratory. *Journal of Power Sources*, 2000. 86(1-2): p. 111-116.
136. Broussely, M. and G. Archdale, Li-ion batteries and portable power source prospects for the next 5-10 years. *Journal of Power Sources*, 2004. 136(2): p. 386-394.

137. Silva, V.S., et al., Proton electrolyte membrane properties and direct methanol fuel cell performance: II. Fuel cell performance and membrane properties effects. *Journal of Power Sources*, 2005. 140(1): p. 41-49.
138. Iwasita, T., Electrocatalysis of methanol oxidation. *Electrochimica Acta*, 2002. 47(22-23): p. 3663-3674.
139. Umeda, M., et al., Porous-microelectrode study on Pt/C catalysts for methanol electrooxidation. *Electrochimica Acta*, 2003. 48(10): p. 1367-1374.
140. SHEN, M., S. ROY, and K. SCOTT, Preparation and characterisation of Pt deposition on ion conducting membrane for direct methanol fuel cell electrodes. *Journal of Applied Electrochemistry*, 2005. 35(11): p. 1103-1109.
141. Burke, L.D. and J.K. Casey, The role of hydrous oxide species on platinum electrocatalysts in the methanol/air fuel cell. *Electrochimica Acta*, 1992. 37(10): p. 1817-1829.
142. Li, W.S., et al., Catalytic oxidation of methanol on molybdate-modified platinum electrode in sulfuric acid solution. *Journal of Power Sources*, 2002. 104(2): p. 281-288.
143. Heinzl, A. and V.M. Barragán, A review of the state-of-the-art of the methanol crossover in direct methanol fuel cells. *Journal of Power Sources*, 1999. 84(1): p. 70-74.
144. Argyropoulos, P., K. Scott, and W.M. Taama, Gas evolution and power performance in direct methanol fuel cells. *Journal of Applied Electrochemistry*, 1999. 29(6): p. 663-671.
145. Lu, G.Q. and C.Y. Wang, Electrochemical and flow characterization of a direct methanol fuel cell. *Journal of Power Sources*, 2004. 134(1): p. 33-40.

146. Lindermeir, A., et al., On the question of MEA preparation for DMFCs. *Journal of Power Sources*, 2004. 129(2): p. 180-187.
147. Jiang, Q., et al., Promoting Effect of Ni in PtNi Bimetallic Electrocatalysts for the Methanol Oxidation Reaction in Alkaline Media: Experimental and Density Functional Theory Studies. *The Journal of Physical Chemistry C*, 2010. 114(46): p. 19714-19722.
148. Su, F., et al., Electrochemical Behavior of Pt Nanoparticles Supported on Meso- and Microporous Carbons for Fuel Cells. *Energy & Fuels*, 2010. 24(7): p. 3727-3732.
149. Maiyalagan, T., T.O. Alaje, and K. Scott, Highly Stable Pt–Ru Nanoparticles Supported on Three-Dimensional Cubic Ordered Mesoporous Carbon (Pt–Ru/CMK-8) as Promising Electrocatalysts for Methanol Oxidation. *The Journal of Physical Chemistry C*, 2012. 116(3): p. 2630-2638.
150. Li, Y., et al., Catalytic performance of Pt nanoparticles on reduced graphene oxide for methanol electro-oxidation. *Carbon*, 2010. 48(4): p. 1124-1130.
151. Zhao, J., et al., Methanol electrocatalytic oxidation on highly dispersed platinum-ruthenium/graphene catalysts prepared in supercritical carbon dioxide-methanol solution. *RSC Advances*, 2012. 2(25): p. 9651-9659.
152. Lu, Y., et al., Nano-PtPd Cubes on Graphene Exhibit Enhanced Activity and Durability in Methanol Electrooxidation after CO Stripping–Cleaning. *The Journal of Physical Chemistry C*, 2013. 117(6): p. 2926-2938.
153. Huang, H. and X. Wang, Pd nanoparticles supported on low-defect graphene sheets: for use as high-performance electrocatalysts for formic acid and methanol oxidation. *Journal of Materials Chemistry*, 2012. 22(42): p. 22533-22541.

154. Zhao, Y., et al., MnO<sub>2</sub> modified multi-walled carbon nanotubes supported Pd nanoparticles for methanol electro-oxidation in alkaline media. *International Journal of Hydrogen Energy*, 2010. 35(19): p. 10522-10526.
155. Liu, R., et al., Preparation of Pd/MnO<sub>2</sub>-reduced graphene oxide nanocomposite for methanol electro-oxidation in alkaline media. *Electrochemistry Communications*, 2013. 26: p. 63-66.
156. Huang, H. and X. Wang, Design and synthesis of Pd-MnO<sub>2</sub> nanolamella-graphene composite as a high-performance multifunctional electrocatalyst towards formic acid and methanol oxidation. *Physical Chemistry Chemical Physics*, 2013. 15(25): p. 10367-10375.
157. Xia, B.Y., et al., Formation of Pt-TiO<sub>2</sub>-rGO 3-phase junctions with significantly enhanced electro-activity for methanol oxidation. *Physical Chemistry Chemical Physics*, 2012. 14(2): p. 473-476.
158. Fan, Y., et al., Pt/TiO<sub>2</sub>-C with hetero interfaces as enhanced catalyst for methanol electrooxidation. *Electrochimica Acta*, 2013. 105: p. 157-161.
159. Zhao, Y., et al., Enhanced electrocatalytic oxidation of methanol on Pd/polypyrrole-graphene in alkaline medium. *Electrochimica Acta*, 2011. 56(5): p. 1967-1972.
160. Qiu, J.-D., et al., Controllable Deposition of Platinum Nanoparticles on Graphene As an Electrocatalyst for Direct Methanol Fuel Cells. *The Journal of Physical Chemistry C*, 2011. 115(31): p. 15639-15645.
161. Park, J.Y. and S. Kim, Preparation and electroactivity of polymer-functionalized graphene oxide-supported platinum nanoparticles catalysts. *International Journal of Hydrogen Energy*, 2013. 38(14): p. 6275-6282.



162. Li, H., et al., Photocatalytic synthesis of highly dispersed Pd nanoparticles on reduced graphene oxide and their application in methanol electro-oxidation. *Catalysis Science & Technology*, 2012. 2(6): p. 1153-1156.
163. Wu, K., et al., Graphene-supported Pd–Pt alloy nanoflowers: In situ growth and their enhanced electrocatalysis towards methanol oxidation. *International Journal of Hydrogen Energy*, 2015. 40(20): p. 6530-6537.
164. Prodromidis, M.I., et al., Preorganized composite material of polyaniline–palladium nanoparticles with high electrocatalytic activity to methanol and ethanol oxidation. *International Journal of Hydrogen Energy*, 2015. 40(21): p. 6745-6753.
165. Siwal, S., et al., Single step synthesis of a polymer supported palladium composite: a potential anode catalyst for the application of methanol oxidation. *RSC Advances*, 2016. 6(53): p. 47212-47219.
166. Yu, P., M. Pemberton, and P. Plasse, PtCo/C cathode catalyst for improved durability in PEMFCs. *Journal of Power Sources*, 2005. 144(1): p. 11-20.
167. Chowdhury, S.R., P. Mukherjee, and S.k. Bhattachrya, Palladium and palladium–copper alloy nano particles as superior catalyst for electrochemical oxidation of methanol for fuel cell applications. *International Journal of Hydrogen Energy*, 2016. 41(38): p. 17072-17083.
168. Thompsett, D., et al., *Handbook of Fuel Cells: Fundamentals, Technology, and Applications*. Vol. 3. 2003, Ney York, : John Wiley & Sons.
169. Radhakrishnan, T. and N. Sandhyarani, Three dimensional assembly of electrocatalytic platinum nanostructures on reduced graphene oxide – An electrochemical approach for high performance catalyst for methanol oxidation. *International Journal of Hydrogen Energy*, 2017. 42(10): p. 7014-7022.

170. Choudhary, M., S. Siwal, and K. Mallick, Single step synthesis of a 'silver-polymer hybrid material' and its catalytic application. *RSC Advances*, 2015. 5(72): p. 58625-58632.
171. Choudhary, M., et al., Polymerization Assisted Reduction Reaction: A Sequential Electron-Proton Transfer Reaction Catalyzed by Gold Nanoparticle. *The Journal of Physical Chemistry C*, 2013. 117(44): p. 23009-23016.
172. Choudhary, M., et al., Polymer stabilized silver nanoparticle: An efficient catalyst for proton-coupled electron transfer reaction and the electrochemical recognition of biomolecule. *Chemical Physics Letters*, 2014. 608(0): p. 145-151.



## CHAPTER 3 EXPERIMENTAL METHODOLOGY

---

### 3.1 Introduction

Platinum group metals (PGM) electro-catalysts are scattered while small particles upon large surface area electron conductive based on an efficient application concerning precious Pt. Consequently, the properties of the metal particles perform a major function in applications of catalysts.

This chapter shows the classification of the catalysis is examined working analytical methods that is comparable to that of their characterizations applied including a complete step by step system to accomplish the aims of this research study. Sample formation and experimental variables implemented within the research are further reported. All the experimental and analytical dealings that were utilized in this study are addressed in this chapter and the entire chapter consist of the following subheading:

- **Materials:** Basic data of all the materials utilized.
- **Research Design:** A comprehensive framework of the complete steady stepladder used to resolve the obstacle of this research.
- **Methodology:** A complete detail on the instrumentation and experimental techniques employed to explain steps concern in the growth in the area of fuel application.

### 3.2 Reagents Materials, and Solvent

As given information of the supplementary chemicals/reagents obtained like analytical grade and accepted without additional refinement. Ultrapure Milli-Q water (of Millipore) including 18.2 M $\Omega$  at 25 °C was utilized to make stock solution.

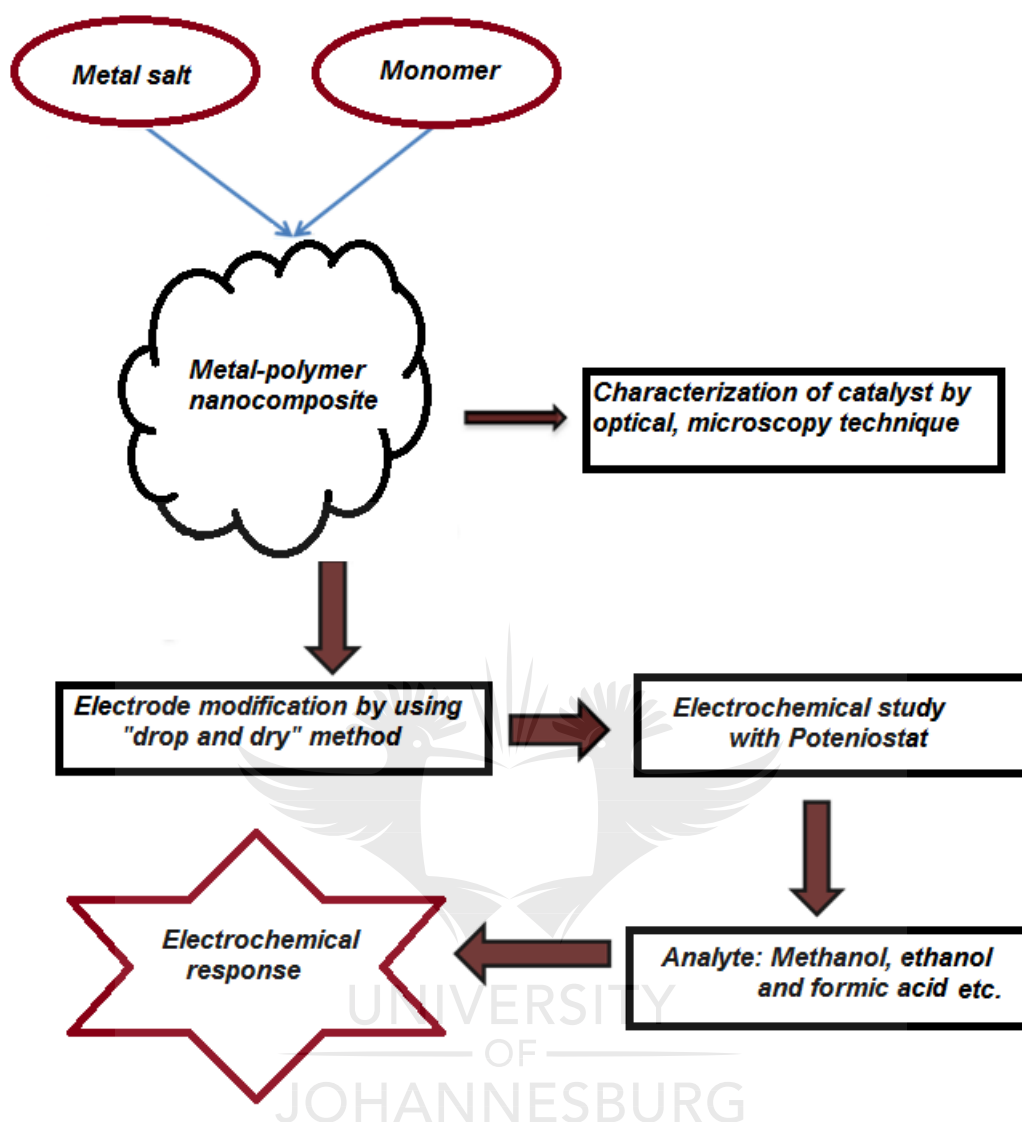
All the materials applied toward the particular outline, are noted inside the tables below;

**Table 3.1** Table and Origin of Materials.

S. No.	Materials	Origin
1.	Palladium tetra chloropalladate	Sigma-aldrich
2.	Methanol	Rochelle chemicals
3.	Pyrene	Sigma-aldrich
4.	Potassium hydroxide	Rochelle chemicals
5.	4-thiophene-3-yl-aniline	Sigma-aldrich
6.	1,8-diaminonaphthalene	Sigma-aldrich
7.	AgNO <sub>3</sub>	Sigma-aldrich
8.	Ammonium persulphate	Sigma-aldrich
9.	Potassium chloride	Rochelle chemicals
10.	Pt auxiliary electrode	BASi
11.	Glassy carbon electrode	BASi
12.	Hg/HgO (1 M NaOH)	BASi
13.	Alumina micro polish powder (1, 0.3 and 0.05 micron)	Buehler
14.	Ultra pure Mili-Q water including 18.2 MΩ at 25 °C	Millipore

### 3.3 Research Plan

The primary focus of the research is toward study some following starts electrochemical sensor progress. Electrochemical analysis were conducted following all fabrication step to ascertain its conformation as awaited results. The required outcomes based upon data where suitable with repetitive steps promote as the forecast of an acceptable result. The following schematic presentation revealing the entire research plan;



**Scheme 3.1** Flow chart of entire research study.

The subsequent steady steps were adopted toward the extension for fuel cell application;

- 1. Electrode and Solution Formation:** Glassy carbon electrode (GCE) was used throughout this work. The cleaning methods were used mechanical polishing for GCE the electrochemical cleaning, aqua regia and piranha solution. The GCE was cleaned by careful polishing with different size alumina slurry (1.0, 0.3 and 0.05  $\mu\text{m}$ ) respectively and sequentially ultrasonicated in distilled water and ethanol for 10 min respectively. In some cases, cathodic cleaning and even rapid etching in piranha solution ( $\text{H}_2\text{SO}_4:\text{H}_2\text{O}_2$ ; 3:1) were used to make sure that the electrode

surface was regenerated. The counter electrode (CE) was usually cleaned by burning it in the flame until it was red-hot followed by rinsing with de-ionized H<sub>2</sub>O, whereas, the reference electrode (RE) (Hg/HgO) was always stored (not in use) in a solution of 1M NaOH.

- 2. Standardization of the electrode:** The following action includes the electrochemical analyses conducted toward make certain the cleanness regarding the electrode and further find its performance during the appearance of blank electrolytes.
- 3. Optical and Electrochemical Analyses:** Potentiometric and optical systems were used to characterize the nanocomposite to obtained relevant data towards the electrode modification for the electro-oxidation of alcohol. The techniques used were; UV (ultra-visible spectroscopy), FTIR (Fourier transform infrared spectroscopy), XRD (X-ray diffraction), SEM (scanning electron microscopy), TEM (transmission electron microscopy), EDX (energy dispersive X-ray spectroscopy), CV (cyclic voltammetry), chronoamperometry and EIS (Electrochemical impedance spectroscopy).
- 4. Preparation of the polymer and polymer-nanocomposite modified stage:** Here the step includes the modification of the bare electrode as the evolution like an electrochemical catalyst for fuel cell application. The electrodes were modified by 'drop and dry' method.
- 5. Electro-oxidation of fuel cell:** This step takes part for the electro-oxidation of analytes (methanol, ethanol and formic acid). The methods adopted here, the steps are cyclic voltammetry (for quantitative) and chronoamperometric (stability).
- 6. Fuel cell Evaluation:** Determination of response to analytes, resistance, responsiveness and oxidation potential.



**Figure 3.1** Structure of a three electrode operation electrochemical cell arrangement. The experimental cell consists a glass vial including a detachable lid having an inlet place as the electrode and gas cleaning. Here, the enough carrying electrolytes (to be contained) were chosen inside a glass vial and the reference electrode (RE), working electrode (WE) and counter electrode (CE) were dipped inside the cell.

The stock solution applied for the study was prepared via applying the generalized **equation 3.1** and **equation 3.2** for dilution.

$$\text{Mass} = \frac{\text{molar mass} \times \text{Molarity} \times \text{Volume}}{1000} \quad \text{Equ. 3.1}$$

$$C_1V_1 = C_2V_2 \quad \text{Eqn. 3.2}$$

Other detail calculations significant will be observed during the experimental outcome regions.

### 3.4 Instrumentation

Scanning electron microscopy (SEM) and energy dispersive X-ray spectroscopy (EDX) were worked to circumscribe the surface morphology about the modified electrodes and presence of metal. EDX linked SEM image captured from a TESCAN (Vega 3 XMU) conducted about 20 kV and were sputter-covered including a small layer of carbon cover.

FTIR analysis conducted applying PerkinElmer Spectrum 100 spectrophotometers. A RigakuUltima IV X-ray diffractometer (XRD) was applied as diffraction analysis. The internal morphology regarding the polymer nanocomposite and nanoparticle held by energy-dispersive X-ray spectroscopy (EDS) linked by transmission electron microscopy (TEM) with working JEM-2100F. A UV-vis 1800 (Shimadzu UV spectrophotometer) was used for the photometric studies. A Biologic SP-300 potentiostat electrochemical Potentiostat/Galvanostat electrochemical workstation was used to perform all the entire electrochemical measurements.

#### **3.4.1 Brunauer-Emmett-Teller (BET) N<sub>2</sub> adsorption method**

Brunauer-Emmett-Teller (BET) study the surface area, pore volume and porosity of supports defined by the BET method working a Micromeritics Accelerated Surface Area and Porosimetry (ASAP) 2010 scheme. The characterization was depended upon the physical adsorption of nitrogen through liquid nitrogen temperature.

##### **3.4.1.1 Sample preparation:**

About 100 mg of the sample was subjected to degassing at 90 °C for 1 hour, followed by 120 °C for 40 minutes and then 150 °C for 1 hour to eliminate moisture, and later at around 260 °C under vacuum to clear the holes of any shreds. After that, the sample weighed under vacuum, subsequent that it was injected into the analysis port and investigated automatically by liquid nitrogen temperature (-196 °C).

#### **3.4.2 Fourier Transform Infrared**

In this study, the chemical structure of washed CNTs and Vulcan were analyzed by FTIR spectroscopy. The analysis was performed using a PerkinElmer Spectrum 100 Spectrophotometer. The analysis of both CNTs samples used was the dried prepared powders, which were put in an oven at 110 °C overnight.



### 3.5 Microscopy Techniques

The microscopy methods applied to crucial parallel methods that assist us to understand the morphological characteristics of a surface with utilizing a beam of electrons toward disclosing an image[1]. In their study, give not just greater magnification but further greater resolution comparison to optical microscopes and enable us to monitor smaller things within relatively much feature. Particularly within the range of metal polymer nanoparticles, electron microscopy techniques are vital toward seeing the differences in the synthesis of nanoparticles. However, before performing in the specification like the exact techniques which is utilized in the articles, that may be suitable to illustrate the principles of electron microscopy concisely.

Here, in the electron microscope is broadly given with the invent of electromagnetic lenses. Alternatively, like the glass lenses in the optical microscope, to monitor the electron beam, the electron microscope applies electromagnetic and electrostatic lenses. It thoroughly observed that if we increased the current the electrons flow quicker, and by this, it gives shorter wavelengths. In electron microscopy, lower wavelengths raise resolution [2].

#### 3.5.1 Transmission Electron Microscopy (TEM)

The TEM runs similar to the origin as optical microscopy, but rather of containing photons TEM holds electrons. TEM applies an electron gun rather of the light bulb and holds magnetic lenses rather of glass lenses [3]. TEM works an electron beam which may be transmitted with the fragile specimen to convey information regarding the composition of the synthesis material. After that, the image is expanded with a group of magnetic lenses till revealing the fluorescent shade or sensible light CCD (charge-coupled device) camera. Later the detected image is displayed within actual time on a monitor or through a computer. TEM is regularly the selected technique and regularly applied in both

commercial and academic toward examining the microstructure and structure of the synthesis material have the thickness smaller than 100 nm; therefore, the electron beam may infiltrate the material during the resolution of 1 Ångstrom (Å) may accomplish below optimum conditions [3].

In all articles within this thesis, TEM has been applied by predefined parameters to show the structure of metal nanoparticles with the polymer.

### **3.5.2 Scanning Electron Microscopy (SEM)**

Under SEM, the electrons are not transmitted within the material, in distinction over the TEM technique. Later the images are generated via detecting secondary electrons that are released from the surface induced with primary electrons. During SEM, the surface is investigated with an electron beam, and the detector takes the image through mapping the detecting signal based upon beam spot. Also, the resolution of SEM is smaller than the TEM; this has the benefit of showing three-dimensional images [4].

In all articles within this thesis, SEM has been utilized to examine the metal nanoparticles and polymer assembling formation to investigate the surface of an electrode material.

## **3.6 Electrochemical Characterization**

The developed fuel cell catalyst was primarily based electrochemical of energy forms. The electrochemical analysis provides us with the data of the redox potential and electrochemical response time about the polymer and polymer-based nanocomposites. Electrochemical studies support the reversible method/coupled, include polarization over potential and therefore represent potential among the forward scan ( $I_F$ ) and reverse scan ( $I_R$ ). The used electrochemical methods to perform this research study were cyclic voltammetry (CV) and chronoamperometric.

### **3.6.1 Electrochemical impedance spectroscopy (EIS)**

Impedance spectroscopy essentially depends upon the theory of electrical immunity. As everybody knows that each circuit component opposes the movement of an electrical

current based upon Ohm's law, that explains the resistance based upon a correlation between voltage and current. Hence, the resistance rate is independent regarding frequency; the current and voltage beacon are in state mutually [5]. Although, while various circuit components have included the method, the concept of resistance is substituted by impedance. Comparable through resistance, impedance further allows us to hold resistance toward the electrical current issue, though electrochemical impedance is estimated with scanning out the current sign via the purpose about a sinusoidal AC potential toward an electrochemical cell.

The electron transferal characteristics about an electrode may be quantified with working electrochemical impedance spectroscopy. Normally, the simple shapes e.g. Randles circuit is arranged to match the impedance yields to determine the charge transfer resistance. Also, under maximum impedance results presented within this thesis, a Nyquist plot is preferred. The Nyquist plot includes semi-circular and linear parts. The plot shows in both electron transfer restricted (semi-circular portion) and diffusion manners (linear part) happening at the corresponding time. The charge carrier resistance ( $R_{CT}$ ) on the electrode surface may be quantified supported on the diameter of the semi-circular portion of the plot. Electrochemical impedance spectroscopy (EIS) is an important method that utilizes an alternating current (AC). This technique is very functional for the characterizing the conductivity and nanostructured surface of nanomaterials. Electrochemical impedance spectroscopy (EIS) is a procedure used to evaluate the electrochemical behaviour of electrode surfaces and/or electrolyte material processes[6]. Electrochemical impedance spectroscopy (EIS) usually used for analyzing electrochemical systems, covering those included in corrosion and electrodeposition. As impedance analyses, a little sinusoidal AC voltage probe is used, and the current response is defined. The AC sign is considered across a broad limit of frequencies to produce an impedance spectrum. EIS spectrum

recorded between two phases: in-phase current response that defines the genuine (resistive) element regarding the impedance, although the out-of-phase current response that decides the imaginary (capacitive) element. In this technique, electron transfer occurs at a high frequency and mass transfer on low frequency. Impedance decisions are generally arranged to equivalent circuits of resistors and capacitors. The Nyquist plot is given in **Fig. 3.2**, that gives a visual insight into the system dynamics.

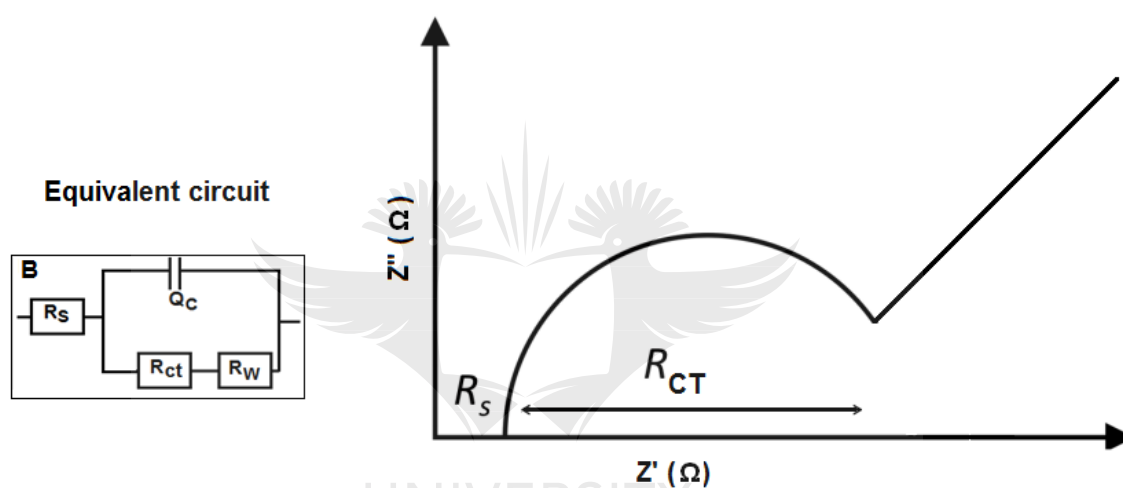


**Figure 3.2** Schematic description of electrochemical cell equivalent circuit (left) and Nyquist plot (right) for impedance spectroscopy.

In **Fig. 3.2**,  $R_{ct}$  is the charge-transfer resistance, that is inversely proportional to the rate of electron transfer;  $R_s$  denotes the solution-phase resistance; and,  $Z_w$  denotes the Warburg impedance, that appears from mass-transfer conditions.  $R_s$  arise originally from the electrolyte resistance and are analytically helpful essentially in sensors. These all component are connected in series with the charge transfer resistance. The Warburg impedance, which may be applied to estimate sufficient diffusion coefficients, is seldom valuable for analytical purposes. In this work, EIS will be used to calculate  $R_{CT}$ ,  $R_s$  and  $C_d$ .

$R_{CT}$  values are influenced by nature of the electrode surface [7], and this gives a better understanding of the electrocatalytic nature of different films.

### 3.6.2 Cyclic voltammetry

There is just one contrast between cyclic voltammetry, and linear sweep voltammetry is that the potential value is investigated at fixed scan rate and is reversed between two voltages states in cyclic voltammetry [8].

Cyclic voltammetry (CV) is a potentiodynamic electrochemical technique that gives both quantitative and qualitative study with quick and reliable characterization tools. CV is very handy electroanalytical techniques as the investigation about electroactive species. This technique is capable of quickly recognizing redox response over a broad potential limit. CV provides knowledge to understanding the kinetics of electron transferal, mechanism and chemical reactions, thermodynamics and for attaining stability of reaction products[9-10].

The cyclic voltammogram (a graph of current versus potential) is accomplished via regulating the current on the working electrode while the potential scan. The scan rate concludes that the reaction rate. Higher the scan rate, faster the scan rate [11-12]. A typical CV plot is shown in **Fig.3.3**.

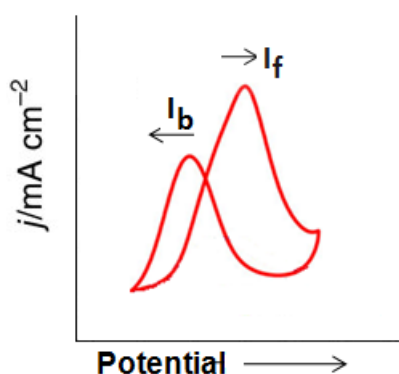


**Figure 3.3** A Typical Cyclic Voltammogram Plot.

A typical voltammograms in **Fig. 3.3** comprises of plotting the current that flows as a function of the potential applied which explain the forward and backwards scan

representing oxidation and reduction reaction respectively. The scan started from the initial potential, moved to its maximum current and then dropped and maintained at a level until it switched back to its initial potential with a reductive scan. In the **Fig. 3.3** the forward scan is the anodic current ( $I_f$ ) describing oxidation of the reductant that occurred from the effect of the loss of an electron. Although, the backwards scan provides the backwards peak that is cathodic current ( $I_b$ ) describing the reduction of the oxidized analyte as effect of an addition of the electron later the potential change.

**Table 3.2** Standard Operating Parameters for CV.

Parameter	Specification
Electrolyte	0.5 M potassium hydroxide to the cell
Methanol	Added 1 M methanol to 0.5 M potassium hydroxide
Working electrode	Catalyst paste (see Working electrode preparation)
Counter electrode	Platinum wire
Reference electrode	Hg/HgO
Scan rate	50 mV/sec
Potential range	Scanning range: -0.8 to 0.2 V

### 3.6.3 Chronoamperometry

Chronoamperometry is an important technique as the quantitative study of a nucleation method. It is helpful technique guides to obtaining the original data of nucleation and growth mechanism during an examined system. Furthermore, the result of the charge for deposition can be concluded. Similarly, here this technique can be used for the measurement regarding a nucleation rate constant and also for adsorption isotherm. By the chronoamperometry, the current versus time being a response to a potential pulse. The

registered current can be analyzed, and its characteristics can be classified from the changes with time.

### 3.6.3.1 Principle of chronoamperometry

From the starting of the transient analysis, the potential of the anode electrode is kept at initial potential ( $E_i$ ) (**Fig. 3.4.a**). Also at  $t=0$  the potential is immediately shifted to a new value  $E_1$ , and similar current time response is registered as shown in **Fig. 3.4.b**.

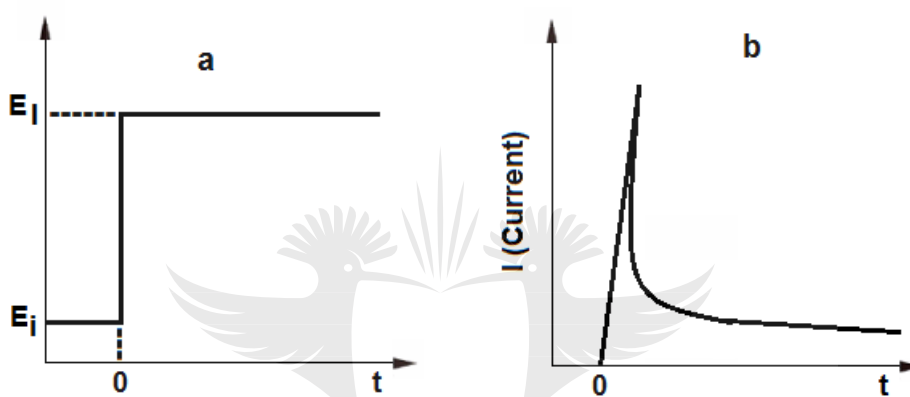


**Figure 3.4** The chronoamperometric analysis. (a) The potential-time profile used through the experiment,  $E_i$  is initial state and  $E_1$  is the potential whether no reduction of O happens or some other potential of concern. (b) The similar response of the current because variations of the potential.

## 3.7 Sub-conclusion

Characterization of synthesized materials is an important step because it proves the identity and also confirms the successful synthesis with a recommendation for their respective applications. The experimental methodology and characterization tools that were used for the material preparation are discussed in detail with their operating principles. Furthermore, the detailed and more focused experimental procedures are discussed in the experimental sections found in following chapters (chapter 4 and chapter 5).

### 3.8 References

1. Kuo, J., *Electron Microscopy: Methods and Protocols*. 2007: Humana Press.
2. Goodhew, P.J.H., J.; Beanland, R., *Electron Microscopy and Analysis*. Third Edition ed. 2000: Taylor & Francis.
3. Williams, D.B. and C.B. Carter, *Transmission Electron Microscopy: A Textbook for Materials Science*. 2009: Springer.
4. Wells, O.C., *Scanning electron microscopy*. 1974: McGraw-Hill.
5. Bard, A.J. and L.R. Faulkner, *Electrochemical Methods: Fundamentals and Applications* 2000: Willey.
6. Barsoukov, E. and J.R. Macdonald, *Impedance Spectroscopy: Theory, Experiment, and Applications*. 2005: John Wiley & Sons Inc. 616.
7. Vayenas, C.G., R.E. White, and M.E. Gamboa-Aldeco, *Modern Aspects of Electrochemistry*. Vol. 42. 2008: Springer.
8. Compton, R.G. and C.E. Banks, *Understanding Voltammetry* 2007: World Scientific.
9. Wang, J., *Analytical Electrochemistry*. 3rd Edition ed. 2006: Wiley. 272.
10. Gosser, D.K., *Cyclic Voltammetry: Simulation and Analysis of Reaction Mechanisms*. 1st Edition ed. 1993: Wiley-VCH. 156.
11. Kissinger, P.T. and W.R. Heineman, *Cyclic voltammetry*. *Journal of Chemical Education*, 1983. **60**(9): p. 702.
12. Monk, P., *Fundamentals of Electroanalytical Chemistry*. 2005, Manchester Metropolitan University, Manchester, UK: John Wiley & Sons, Ltd. 19.



## CHAPTER 4

# SINGLE STEP SYNTHESIS OF POLYMER SUPPORTED PALLADIUM COMPOSITE: A POTENTIAL ANODE CATALYST FOR THE APPLICATION OF METHANOL OXIDATION

---

### 4.1 Introduction

In general, two different classes of materials, such as, inorganic and organic molecule or polymer, has been applied as hosts to stabilize two different kinds of palladium species, ionic palladium and metallic palladium. Due to the unique properties of the polymer, they often used in depositing appropriate palladium species for the various application purposes. The well-known application of palladium as a catalyst is carbon-carbon bond formation reaction which are commonly used for the synthesis of natural products, pharmaceutical products, fine chemicals and the manufacturing of long chain organic molecules for organo-electronics applications [1, 2]. The use of palladium nanoparticles in catalysis is not only industrially important [3] but also scientifically interesting since they provide details of the sensitive relationship between the catalytic activity and the nanoparticle size and shape as well as the nature of the surrounding media [4]. The incorporation of palladium in polymers has attracted attention because the composite architectures provide synergistically useful functionality and mechanical stability. Many investigations have been published regarding the incorporation of the palladium into a polymer matrix for versatile applications [5-10].

Electro-oxidation of small organic molecules, particularly alcohol, has attracted considerable attention for to the development of liquid fuel cells due to high energy densities, low operating temperature and low pollutant emission [11]. Though platinum is the most efficient electro catalysts for methanol fuel cell application but the platinum based catalysts are less tolerant for carbon monoxide poisoning that restrict the catalyst from the

widespread application in fuel cells. Among the various replacement of platinum based catalysts, palladium with different support materials received considerable attention because of their superior activity and greater resistance to carbon monoxide poisoning [12]. Nano-structured palladium catalyst on multi-walled carbon nano tubes, [13] active carbon fibers, [13] carbon microspheres and hollow spheres [14, 15] using PdCl<sub>2</sub> salt as the metal precursor has been reported as the promising anode catalysts for the oxidation of methanol. Among them Pd-carbon nanotube system are considered as the highly active catalyst due to the smaller size and higher dispersion of the metal. In another study, the performance of Pd-multi-walled carbon nanotube was tested for the oxidation of methanol, ethanol and glycerol and the results exhibited high activity of the catalyst for the oxidation reactions of all alcohols [16]. Reduced graphene oxide in combination with Nafion as a support for the nanostructured palladium has been reported as a promising electrocatalyst for ethanol oxidation [17]. Dispersed palladium nanoparticles on the surface of vanadium oxide nanotubes [18] and  $\beta$ -MnO<sub>2</sub> [19] have been exhibited excellent electrocatalytic methanol oxidation reaction under alkaline medium. Palladium nanoparticles decorated graphene was utilized for the efficient electro-oxidation of methanol under strong alkaline condition [20].

Very few examples are available in the literature regarding the polymer based catalyst for the electrooxidation of alcohol. Palladium nanoparticles supported on polypyrrole-functionalized graphene was reported as a very active catalyst for the electro-oxidation of methanol [21]. The poly-(diphenylbutadiene) polymer nanofiber supported metallic palladium showed the catalytic activity for the oxidation of ethanol [22]. Reports are also available for the polyaniline, a conducting polymer, supported Pt-Ru and Pt-Sn binary catalyst for the electrochemical oxidation of methanol and ethanol, where binary system

performed better catalytic activity than the Pt alone [23]. The conducting polymers also serve as an excellent component for the various energy related applications [24-26].

In this current study, we report the formation of a palladium-polymer composite material, Pd(I)-poly [4-(thiophen-3yl)-aniline], Pd-pTA, by using the in-situ polymerization and composite formation (IPCF) approach [27-31] We have chosen 4-(thiophen-3yl)-aniline for this experiment because the molecule has nicely responded for the IPCF type of reaction for the synthesis of Pd-pTA composite. IPCF technique for the synthesis of composite material have potential advantages in the field of ‘synthetic material science’ because the reaction produces both the polymer and the metal component simultaneously and thus facilitates an intimate contact between them through functionalization. The composite material was characterized using various optical and microscopic techniques. Surface characterization techniques have also been employed to extract further information about the composite material. The synthesized material has been used as a catalyst for the electro-oxidation of methanol.

## **4.2 Experimental procedure**

### **4.2.1 Materials:**

All the chemicals and the solvents used for this experiment were of analytical purity and used without further purification. Ultra-pure water (specific resistivity  $>17 \text{ M}\Omega \text{ cm}$ ) was used in this experiment wherever required.

### **4.2.2 Material characterization:**

TEM studies were performed at an acceleration voltage of 197 kV by using a Philips CM200 TEM instrument equipped with a  $\text{LaB}_6$  source. The TEM samples were prepared by depositing small amount of synthesized material onto a TEM grid (200 mesh size Cu-grid) coated with a lacy carbon film. The SEM studies were performed at 5 kV by using an FEI Quanta 400 instrument. As a precaution to prevent possible charging, the samples were sputter-coated with a thin, uniform layer of Au-Pd. The X-ray diffraction (XRD)

patterns were recorded on a Shimadzu XD-3A X-ray diffractometer operating at 20 kV using Cu-K $\alpha$  radiation ( $\lambda = 0.1542$  nm). The measurements were performed over a diffraction angle range of  $2\theta = 10^\circ$  to  $90^\circ$ . X-ray photoelectron spectra (XPS) were collected in a UHV chamber attached to a Physical Electronics 560 ESCA/SAM instrument. Fourier transform infrared spectroscopy (FTIR) spectra were collected utilizing a Shimadzu IRAffinity-1 with a spectral resolution of  $0.5\text{ cm}^{-1}$ . The UV-vis spectra were measured using a Shimadzu UV-1800 spectrophotometer using with a quartz cuvette. To measure the fluorescence property of the material a spectrofluorophotometer (RF-5301PC, Shimadzu), attached with a light source of 150W Xenon lamp, was used for this study. The surface areas were calculated by the Brunauer-Emmett-Teller (BET) method, and the pore size distribution was calculated by applying the Barrett-Joyner-Halenda (BJH) theory. Electrochemical studies was carried out with a, Bio-Logic, SP-200, potentiostat connected to a data controller. A three-electrode system was used in the experiment with a glassy carbon electrode (GCE) as the working electrode. Ag/AgCl electrode (saturated KCl) and a Pt-electrode were used as the reference and counter electrodes, respectively.

#### **4.2.3 Preparation of Pd-pTA composite catalyst:**

In a typical experiment, 0.350 g of 4-(thiophen-3-yl) aniline was dissolved in 10 mL of methanol and a separate stock solution of K<sub>2</sub>PdCl<sub>4</sub> (0.0326 g of K<sub>2</sub>PdCl<sub>4</sub> in 10 mL of water) were prepared. In a small glass beaker, 3.5 mL of K<sub>2</sub>PdCl<sub>4</sub> stock solution was added drop wise to the 10 mL of methanolic solution of the 4-(thiophen-3-yl) aniline under continuous stirring conditions. During the addition, the solution took on a yellow colour, while at the end, a yellowish precipitation, Pd-pTA, was formed at the bottom of the beaker. Entire reaction was performed under ambient condition. The material was allowed to settle for 30 min after which the colloidal solution was taken from the bottom of the beaker and pipetted onto lacey, carbon-coated, copper mesh grids for TEM study and after the TEM

study the same grid was sputter coated with a conducting layer a few nanometres thick of Au-Pd for SEM study. The required amount of material was used for UV-vis, IR and PL spectroscopy studies. The remaining portion of the compound was dried under vacuum at 60<sup>0</sup> C and used for XRD, XPS and BET measurements as well as the studies for the electrochemical oxidation of methanol. For the comparative study, poly [4-(thiophen-3yl)-aniline], pTA, has been synthesized using ammonium persulfate (APS) as an oxidizing agent.

#### **4.2.4 Electrochemical Measurements:**

A GCE was carefully polished with alumina powder and subsequently cleaned with ethanol and deionized water. The synthesized composite material (Pd-pTA) was dropped onto the GCE surface, dried in the air at room temperature and used for electrochemical measurements at room temperature. For the electro-oxidation study of methanol, the cyclic voltammograms were recorded at a scan rate of 50 mV/s in a mixture of KOH (0.5 mol dm<sup>-3</sup>) and methanol (1.0 mol dm<sup>-3</sup>).

### **4.3 Result and discussion:**

#### **4.3.1 Characterization of the compound**

The TEM image (figure 4.1A) indicates a thin film-like morphology with a smooth surface of Pd-pTA, whereas, the low magnification SEM image (figure 4.1B) shows the fiber-like morphology of the synthesized metal-polymer composite material. The XRD pattern of polyaniline and the derivatives of polyaniline generally depend on the length of the polymeric chains and the oxidation states. The pattern also depend on the synthetic routes, solvent and oxidizing agent used for the synthesis. In this current study the XRD spectrum (figure 4.1C) for Pd-pTA shows three major peaks at 17.0, 23.5 and 27.8 which correspond to (011), (020) and (200) crystal planes. The XRD pattern also confirmed the crystalline character of the material and no evidence of the formation of metallic palladium species.

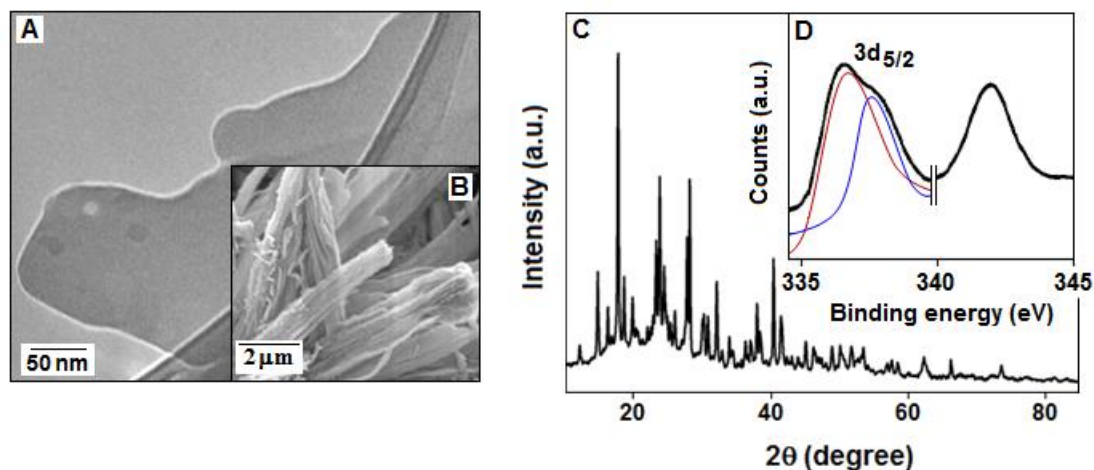


**Figure 4.1** (A) TEM and (B) SEM image of the Pd-pTA composite. (C) The XRD patterns of the Pd-pTA composite and the XPS signal (D) indicates the presence of characteristic ionic palladium species in the sample.

To investigate the oxidation state of palladium in Pd-pTA the XPS technique was employed. The characteristic XPS peaks (figure 4.1D) correspond to curve-fitting for palladium 3d spectra consisting of the Pd 3d<sup>5/2</sup> and Pd 3<sup>3/2</sup> spin-orbital splitting. In this work we have used only the binding energy value of the Pd 3d<sup>5/2</sup> line to determine the oxidation state of palladium. In general, the peak positioned at 335.7 eV indicates the metallic state of palladium whereas the peak at approximately 337.75 eV can be assigned to the Pd (II) state [32]. In the present experiment the synthesized Pd-pT3A shows an asymmetric broad spectrum within the range 335.0-340.0 eV and after deconvolution two separate peaks appeared at 336.75 and 337.55 eV. The peak at 337.55 eV is due to the presence of unreacted Pd (II) whereas the new peak that appeared at 336.75 eV is due to the presence of Pd (I) in the sample [32, 33]. Both the palladium species could coordinate and stabilize with chain nitrogen of the polymer [34]. The optical property of the synthesized composite material (Pd-pTA) and the polymer alone (pTA) were characterized using UV-visible and photoluminescence (PL) spectroscopy methods.

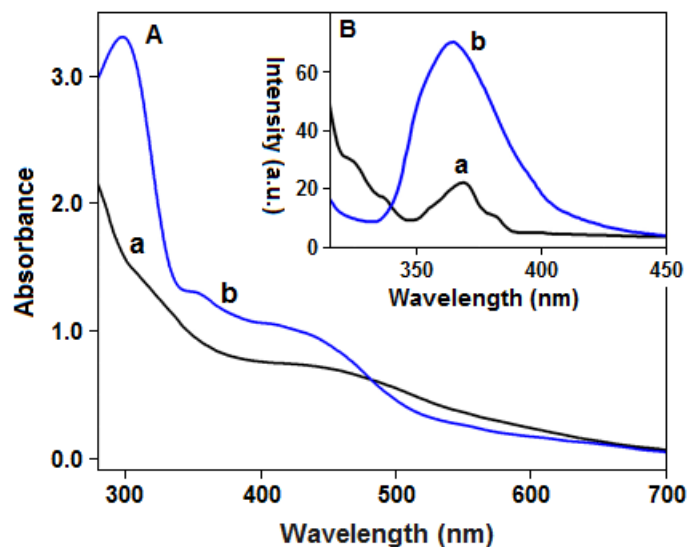


**Figure 4.2** (A) The UV-visible spectra of *pTA* (a) and *Pd-pTA* (b). (B) The photoluminescence spectra for *pTA* (a) and *Pd-pTA* (b).

In the spectrum (a) and (b), figure 4.2A, a broad band within the range of 380-520 nm can be assigned for polaron–bipolaron transition for *pTA* and *Pd-pTA*, respectively. In spectrum (b), a sharp absorption peak at 300 nm is clearly visible which are due to the  $\pi-\pi^*$  transition of the benzenoid rings. Photoluminescence spectra for the pure polymer and *Pd-polymer* were measured in the range of 310-440 nm (figure 4.2B) and the wavelength of excitation for the samples was chosen 300 nm. In the current experiment, the emission peaks for both the samples were observed at about 370 nm and it is also evident from the figure that the intensity of the spectra for *Pd-pTA* is higher than that of the pure polymer. It has been well documented that benzenoid unit present in the polymer backbone demonstrate the fluorescence property [35]. The photoluminescence property of polymer is caused by the benzenoid unit (amine group) and it is quenched when such a group is adjacent to the quinoid unit (imine group) or converted to a quinoid unit [35]. For both samples in the present work the benzenoid groups are predominant as compared with the quinoid units. The presence of both amine group (electron donating group) and ionic species, Pd (I), enhances the electron mobility in the *Pd-pTA* composite, which in turn



favours the formation of singlet excitons. The singlet exciton states decay radiatively to the ground state resulting in enhanced photoluminescence [36]. A broad spectrum appeared for Pd-pTA composite and may be attributed due to the formation of more density of states due to the presence of ionic palladium. For the pure polymer, the fluorescence spectrum shows that emission occurs at 368 nm with a shoulder at 381 nm originate from single chain or intra-chain excitons and inter-chain excitons, respectively [37].

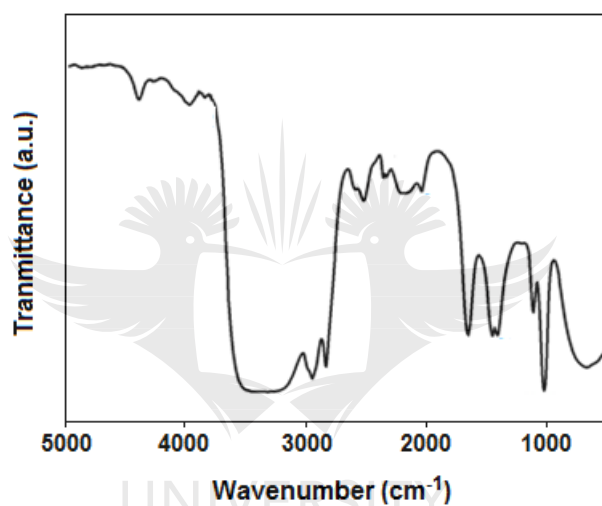


**Figure 4.3** FTIR spectra of Pd-pTA.

The presence of quinoid unit in the Pd-pTA composite has been confirmed from the Fourier transform infrared spectrum (figure 4.3), where the vibrational signature at  $1660\text{ cm}^{-1}$  indicates the presence of  $\text{N}=\text{Q}=\text{N}$  (Q represents a quinoid ring structure). A doublet band with the peak positions at  $1447$  and  $1410\text{ cm}^{-1}$  can be assigned to the  $\nu_3$  mode of thiophene [38]. The  $\nu_3$  mode is a ring vibration that consists primarily of the symmetric stretching of the  $\text{C}=\text{C}$  bonds of thiophene [39]. The vibration bands at  $1108$  and  $1023\text{ cm}^{-1}$  are due to the aromatic  $\text{C}-\text{H}$  in-plane bending modes.

The mechanism of the IPCF type of polymerization process comprises the release of electrons during the reaction between monomer and metal salt (oxidizing agent). In



general, the released electrons reduce the metal ions, such as, gold, silver and palladium, to their respective atomic state, which ultimately forms their corresponding nanoparticles [40-42]. However, in the present experiment we found the reaction between 4-(thiophen-3yl)-aniline and  $K_2PdCl_4$  evidences the formation of Pd(I) and poly[4-(thiophen-3yl)-aniline]. The polymer is an aniline derivatives have several amine as well as imine moieties which can act as a macro ligand, [34] that coordinate with the Pd(I) species. The electron microscopy characterization also showed no evidence for the formation of palladium nanoparticles. The TEM result also corroborate with the previously described XPS data. Therefore, to explain our data, the partial reduction of Pd(II) to Pd(I) species becomes an attractive proposal. This would lead similar to, though not identical, the formation of Pd(I)-carbonyl carboxylate complex [43] which can be envisaged as a model for such Pd(I) intermediates. The chemistry of Pd(I) complexes has been intensively developed with the special interest due to both the unusual oxidation state of Pd and the potentially important role of Pd(I) complexes in catalytic processes [44].

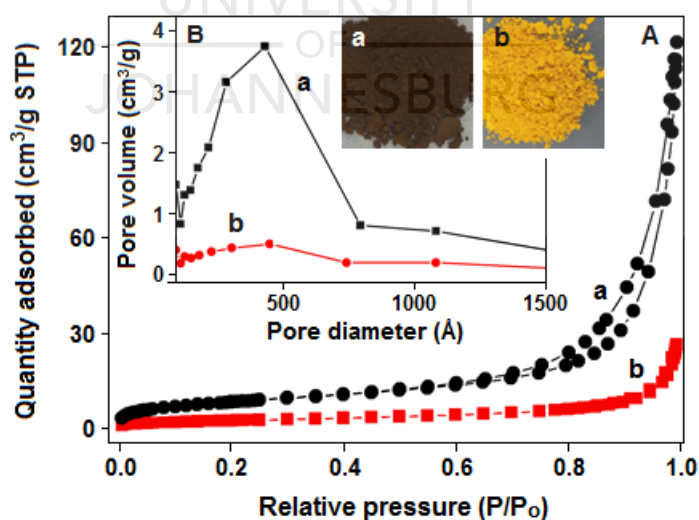


**Figure 4.4** The optical images of (a) *pTA* and (b) *Pd-pTA*. (A) Nitrogen adsorption and desorption isotherms and (B) pore size distribution of the (a) *pTA* and (b) *Pd-pTA*.

The figure 4.4 is the nitrogen adsorption and desorption isotherm for both the samples, pTA (a) and Pd-pTA (b), and are follows type II isotherm with a typical H3-type hysteresis loop according to the IUPAC (International Union of Pure and Applied Chemistry) classification. The BET surface areas of the pTA and Pd-pTA are  $30.26 \text{ m}^2\text{g}^{-1}$  and  $9.32 \text{ m}^2\text{g}^{-1}$ , respectively, and the average pore diameter for both the samples are 40 nm.

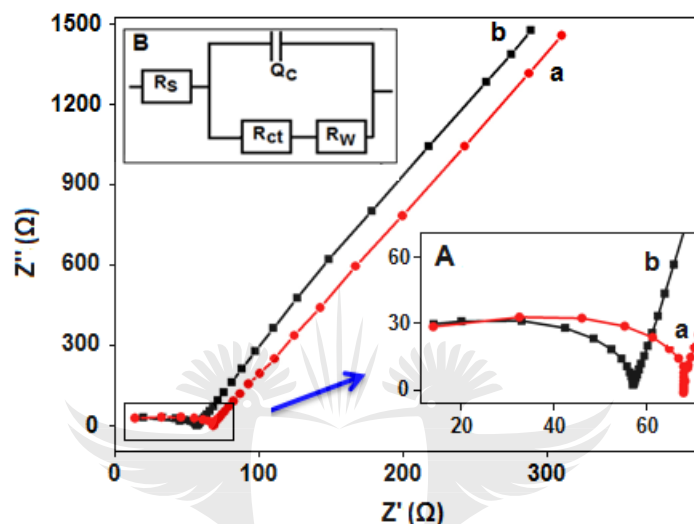


**Figure 4.5** The electrochemical impedance spectroscopy analysis for the (a) pTA and (b) Pd-pTA in 0.50M KOH within the frequency ranges from 3 MHz to 10 Hz. The electron transfer resistance values for (a) pTA and (b) Pd-pTA are 68.60 ohm and 58.30 ohm, respectively.

Impedance spectroscopy is an effective method for probing the features of surface-modified electrodes. The complex impedance can be presented as the sum of the real,  $Z'$ , and imaginary,  $Z''$ , components that originate mainly from the resistance and capacitance of the cell, respectively. A typical shape of a Faradaic impedance spectrum, presented in the form of a Nyquist plot in figure 4.5 (main panel), includes a semicircle region lying on the  $Z'$ -axis followed by a straight line. The semicircle portion, observed at higher frequencies, corresponds to the electron-transfer-limited process, whereas the linear part is characteristic of the lower frequencies range and represents the diffusion-limited electron-transfer process. From the figure it is clear that almost similar slope values for both the

samples which indicate the identical ion diffusion rate. The semicircle diameter equals to the electron transfer resistance values at the electrode surface for pTA (a) and Pd-pTA (b) are 68.60 ohm and 58.30 ohm, respectively (figure 4.5A). For the sample pTA, the electron transfer resistance was expanded which indicated the polymer performs as a kinetic barrier for the electron transfer process, whereas, in Pd-pTA the electron transfer resistance value was decreased due to the presence of ionic palladium species that participate for a better charge transfer mechanism. The electrochemical cell equivalent circuit for both the samples are identical in nature (figure 4.5B is for Pd-pTA), where  $R_{ct}$  represents the charge transfer resistance of the modified electrode and  $R_w$  is the diffusion coefficient of the electroactive species. The term,  $R_s$  represents the total ohmic resistance of solution and electrode whereas  $Q_c$  designate the capacitance of the double layer. The electrochemical active surface area of the as synthesized composite material Pd-pTA was  $0.70 \text{ m}^2\text{g}^{-1}$  in alkaline media, which is the comparable value as referred in the literature [45].

#### **4.3.2 Performance of Pd-pTA as an electrocatalyst for methanol oxidation reaction**

The composite material, Pd-pTA, has been tested as an electrocatalyst towards the oxidation of methanol and was monitored by cyclic voltammetric technique. We have also checked the performance of bare electrode and pTA modified electrode in the presence and absence of methanol.

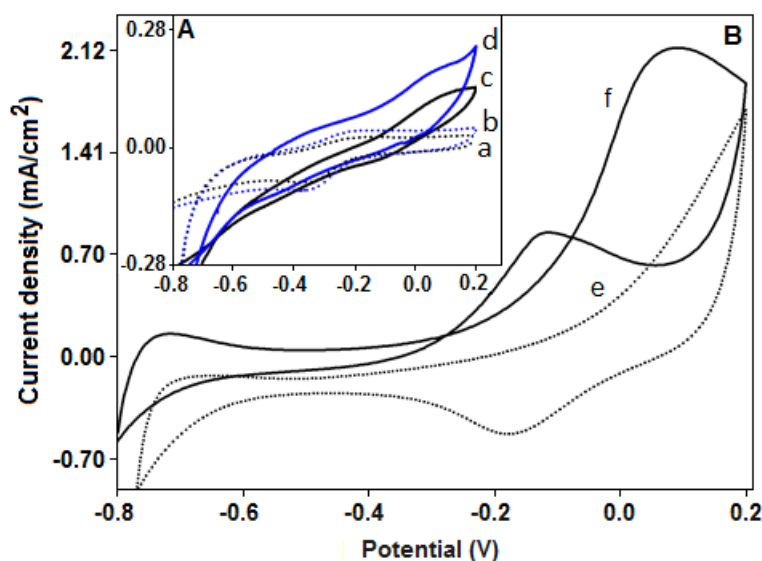


**Figure 4.6** (A) Cyclic voltammogram of bare GCE (curve ‘a’), *p*TA modified GCE (curve ‘b’) in the absence of methanol, whereas, the curve ‘c’ and curve ‘d’ represent the voltammogramme for bare GCE and *p*TA modified GCE, respectively, in the presence of 1.0 mol dm<sup>-3</sup> methanol and 0.5 mol dm<sup>-3</sup> KOH under the scan rate of 50 mVs<sup>-1</sup>. (B) Cyclic voltammogram of Pd-*p*TA modified GCE, in the absence of methanol (curve ‘e’) and in the presence of 1 mol dm<sup>-3</sup> methanol (curve ‘f’), in 0.5 mol dm<sup>-3</sup> KOH under the scan rate of 50 mVs<sup>-1</sup>.

In figure 4.6A, two cyclic voltammetric signatures, ‘a’ and ‘b’, are for bare and *p*TA modified electrode, respectively, in 0.5 mol dm<sup>-3</sup> KOH solution. Due to the addition of 1.0 mol dm<sup>-3</sup> of methanol in the presence of 0.5 mol dm<sup>-3</sup> KOH solution, the current density values, as obtained from voltammogram signals, for both bare and *p*T3A modified electrodes have been slightly improved, designated as ‘c’ and ‘d’, respectively. In the main panel (figure 4.6B), cyclic voltammogram of Pd-*p*TA modified glassy carbon electrode (curve ‘e’), in absence of methanol, shows the maximum current density value of 1.70 mA cm<sup>-2</sup> at 0.2 V but when the GC electrode was modified with Pd-*p*T3A, in the presence of 1.0 mol dm<sup>-3</sup> methanol, during the forward scan, the current density value reached at 2.12 mA cm<sup>-2</sup> at 0.09 V, curve ‘f’, in 0.5 mol dm<sup>-3</sup> KOH under the scan rate of 50 mV/s. The CV curves consist of two well-defined peaks at the forward and reverse scans. The peak in the forward scan is attributed to the oxidation of methanol molecules while the one in the

reverse scan is related to the oxidation of intermediate products, mainly carbon monoxide [20].

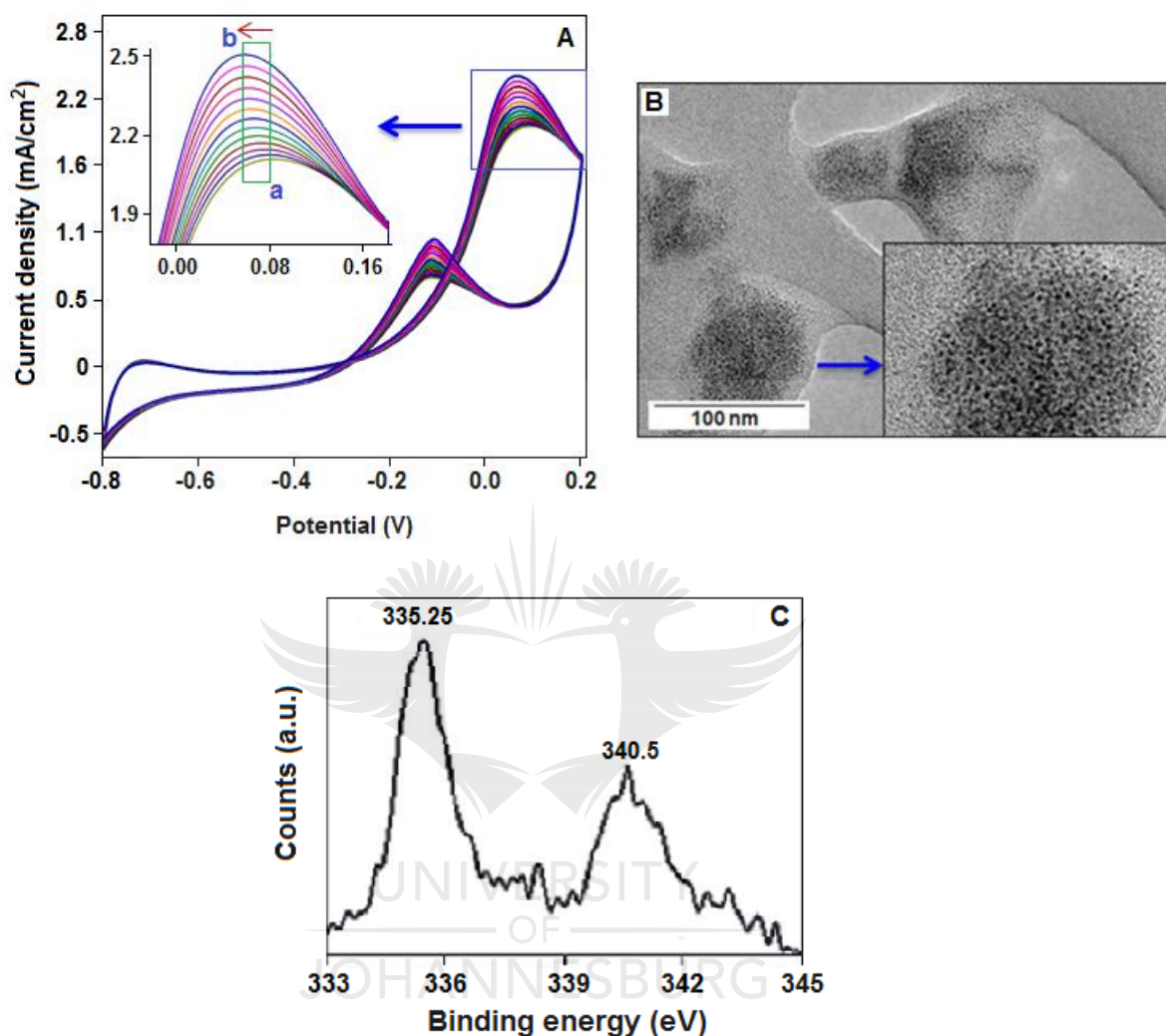


**Figure 4.7** (A) Represents 10 consecutive scans (cyclic voltammograms) in the presence of 1.0 mol dm<sup>-3</sup> methanol and 0.5 mol dm<sup>-3</sup> KOH. The magnified section shows, from 'a' (first scan) to 'b' (tenth scan), the increase of current density (peak height) with the shifting of peak position towards lower potential direction. (B) Polymer stabilized palladium nanoparticles (sample collected from the working electrode at the end of the experiment). (C) The characteristic XPS peak with the binding energy value 335.23 eV for the Pd 3d<sub>5/2</sub> line indicates the presence of metallic state of palladium.

It is also important to mention that a gradual increase of current density values has been observed during the repeated scan with the decreasing of peak potential value (Figure 4.7A). The magnified figure, marked by an arrow, of the methanol oxidation peaks indicates the decrease of potential values from 0.090 V (point 'a') to 0.065 V (point 'b')

along with the increase of current density values from 2.12 to 2.54 mA cm<sup>-2</sup>. The phenomenon of the above event could be explained in the light of nanoparticle catalyzed reaction where the transformation of ionic palladium to palladium atoms which leads to the formation of polymer stabilized nanoparticles, as evidenced by the TEM image of their covered material from the working electrode (Figure 4.7B), that expedite the catalytic performance of the composite for the methanol oxidation process by lowering the potential values with the increase of current density values. The histogram, the particle frequency as a function of particle size, (supporting information, figure S5) shows that 85% of the palladium nanoparticles are approximately within the range between 2-3 nm. The characteristic XPS peak with the binding energy value 335.25 eV for the Pd 3d<sup>5/2</sup> line indicates the presence of metallic palladium within the polymer matrix (Figure 4.7C).

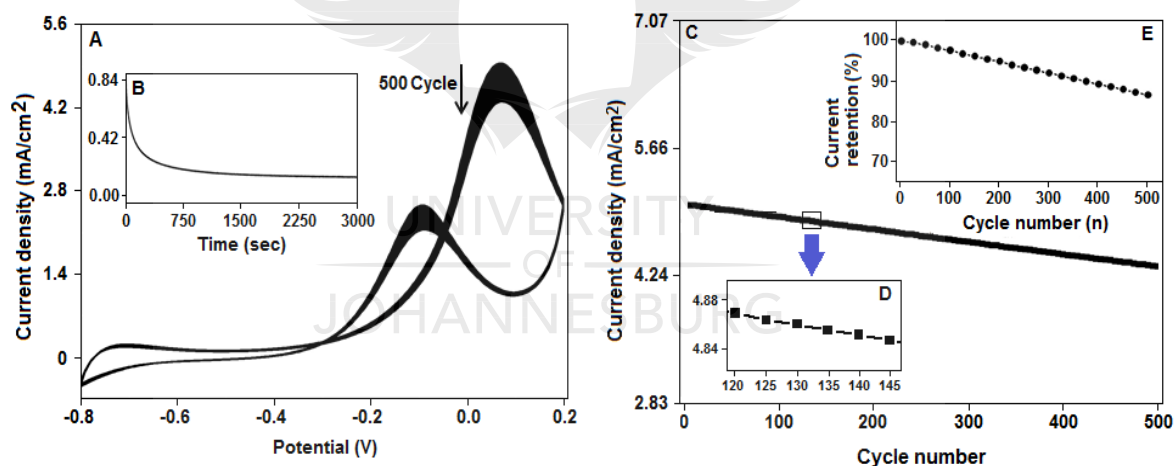


**Figure 4.8** (A) The stability study of Pd-*p*TA catalyst on glassy carbon electrode in the presence of 1.0 mol dm<sup>-3</sup> methanol in 0.5 mol dm<sup>-3</sup> KOH under the scan rate of 50 mV/s for 500 cycles. (B) The chronoamperometric response for the Pd-*p*TA catalyst in the presence of 1.0 mol dm<sup>-3</sup> methanol and 0.5 mol dm<sup>-3</sup> KOH at 30 °C at the fixed potential of 0.07V for the period of 3000 seconds. (C) show the linear relation between the current density (obtained from anodic peak) and the cycle number, obtained from the cyclic voltammogram data (A). (D) A fraction of the linear plot is shown by an arrow at higher magnification. (E) Current retention capability of the catalyst, which is 86.4%, has been calculated from.

The highest current density achieved by using Pd-*p*TA modified glassy carbon electrode in the presence of 1.0 mol dm<sup>-3</sup> methanol and 0.5 mol dm<sup>-3</sup> KOH was 5.03 mA cm<sup>-2</sup> at 0.065

V (Figure 4.8A). The electrocatalytic cycling stability of Pd-pTA modified electrode in other words the deactivation of the catalyst has also been studied in this experiment and we have found that the net decrease of current density was  $0.69 \text{ mA cm}^{-2}$  after 500 cycles, which indicate a stable catalyst for the methanol oxidation reaction (figure 4.8A). The long-term stability and durability of the polymer based catalyst was further examined by chronoamperometric measurements. For methanol oxidation reaction, the catalyst modified electrode was biased at the fixed potential of 0.07V and the changes of the oxidation current with time (for 3000 seconds) were monitored. Figure 4.8B shows the chronoamperometric response of the catalyst (Pd-pTA) for  $1.0 \text{ mol dm}^{-3}$  methanol in  $0.5 \text{ mol dm}^{-3}$  KOH at  $30^{\circ} \text{C}$ . For the catalyst, a gradual decay for a period of 750 sec, possibly suggesting catalyst poisoning by chemisorbed carbonaceous species formed during the oxidation of methanol, and after that the current appears to be fairly stable within the rest of the time period for the experiment, suggesting the better tolerance of the catalyst at the later stage. A similar incident has also been observed when we have performed the stability study of the catalyst (figure 4.8A). After achieving the highest current density, which is  $5.03 \text{ mA cm}^{-2}$ , we had allow the instrument to run 500 cycles and we found the net decrease of current density was  $0.69 \text{ mA/cm}^2$  with the  $I_F/I_B$  ratio for the first scan and the last scan ( $500^{\text{th}}$ ) were 1.939 and 2.011, respectively, has corroborate with the chronoamperometric study. The  $I_F/I_B$  ratio evaluating the tolerance efficiency of the catalyst, higher is the ratio better is the tolerance of the catalyst, which reveal that methanol can be more effectively oxidized on Pd-pTA modified electrode during the forward potential scan to generate relatively less carbon monoxide.

In the figure 4.8C, main panel, a liner plot, obtained from the figure 4.8A, using the peak potential values of the forward scan as a function of cycle number and a small fraction of the plot, has been magnified and marked by an arrow (figure 4.8D), indicates the



steadiness of the reaction. Figure 4.8E shows the long term performance of the catalyst, with the current retention value of 86.4% (based on the forward peak potential value) after 500 cycles.

**Table 4.1** A comparative data on the Pd-based catalyst for the electro-oxidation of methanol.

Entry	Catalyst	Current density (mA cm <sup>-2</sup> )	Reference
1	Commercial Pd/C catalyst	0.36	[41]
2	Pd-nanoparticles on graphene oxide	1.6	[41]
3	Carbon (Vulcan XC-72)-Pd (20 wt%)	10	[42]
4	MnO <sub>2</sub> -graphene oxide-Pd nanoparticles	20.4	[43]
5	Pd nanoparticles-carbon nanodots	3.42	[44]
6	Palladium selenides	3.18	[45]
7	Pd-SnO <sub>2</sub> -TiO <sub>2</sub> -MWCNT	0.285	[46]
8	Electrodeposited Pd on polyaniline	0.82	[47]
9	Palladium-polystyrene composite	0.17	[48]
10	Pd(I)-poly[4-(thiophen-3yl)-aniline]	5.03	Current work

A comparative survey on the electro-oxidation of methanol for various palladium based catalysts is incorporated in this report as a ready reference [46-53] (Table: 4.1, based on the achieved current densities, mA cm<sup>-2</sup>). From the table we have found that three component MnO<sub>2</sub>-graphene oxide-Pd nanoparticles catalyst system [48] shows the highest performance in terms of current density value (20.4 mA cm<sup>-2</sup>) for the electro-oxidation of methanol followed by Carbon (Vulcan XC-72)-Pd (20 wt%) system (current density: 10 mA cm<sup>-2</sup>), [47] where the Pd loading is very high as compared with the current polymer based system, Pd-pT3A (1.02 wt% of Pd), where we have achieved the highest current density value 5.03 mA cm<sup>-2</sup>. Other comparable systems, for the electro-oxidation of



methanol, are Pd nanoparticles-carbon nanodots [49] and palladium selenides [50] showed the current density values 3.42 and 3.18 mA cm<sup>-2</sup>, respectively.

#### **4.4 Sub-conclusion**

The present article reports a single step synthesis route of Pd-polymer composite material with an excellent performance on methanol oxidation reaction in alkaline media. The simple preparation method as well as the stability and the recyclability performance indicate that the material could have potential in direct methanol fuel cell application. To the best of our knowledge, this is the first kind of report where polymer supported ionic palladium has been used as a catalyst for the electro-oxidation of methanol. But it is also important to mention that during the electrochemical reaction the in situ formation of the palladium nanoparticles has been observed and that could play the role as an efficient catalyst for the significant improvement of the electro-oxidation process of methanol.



#### 4.5 References

1. Hassan, J., et al., Aryl–Aryl Bond Formation One Century after the Discovery of the Ullmann Reaction. *Chemical Reviews*, 2002. 102(5): p. 1359-1470.
2. Miyaura, N. and A. Suzuki, Palladium-Catalyzed Cross-Coupling Reactions. *Chemical reviews*, 1995. 95(7): p. 2457-2483
3. Bard, A.J., Photoelectrochemistry. *Science*, 1980. 207(4427): p. 139-144.
4. Mizukoshi, Y., et al., Sonochemical Preparation of Bimetallic Nanoparticles of Gold/Palladium in Aqueous Solution. *The Journal of Physical Chemistry B*, 1997. 101(36): p. 7033-7037.
5. Stefania, S., et al., Polymer-encapsulated metal nanoparticles: optical, structural, micro-analytical and hydrogenation studies of a composite material. *Nanotechnology*, 2008. 19(7): p. 075708.
6. Choudhary, M., et al., In situ generation of a high-performance Pd-polypyrrole composite with multi-functional catalytic properties. *Dalton Transactions*, 2014. 43(17): p. 6396-6405.
7. Choudhary, M., et al., Catalytic performance of the in situ synthesized palladium-polymer nanocomposite. *New Journal of Chemistry*, 2016.
8. Mahato, S.K., et al., Polymer-Stabilized Palladium Nanoparticles for the Chemoselective Transfer Hydrogenation of  $\alpha,\beta$ -Unsaturated Carbonyls: Single-Step Bottom-Up Approach. *ChemCatChem*, 2014. 6(5): p. 1419-1426.
9. Ul Islam, R., et al., Palladium–Poly(3-aminoquinoline) Hollow-Sphere Composite: Application in Sonogashira Coupling Reactions. *ChemCatChem*, 2013. 5(8): p. 2453-2461.

10. Choudhary, M., et al., Template-less synthesis of polymer hollow spheres: an efficient catalyst for Suzuki coupling reaction. *Applied Organometallic Chemistry*, 2013. 27(9): p. 523-528.
11. Huang, H. and X. Wang, Design and synthesis of Pd-MnO<sub>2</sub> nanolamella-graphene composite as a high-performance multifunctional electrocatalyst towards formic acid and methanol oxidation. *Physical Chemistry Chemical Physics*, 2013. 15(25): p. 10367-10375.
12. Hoshi, N., et al., Structural Effects of Electrochemical Oxidation of Formic Acid on Single Crystal Electrodes of Palladium. *The Journal of Physical Chemistry B*, 2006. 110(25): p. 12480-12484.
13. Zheng, H.T., et al., Effect of support on the activity of Pd electrocatalyst for ethanol oxidation. *Journal of Power Sources*, 2006. 163(1): p. 371-375.
14. Xu, C., et al., Methanol and ethanol electrooxidation on Pt and Pd supported on carbon microspheres in alkaline media. *Electrochemistry Communications*, 2007. 9(5): p. 997-1001.
15. Hu, F.P., et al., Improved performance of Pd electrocatalyst supported on ultrahigh surface area hollow carbon spheres for direct alcohol fuel cells. *Journal of Power Sources*, 2008. 177(1): p. 61-66.
16. Bambagioni, V., et al., Pd and Pt–Ru anode electrocatalysts supported on multi-walled carbon nanotubes and their use in passive and active direct alcohol fuel cells with an anion-exchange membrane (alcohol = methanol, ethanol, glycerol). *Journal of Power Sources*, 2009. 190(2): p. 241-251.
17. Ghosh, S., et al., Facile synthesis of Pd nanostructures in hexagonal mesophases as a promising electrocatalyst for ethanol oxidation. *Journal of Materials Chemistry A*, 2015. 3(18): p. 9517-9527.

18. Zhang, K.-F., et al., Vanadium oxide nanotubes as the support of Pd catalysts for methanol oxidation in alkaline solution. *Journal of Power Sources*, 2006. 162(2): p. 1077-1081.
19. Xu, M.-W., et al., Novel Pd/ $\beta$ -MnO<sub>2</sub> nanotubes composites as catalysts for methanol oxidation in alkaline solution. *Journal of Power Sources*, 2008. 175(1): p. 217-220.
20. Singh, R.N. and R. Awasthi, Graphene support for enhanced electrocatalytic activity of Pd for alcohol oxidation. *Catalysis Science & Technology*, 2011. 1(5): p. 778-783.
21. Zhao, Y., et al., Enhanced electrocatalytic oxidation of methanol on Pd/polypyrrole-graphene in alkaline medium. *Electrochimica Acta*, 2011. 56(5): p. 1967-1972.
22. Ghosh, S., et al., Conducting polymer-supported palladium nanoplates for applications in direct alcohol oxidation. *International Journal of Hydrogen Energy*, 2015. 40(14): p. 4951-4959.
23. Hable, C. and M.S. Wrighton, Electrocatalytic oxidation of methanol and ethanol: a comparison of platinum-tin and platinum-ruthenium catalyst particles in a conducting polyaniline matrix. *Langmuir* 1993. 9: p. 3284-3290.
24. Ghosh, S., T. Maiyalagan, and R.N. Basu, Nanostructured conducting polymers for energy applications: towards a sustainable platform. *Nanoscale*, 2016. 8(13): p. 6921-6947.
25. Ghosh, S., et al., Visible-light active conducting polymer nanostructures with superior photocatalytic activity. *Scientific Reports*, 2015. 5: p. 18002.

26. Yin, Z. and Q. Zheng, Controlled Synthesis and Energy Applications of One-Dimensional Conducting Polymer Nanostructures: An Overview. *Advanced Energy Materials*, 2012. 2(2): p. 179-218.
27. Mallick, K., et al., Fabrication of a Metal Nanoparticles and Polymer Nanofibers Composite Material by an in Situ Chemical Synthetic Route. *Langmuir*, 2005. 21(17): p. 7964-7967.
28. Mallick, K., et al., Polymerization of Aniline by Auric Acid: Formation of Gold Decorated Polyaniline Nanoballs. *Macromolecular Rapid Communications*, 2005. 26(4): p. 232-235.
29. Mallick, K., M.J. Witcomb, and M.S. Scurrall, Formation of palladium nanoparticles in poly (o-methoxyaniline) macromolecule fibers: An in-situ chemical synthesis method. *The European Physical Journal E*, 2006. 19(2): p. 149-154.
30. Mallick, K., M.J. Witcomb, and M.S. Scurrall, In situ synthesis of copper nanoparticles and poly(o-toluidine): A metal-polymer composite material. *European Polymer Journal*, 2006. 42(3): p. 670-675.
31. Mallick, K., M. Witcomb, and M. Scurrall, Fabrication of a nanostructured gold-polymer composite material. *The European Physical Journal E*, 2006. 20(3): p. 347-353.
32. Mathew, J.P. and M. Srinivasan, Photoelectron spectroscopy (XPS) studies on some palladium catalysts. *European Polymer Journal*, 1995. 31(9): p. 835-839.
33. Zharmagambetova, A.K., V.A. Golodov, and Y.P. Saltykov, The study of the composition and catalytic properties of palladium(II) complexes with poly(VINYLPYRIDINE). *Journal of Molecular Catalysis*, 1989. 55(1): p. 406-414.

34. Likhar, P.R., et al., Highly Efficient and Reusable Polyaniline-Supported Palladium Catalysts for Open-Air Oxidative Heck Reactions under Base- and Ligand-Free Conditions. *Advanced Synthesis & Catalysis*, 2008. 350(13): p. 1968-1974.
35. Shimano, J.Y. and A.G. MacDiarmid, Polyaniline, a dynamic block copolymer: key to attaining its intrinsic conductivity? *Synthetic Metals*, 2001. 123(2): p. 251-262.
36. Wise, D.L., et al., Photonic polymer systems-Fundamentals, methods and applications. 1998, New York: CRC Press. 968.
37. Liu, J., Y. Shi, and Y. Yang, Improving the performance of polymer light-emitting diodes using polymer solid solutions. *Applied Physics Letters*, 2001. 79(5): p. 578-580.
38. El-Azhary, A.A. and R.H. Hilal, Vibrational analysis of the spectra of furan and thiophene. *Spectrochimica Acta Part A: Molecular and Biomolecular Spectroscopy*, 1997. 53(9): p. 1365-1373.
39. Scott, D.W., A valence force field for thiophene and its deuterium and methyl derivatives. *Journal of Molecular Spectroscopy*, 1969. 31(1): p. 451-463.
40. Kaushik, M., J.W. Mike, and S.S. Mike, Directional assembly of polyaniline functionalized gold nanoparticles. *Journal of Physics: Condensed Matter*, 2007. 19(19): p. 196225.
41. Mallick, K., et al., Low-temperature magnetic property of polymer encapsulated gold nanoparticles. *Journal of Applied Physics*, 2009. 106(7): p. 074303.
42. Taher, A., et al., Suzuki coupling reaction in the presence of polymer immobilized palladium nanoparticles: a heterogeneous catalytic pathway. *New Journal of Chemistry*, 2015. 39(7): p. 5589-5596.

43. Shishilov, O.N., et al., Palladium(II) carboxylates and palladium(I) carbonyl carboxylate complexes as catalysts for olefin cyclopropanation with ethyl diazoacetate. *Dalton Transactions*, 2009(33): p. 6626-6633.
44. Davidson, J.M. and C. Triggs, Reaction of metal ion complexes with hydrocarbons. Part I. 'Palladation' and some other new electrophilic substitution reactions. The preparation of palladium(I). *Journal of the Chemical Society A: Inorganic, Physical, Theoretical*, 1968(0): p. 1324-1330.
45. Prodromidis, M.I., et al., Preorganized composite material of polyaniline–palladium nanoparticles with high electrocatalytic activity to methanol and ethanol oxidation. *International Journal of Hydrogen Energy*, 2015. 40(21): p. 6745-6753.
46. Li, H., et al., Photocatalytic synthesis of highly dispersed Pd nanoparticles on reduced graphene oxide and their application in methanol electro-oxidation. *Catalysis Science & Technology*, 2012. 2(6): p. 1153-1156.
47. Hu, G., et al., Palladium nanocrystals supported on helical carbon nanofibers for highly efficient electro-oxidation of formic acid, methanol and ethanol in alkaline electrolytes. *Journal of Power Sources*, 2012. 209: p. 236-242.
48. Liu, R., et al., Preparation of Pd/MnO<sub>2</sub>-reduced graphene oxide nanocomposite for methanol electro-oxidation in alkaline media. *Electrochemistry Communications*, 2013. 26: p. 63-66.
49. Wei, W. and W. Chen, "Naked" Pd nanoparticles supported on carbon nanodots as efficient anode catalysts for methanol oxidation in alkaline fuel cells. *Journal of Power Sources*, 2012. 204: p. 85-88.
50. Madhu and R.N. Singh, Palladium selenides as active methanol tolerant cathode materials for direct methanol fuel cell. *International Journal of Hydrogen Energy*, 2011. 36(16): p. 10006-10012.

51. An, H., et al., Synthesis and performance of palladium-based catalysts for methanol and ethanol oxidation in alkaline fuel cells. *Electrochimica Acta*, 2013. 102: p. 79-87.
52. Hatchett, D.W., et al., The electrochemical reduction of PdCl<sub>4</sub><sup>2-</sup> and PdCl<sub>6</sub><sup>2-</sup> in polyaniline: Influence of Pd deposit morphology on methanol oxidation in alkaline solution. *Electrochimica Acta*, 2011. 56(17): p. 6060-6070.
53. Zhang, N., et al., Preparation and characterization of nano-sized PS@Pd core-shell architectures with a one-pot method. *RSC Advances*, 2016. 6(2): p. 1376-1379.





## CHAPTER 5

# PALLADIUM-POLYMER NANOCOMPOSITE: AN ANODE CATALYST FOR THE ELECTROCHEMICAL OXIDATION OF METHANOL

---

### 5.1 Introduction

The need for functional materials have been significantly increases for a number of advanced applications in recently years. Materials based on nano-sized metals represent a potential candidate for the solution to many technological demands as they exhibit extraordinary properties as compared with the balk metals. For an effective application, to control of these small objects is a real challenge as they agglomerate rapidly because of the high surface energy. The nano-sized metals are also very prone to oxidation, another limitation for application point of view, even due to the minimum exposure of aerial oxygen. Stabilizing the nanomaterials using a polymer is a successful option where the polymer matrices serve both as the support as well as the stabilizer of the nanoparticles that provide a mechanism to prevent particle agglomeration.

A facile *in-situ* synthesis route has been reported for the preparation of polymer stabilized silver nanoparticles where silver nanoparticles are shown to have an excellent catalytic activity for the proton-coupled electron transfer reaction [1].The silver-polymer nanocomposite material also perform as an efficient electro-catalyst for the oxidation of ascorbic acid [1]. A gold-polymer supramolecular architecture showed the electrochemical sensing performance for the detection of biomolecules, where the gold nanoparticles play the role of a catalyst [2]. Polymer stabilized palladium nanoparticles have attracted much attention as a new research direction in catalysis where metal particles play the role of catalyst for various organic transformation reactions [3-5].

Palladium based catalysts are emerged as a good electrode material for alcohol oxidation in alkaline medium and the electrocatalytic performance of palladium depends on shape, size and the distribution on the support material [6]. Efforts have been made to facilitate the catalytic activity of palladium by controlling the size and shape of the nanocrystals [7] and also to improve the dispersion of the nanoparticles on various support materials, such as, metal oxides [8] and various carbon based materials [9-11]. Reports are also available on the polymer supported catalyst for the electro-oxidation of alcohol. The three component palladium-polypyrrole-graphene system was reported as an active catalyst system for the electro-oxidation of methanol [12]. Again, palladium nanoparticles supported on poly-(diphenylbutadiene) also displayed the catalytic activity for the oxidation of ethanol [13]. The polyaniline supported bimetallic system, Pt-Ru and Pt-Sn, showed superior catalytic activity for both methanol and ethanol oxidation than the Pt alone [14]. Palladium-polyaniline composite has been reported as an electrocatalyst for methanol and ethanol oxidation [15].

In addition to that, various carbon based material can also perform as an excellent support system for the metal catalyst for methanol oxidation reaction. Reduced graphene oxide supported Pd-Pt alloy showed superior electrocatalytic activity, stability and carbon monoxide tolerance towards the methanol oxidation reaction in the presence of sodium hydroxide electrolyte [16]. Uniformly deposited Pt-Rh nanoparticles on the  $\beta$ -cyclodextrin functionalized carbon nanotubes exhibit excellent electrocatalytic performance for methanol electro-oxidation due to the smaller particle size and uniform deposition of the nanoparticles [17]. Graphite supported bimetallic Pd-Cu system, synthesized through single-pot hydrothermal reduction method, has been reported synergistic and enhanced electro-catalytic activity towards the oxidation of methanol in alkali medium [18]. Carbon black supported Pd-Ni system demonstrated a higher catalytic activity and higher carbon

monoxide poisoning tolerance for methanol oxidation reaction than carbon supported Pd system alone [19]. Pt nanoparticles supported on sulphur-modified carbon nanotubes, with electrochemically active surface area  $88.4 \text{ m}^2 \text{ g}^{-1}$ , showed efficient catalytic activity for methanol electro-oxidation reaction [20]. A single-step electrodeposition approach has also been reported, to grow the morphology controlled Pt-nanostructure on reduced graphene oxide, towards methanol oxidation for fuel cell application under alkaline medium [21].

In this current work, we describe a single-step wet chemical route for the synthesis of palladium-polymer composite material, where potassium tetrachloropalladate (II) and the diamine derivatives of naphthalene, 1,8-diaminonaphthalene, has been used as the precursors. During the reaction diaminonaphthalene has been oxidized to produce poly-(diaminonaphthalene), *p*DAN, and on the other hand palladium salt was reduced to form palladium nanoparticles. In the above reaction, both nanoparticle formation and polymerization are happened concurrently and produced metal-polymer composite material (Pd-*p*DAN) that has been used as a catalyst for the electrochemical oxidation of methanol under alkaline condition.

## 5.2 Experiment section

### 5.2.1 Materials

All the chemicals and the solvents used for this experiment were of analytical purity and no further purification process was involved unless otherwise specifically mentioned. Ultra-pure water (electrical conductivity  $\sim 5.5 \times 10^{-6} \text{ S.cm}^{-1}$ ) was used in this experiment wherever required.

### 5.2.2 Material characterization

Microscopy studies of the synthesized material were performed using JEOL (JEM-2100) transmission electron microscope (TEM) instrument equipped with a LaB<sub>6</sub> electron source.

The sample for TEM analysis was prepared by depositing small amount of synthesized material onto a 200 mesh size Cu-grid coated with a lacy carbon film. The X-ray diffraction (XRD) patterns were recorded on a Shimadzu XD-3A X-ray diffractometer operating at 20 kV using Cu-K $\alpha$  radiation ( $\lambda = 0.1542$  nm) within the diffraction angle range ( $2\theta$ ) from 10° to 90°. X-ray photoelectron spectra (XPS) were collected using a Physical Electronics 560 ESCA/SAM instrument. Fourier transform infrared spectroscopy (FTIR) study was performed using a Shimadzu IRAffinity-1. Electrochemical studies was carried out with a, Bio-Logic, SP-200, potentiostat connected to a data controller. A three-electrode system was used in the experiment with a glassy carbon electrode (GCE) as the working electrode, whereas, Ag/AgCl electrode (saturated KCl) and a Pt-electrode were used as the reference and counter electrodes, respectively.

### 5.2.3 Preparation of a Pd-*p*DAN composite catalyst

In a typical experiment, 0.240 g of 1, 8-diaminonaphthalene was dissolved in 10 mL of methanol. The aqueous solution of potassium tetrachloropalladate (II) (5 mL of  $0.5 \times 10^{-2} \text{ mol dm}^{-3}$ ) was slowly added to the dissolved organic molecule under stirring conditions in a 50 mL conical flask. During the addition, a brownish colloidal material was formed. The entire reaction was performed under ambient condition for the period of 120 min. During the reaction a dark brown precipitation was formed at the bottom of the flask. Few drops of the colloidal material was deposited onto the carbon-coated copper grid for TEM study and the required amount of material was used for infra-red analysis. The remaining portion of the compound was dried under vacuum at 60 °C and used for XRD and XPS measurements. The solid material was also tested as an anode catalyst for the electro-oxidation of methanol.

For the control study, poly (1, 8-diaminonaphthalene), *p*DAN, has been synthesized using ammonium persulfate (APS) as an oxidizing agent (maintaining the identical concentration of monomer and oxidizing agent as above).

#### 5.2.4 Electrochemical measurements

A glassy carbon electrodes (GCE) was polished with alumina and cleaned with acetone and deionized water, respectively. The synthesized composite materials (*p*DAN and Pd-*p*DAN) were dropped onto the GCE surface, dried at room temperature and used for electrochemical measurements. For the electro-oxidation study of methanol, the cyclic voltammograms were recorded at a scan rate of 50 mV.s<sup>-1</sup> in a mixed solution of KOH (0.5 mol dm<sup>-3</sup>) and methanol (1.0 mol dm<sup>-3</sup>).

### 5.3 Result and discussion:

The synthesis of conjugated polymer encapsulated metal nanoparticles, such as, gold [16], silver [17], palladium [18] and copper [19] have been reported by using the IPCF technique [16-19], where metal-polymer nanocomposite has been produced through a single step reaction and have an intimate contact between the particles and the polymer through functionalization [20]. In this current report, the polymerization of diamine derivatives of naphthalene, 1,8-diaminonaphthalene, follows the similar mechanism like aniline polymerization [21] and during the process, the released electrons reduced the potassium tetrachloropalladate (II) to form palladium atoms. The coalescence of these atoms formed palladium nanoparticles, which were encapsulated by the poly (1,8-diaminonaphthalene).

In the IR spectrum (Figure 5.1), the broad absorption bands in the range of 3100-3600 cm<sup>-1</sup> is due to the N-H stretching mode for both the polymer samples, *p*DAN, spectrum (a) and Pd-*p*DAN, spectrum (b). For the Pd-*p*DAN sample, the bands at 2949 and 2838 cm<sup>-1</sup> are

clearly visible and are due to the aromatic C-H stretching vibration. In the IR spectra, the vibrational band at  $1647\text{ cm}^{-1}$ , for both the samples, corresponds to the group  $\text{N}=\text{Q}=\text{N}$  (where Q represents a quinoid ring). The adjacent lower intensity bands are responsible for the N-B-N group (where B represents a benzenoid ring) for both the samples. The band at  $1280\text{ cm}^{-1}$  is assigned for the C-N stretching vibration of the secondary aromatic amine and only visible for Pd-*p*DAN sample. The absorption bands at  $1107$  and  $1014\text{ cm}^{-1}$  are due to the aromatic C-H in-plane bending vibration and are visible for both the samples but with different intensity. The IR spectrum confirms the formation of polymer with the presence of both benzenoid and quinoid ring structure in both the cases.

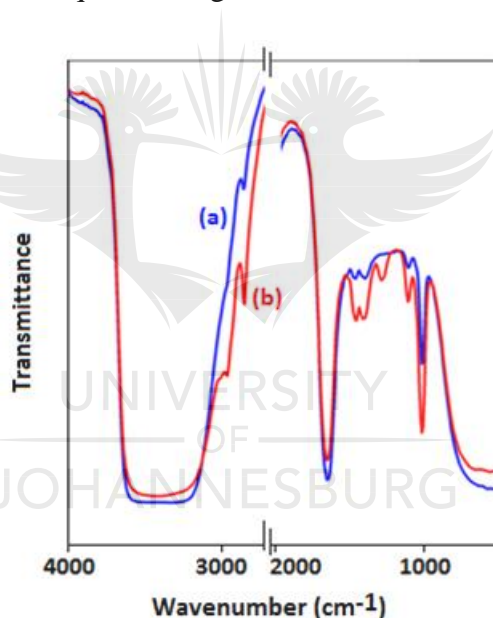


**Figure 5.1** The Fourier transform infrared images for *p*DAN, spectrum (a) and Pd-*p*DAN spectrum (b).

The transmission electron microscopy (TEM) image of Pd-*p*DAN shows a chain like structure where the diameter of the chain is within the range of 50-60 nm (Figure 5.2A). The magnified TEM image (Figure 5.2B) shows the distribution of dark spots along the core of the polymer chains. The in-set image (figure 5.2C), clearly shows that the dark spots are the nanoparticulates. A typical EDX spectra (Figure 5.2D) obtained from the

electron beam being focused on the dark spots in the polymer matrix and indicate that these spots are for the palladium particles, with the diameter of 3-4 nm.

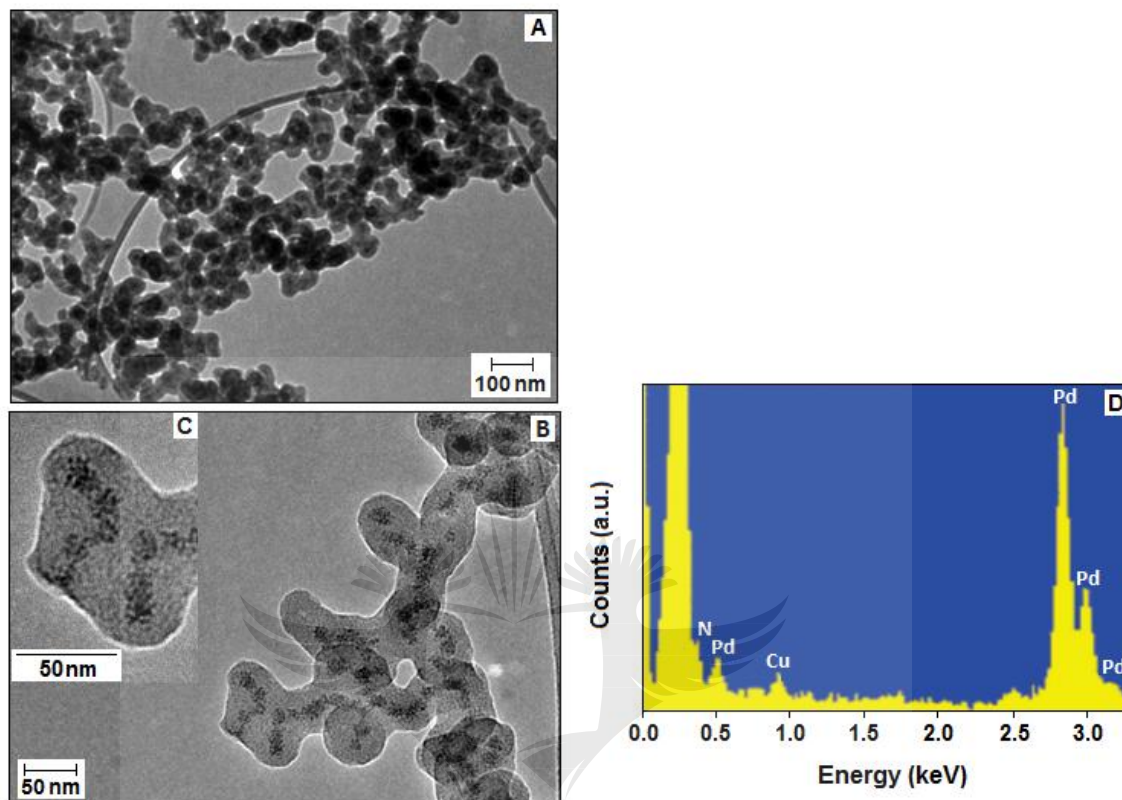


**Figure 5.2** (A) The TEM image shows a chain like structure of Pd-*p*DAN. (B) The magnified TEM image shows the distribution of palladium nanoparticles along the core of the polymer chains. (C) The in-set TEM image shows the nanoparticulates within the polymer. (D) A typical EDX spectra indicates the presence of palladium in the sample (the copper peak is derived from the TEM support grid).

To confirm the metallic character of the palladium, X-ray Diffraction (XRD) and X-ray photoelectron spectroscopy (XPS) studies were performed. The figure 5.3A shows the XRD pattern of polymer (*p*DAN), spectrum (a), and metal-polymer nanocomposite (Pd-*p*DAN), spectrum (b). From the pattern it is clear that the polymer is crystalline in nature. The spectrum (b) produce the evidence of metallic palladium in the polymer based composite. The peaks in the spectrum (b) at 40.2°, 46.5°, 68.0°, 82.2° and 86.7° representing the (111), (200), (220), (311) and (222) Bragg reflection, respectively. In the XPS spectrum (figure 5.3B), the Pd3d region shows the spin-orbit splitting between 3d<sub>5/2</sub>



and  $3d_{3/2}$  is separated by 4.9 eV, with the peak positions at binding energies of 335.20 and 340.05 eV, respectively, and that indicates the metallic property of the palladium in the polymer.

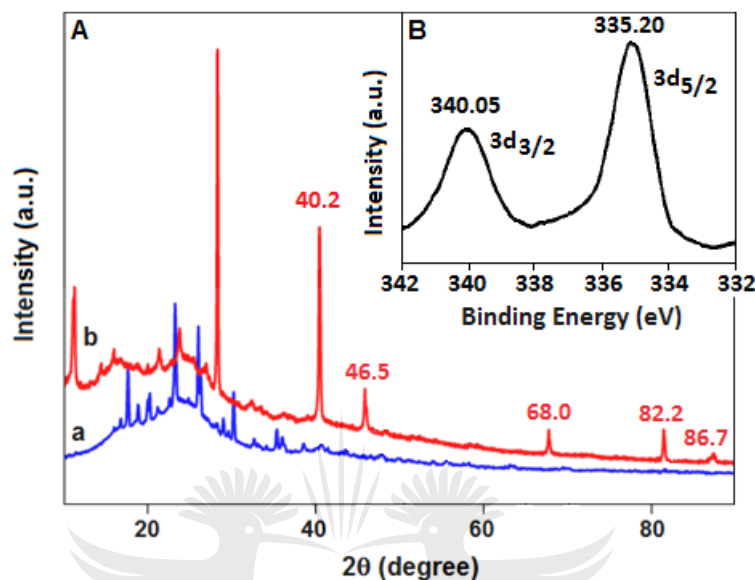


**Figure 5.3** (A) X-ray Diffraction pattern for (a) *p*DAN and (b) Pd-*p*DAN. In the spectrum (b), the peaks at 40.2°, 46.5°, 68.0°, 82.2° and 86.7° representing the (111), (200), (220), (311) and (222) Bragg reflection, respectively, indicates the crystalline nature of the palladium nanoparticles. (B) Palladium 3d X-ray photoelectron spectroscopy of Pd-*p*DAN. The peaks at binding energies at 335.20 eV and 340.05 eV for  $3d_{5/2}$  and  $3d_{3/2}$ , respectively, are indicative of metallic palladium.

Impedance spectroscopy is an effective method for probing the features of surface-modified working electrode. The complex impedance can be presented as the sum of the real ( $Z'$ ) and imaginary ( $Z''$ ) components that originate mainly from the capacitor's resistance and reactance, respectively. The relation between  $Z'$  and  $Z''$  part of the impedance for the samples (a) *p*DAN and (b) Pd-*p*DAN was tested in terms of Nyquist plot under the alkaline condition (KOH, 0.5 mol dm<sup>-3</sup>) within the frequency range from 7 MHz to 10 Hz and illustrated in the figure 5.4A. The Nyquist plot, in the main panel, includes a semicircle region lying on the  $Z'$ -axis followed by a straight line. The semicircle portion, observed at higher frequency region, corresponds to the electron-transfer limited process,



whereas the linear part is characteristic of the lower frequency range represents the diffusion-limited electron-transfer process. From the figure 5.4A, main panel, it is clear that almost identical slope values were obtained for *p*DAN and Pd-*p*DAN and which indicate the equal ion diffusion rate for both the samples. In the Nyquist plot, the semicircle diameter represent to the electron transfer resistance values at the electrode surface and which are 62.26 and 18.76 ohm for *p*DAN (a) and Pd-*p*DAN (b), respectively (Figure 5.4B). For the sample *p*DAN, the electron transfer resistance value was high (62.26 ohm) and that indicate the polymer performs as a kinetic barrier for the electron transfer process. For the sample Pd-*p*DAN, the electron transfer resistance value was decreased (18.76 ohm) due to the presence of palladium nanoparticles that contribute for an improved charge transfer mechanism. The electrochemical cell equivalent circuit for both the samples are identical in nature (Figure 5.4C) where  $R_{CT}$  represents the charge transfer resistance of the modified electrode and  $R_w$  is the diffusion coefficient of the electroactive species. The term,  $R_s$  represents the total ohmic resistance of the solution and the electrode whereas  $Q_C$  designate the capacitance of the double layer. In figure 5.4D, two cyclic voltammogram signatures, 'a' and 'b', are for bare and *p*DAN modified working electrode, respectively, in absence of methanol under the alkaline condition. In the presence of methanol ( $1.0 \text{ mol dm}^{-3}$ ) the current density value for the bare electrode was slightly improved, compared with (a) and (b), as evidenced by the voltammogram signal (c). For the *p*DAN modified electrode further improvement of the current density has been observed with the anodic peak current value  $0.22 \text{ mA cm}^{-2}$  and the pattern of the voltammogram (d) resembles like the typical methanol electro-oxidation signal [22]. In the main panel, figure 5.4E shows the voltammogram (curve 'e') of Pd-*p*DAN modified glassy carbon electrode in absence of methanol with the maximum current density of  $0.54 \text{ mA cm}^{-2}$  at 0.2 V, whereas, in presence of methanol ( $1.0 \text{ mol dm}^{-3}$ ), during the forward scan,

the highest current density value was reached to  $1.26 \text{ mA} \cdot \text{cm}^{-2}$  at  $-0.05 \text{ V}$ , curve (f), in the presence of KOH ( $0.5 \text{ mol dm}^{-3}$ ) under the scan rate of  $50 \text{ mV/s}$ . The electrochemical active surface area of the as synthesized composite material Pd-pDAN was found to be  $6.04 \text{ m}^2 \cdot \text{g}^{-1}$  in alkaline media, which was calculated based on the voltammogram (e) within the potential range from  $-0.45 \text{ V}$  to  $0.2 \text{ V}$ . The voltammogram (e) consist of two well-defined peaks at the forward and reverse scans. The peak in the forward scan is attributed to the oxidation of methanol molecules while the one in the reverse scan is related to the intermediate products, mainly the formation of carbon monoxide [23].

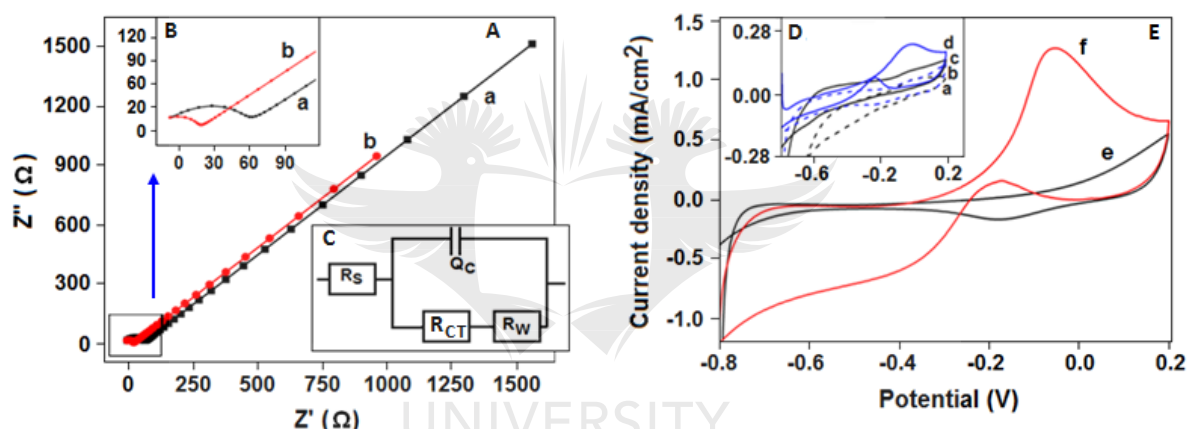


**Figure 5.4** (A) In the main panel, the electrochemical impedance spectra for the (a) pDAN and (b) Pd-pDAN in KOH ( $0.5 \text{ mol dm}^{-3}$ ) within the frequency ranges from  $7 \text{ MHz}$  to  $10 \text{ Hz}$ . (B) The in-set image shows the magnified  $Z'$  axis, where the electron transfer resistance values for both the samples are clearly visible: (a) pDAN ( $62.26 \text{ ohm}$ ) and (b) Pd-pDAN ( $18.76 \text{ ohm}$ ). (C) The electrochemical cell equivalent circuit for Pd-pDAN. (D) Cyclic voltammogram of bare (a) and pDAN modified (b) GCE, in KOH ( $0.5 \text{ mol dm}^{-3}$ ). Cyclic voltammogram of bare (c) and pDAN modified (d) GCE in the presence of KOH ( $0.5 \text{ mol dm}^{-3}$ ) and methanol ( $1.0 \text{ mol dm}^{-3}$ ). (E) In the main panel, cyclic voltammetry, current vs potential graphs for Pd-pDAN modified GCE, in absence of methanol, voltammogram (e), and in the presence of methanol ( $1.0 \text{ mol dm}^{-3}$ ), voltammogram (f), in KOH ( $0.5 \text{ mol dm}^{-3}$ ).

The highest current density value was obtained for the electrocatalytic oxidation of methanol was  $1.7 \text{ mA cm}^{-2}$  ( $84.5 \text{ mA} \cdot \text{cm}^{-2} / \text{mg}$  of Pd) for the Pd-pTA catalyst (figure 5.5A) and the current density decreases progressively with the number of scanning. A stable current density value has been obtained, which is  $1.42 \text{ mA} \cdot \text{cm}^{-2}$  ( $71.0 \text{ mA} \cdot \text{cm}^{-2} / \text{mg}$

of Pd) approximately after 100 cycles. Chronoamperometric study was performed to find the long-term performance of the Pd-*p*DAN catalyst toward methanol oxidation reaction. For this study, the working electrode was biased at the potential of -0.05V for the period of 3000 seconds in the presence of methanol (1.0 mol $\text{dm}^{-3}$ ) and KOH (0.5 mol $\text{dm}^{-3}$ ). The Figure 5.5B shows a sharp initial decay followed by a gradual decay in the current density for the period of 25 min suggesting the initial deactivation of the catalyst by the chemisorbed carbonaceous species due the oxidation of methanol [24]. In the later stage the current appears to be stable and that indicates the better tolerance of the catalyst. In the figure 5.5C, main panel, a liner plot obtained from the stability study (figure 5A) using the peak potential values of the forward scan as a function of cycle number, indicates a steady decrease of current density. Figure 5.5D shows the current retention value, which is 83.8%, calculated based on the forward peak potential value for the first 100 cycles of the figure 5.5A. After 100 cycles no apparent decrease of current density has been noticed (not shown in the figure).

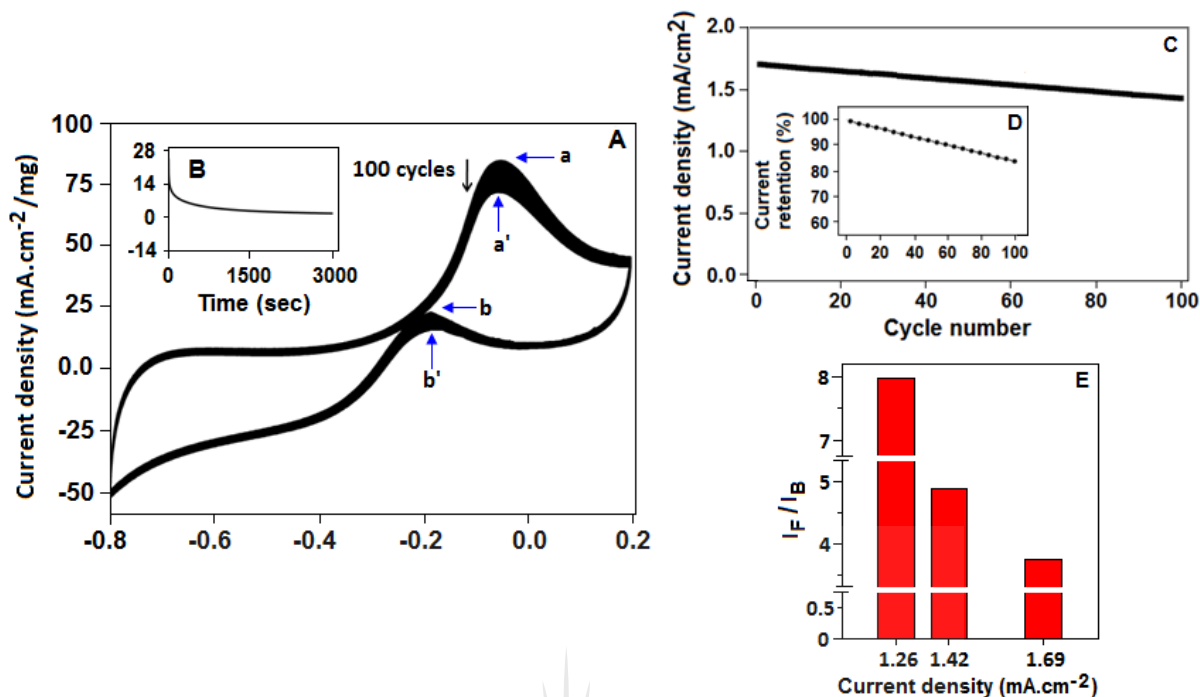


**Figure 5.5** (A) The stability study of Pd-*p*DAN modified electrode in the presence of methanol (1.0 mol dm<sup>-3</sup>) and KOH (0.5 mol dm<sup>-3</sup>) under the scan rate of 50 mV/s for 100 cycles. (B) The chronoamperometric response for the Pd-*p*DAN modified electrode presence of methanol (1.0 mol dm<sup>-3</sup>) and KOH (0.5 mol dm<sup>-3</sup>) at 30 °C under the fixed potential of -0.05V for the period of 3000 seconds. (C) A linear relation between the current density (anodic peak during the forward scan) and the cycle number; obtained from the cyclic voltammogram data (figure 5A). (D) Current retention graph calculated from the cyclic voltammogram data (figure 5A). (E) The bar diagram shows the relation between current density and the I<sub>F</sub>/I<sub>B</sub> ratio.

We also have calculated the ratio of the current density peak values for the forward scan (I<sub>F</sub>) and the backward scan (I<sub>B</sub>), a critical parameter for evaluating the carbon monoxide tolerance efficiency of the catalyst. The graphical representation, figure 5.5E, shows the relation between current density (methanol oxidation peak) and I<sub>F</sub>/I<sub>B</sub> ratio at the different stage of the reaction. At the initial stage, the I<sub>F</sub>/I<sub>B</sub> ratio was 7.98, figure 4E, voltammogram (f), and the ratio drops down to 3.75 (a / b, figure 5.5A) when maximum methanol oxidation was achieved. A stable ratio with the value of 4.89 (a'/b', figure 5.5A) indicates that carbon monoxide formation is directly proportional to the oxidation of alcohol and no further deactivation of the catalyst has been observed, for the another 200 cycles(not shown in the figure).

It is also important to mention that in our previous study [25] we have used polymer stabilized ionic palladium as an electrocatalyst for methanol oxidation reaction and found better catalytic performance, in terms of current density, as compared with the present system, where preformed palladium nanoparticles was used as a catalyst. The most sensible justification of this behaviour could be explained according to the mechanism where the superior performance of the growing metal nanoparticles as redox catalysts was explained [26-28]. But for Pd-*p*DAN system, a stable and higher value of  $I_F/I_B$  ratio was obtained, which evidenced as the less carbon monoxide formation, when palladium nanoparticles were used as an electro-catalyst for methanol oxidation reaction.

#### **5.4 Sub-conclusion:**

The present article reports a polymer stabilized palladium nanoparticles has been prepared by a simple one-pot wet-chemical synthesis method at room temperature. Optical characterization produced the evidence for the quinoid and benzenoid ring structure in the polymer. The microscopic and surface characterization techniques confirmed the presence of the crystalline metallic palladium nanoparticles within the polymer. The integrated architecture of metal-polymer nanocomposite show excellent stability towards the electrocatalytic methanol oxidation in alkaline media.

## 5.5 References

1. Choudhary, M., et al., Polymer stabilized silver nanoparticle: An efficient catalyst for proton-coupled electron transfer reaction and the electrochemical recognition of biomolecule. *Chemical Physics Letters*, 2014. 608(0): p. 145-151.
2. Choudhary, M., et al., Recognition of biomolecules using gold-polymer composites: metal nanoparticles play the role of the catalyst. *Journal of Materials Science*, 2015: p. 1-9.
3. Islam, R.U., et al., Conjugated polymer stabilized palladium nanoparticles as a versatile catalyst for Suzuki cross-coupling reactions for both aryl and heteroaryl bromide systems. *Catalysis Science & Technology*, 2011. 1(2): p. 308-315.
4. Ul Islam, R., et al., Palladium–Poly(3-aminoquinoline) Hollow-Sphere Composite: Application in Sonogashira Coupling Reactions. *ChemCatChem*, 2013. 5(8): p. 2453-2461.
5. Mahato, S.K., et al., Polymer-Stabilized Palladium Nanoparticles for the Chemoselective Transfer Hydrogenation of  $\alpha,\beta$ -Unsaturated Carbonyls: Single-Step Bottom-Up Approach. *ChemCatChem*, 2014. 6(5): p. 1419-1426.
6. Liu, H., et al., A review of anode catalysis in the direct methanol fuel cell. *Journal of Power Sources*, 2006. 155(2): p. 95-110.
7. Zhang, H.-X., et al., Palladium nanocrystals bound by {110} or {100} facets: from one pot synthesis to electrochemistry. *Chemical Communications*, 2012. 48(67): p. 8362-8364.
8. Yang, H.H., et al., Pd Nanoparticles Supported on TiO<sub>2</sub> Nanotubes for Ethanol Oxidation in Alkaline Media. *Advanced Materials Research*, 2010. 132: p. 8.

9. Chen, X., et al., Synthesis of “Clean” and Well-Dispersive Pd Nanoparticles with Excellent Electrocatalytic Property on Graphene Oxide. *Journal of the American Chemical Society*, 2011. 133(11): p. 3693-3695.
10. Li, H., et al., Photocatalytic synthesis of highly dispersed Pd nanoparticles on reduced graphene oxide and their application in methanol electro-oxidation. *Catalysis Science & Technology*, 2012. 2(6): p. 1153-1156.
11. Xu, C., Y. Liu, and D. Yuan, Pt and Pd supported on carbon microspheres for alcohol electrooxidation in alkaline media. *International Journal of Electrochemical Science*, 2007. 2: p. 7.
12. Zhao, Y., et al., Enhanced electrocatalytic oxidation of methanol on Pd/polypyrrole-graphene in alkaline medium. *Electrochimica Acta*, 2011. 56(5): p. 1967-1972.
13. Ghosh, S., et al., Conducting polymer-supported palladium nanoplates for applications in direct alcohol oxidation. *International Journal of Hydrogen Energy*, 2015. 40(14): p. 4951-4959.
14. Hable, C. and M.S. Wrighton, Electrocatalytic oxidation of methanol and ethanol: a comparison of platinum-tin and platinum-ruthenium catalyst particles in a conducting polyaniline matrix. *Langmuir* 1993. 9: p. 3284-3290.
15. Prodromidis, M.I., et al., Preorganized composite material of polyaniline-palladium nanoparticles with high electrocatalytic activity to methanol and ethanol oxidation. *International Journal of Hydrogen Energy*, 2015. 40(21): p. 6745-6753.
16. Wu, K., et al., Graphene-supported Pd-Pt alloy nanoflowers: In situ growth and their enhanced electrocatalysis towards methanol oxidation. *International Journal of Hydrogen Energy*, 2015. 40(20): p. 6530-6537.

17. Li, L., et al., One-pot synthesis of PtRh/ $\beta$ -CD-CNTs for methanol oxidation. *International Journal of Hydrogen Energy*, 2015. 40(43): p. 14866-14874.
18. Chowdhury, S.R., P. Mukherjee, and S.k. Bhattacharya, Palladium and palladium–copper alloy nano particles as superior catalyst for electrochemical oxidation of methanol for fuel cell applications. *International Journal of Hydrogen Energy*, 2016. 41(38): p. 17072-17083.
19. Calderón, J.C., et al., Palladium–nickel catalysts supported on different chemically-treated carbon blacks for methanol oxidation in alkaline media. *International Journal of Hydrogen Energy*, 2016. 41(43): p. 19556-19569.
20. Ahmadi, R. and M.K. Amini, Synthesis and characterization of Pt nanoparticles on sulfur-modified carbon nanotubes for methanol oxidation. *International Journal of Hydrogen Energy*, 2011. 36(12): p. 7275-7283.
21. Radhakrishnan, T. and N. Sandhyarani, Three dimensional assembly of electrocatalytic platinum nanostructures on reduced graphene oxide – An electrochemical approach for high performance catalyst for methanol oxidation. *International Journal of Hydrogen Energy*, 2017. 42(10): p. 7014-7022.
22. Mallick, K., M. Witcomb, and M. Scurrall, Fabrication of a nanostructured gold-polymer composite material. *The European Physical Journal E*, 2006. 20(3): p. 347-353.
23. Choudhary, M., S. Siwal, and K. Mallick, Single step synthesis of a 'silver-polymer hybrid material' and its catalytic application. *RSC Advances*, 2015. 5(72): p. 58625-58632.
24. Mallick, K., et al., Fabrication of a Metal Nanoparticles and Polymer Nanofibers Composite Material by an in Situ Chemical Synthetic Route. *Langmuir*, 2005. 21(17): p. 7964-7967.



25. Mallick, K., M.J. Witcomb, and M.S. Scurrall, In situ synthesis of copper nanoparticles and poly(o-toluidine): A metal-polymer composite material. *European Polymer Journal*, 2006. 42(3): p. 670-675.
26. Kaushik, M., J.W. Mike, and S.S. Mike, Directional assembly of polyaniline functionalized gold nanoparticles. *Journal of Physics: Condensed Matter*, 2007. 19(19): p. 196225.
27. Kang, E.T., K.G. Neoh, and K.L. Tan, Polyaniline: A polymer with many interesting intrinsic redox states. *Progress in Polymer Science*, 1998. 23: p. 277-324.
28. Yang, C., M. Zhou, and L. Gao, Highly Alloyed PtRu Nanoparticles Confined in Porous Carbon Structure as a Durable Electrocatalyst for Methanol Oxidation. *ACS Applied Materials & Interfaces*, 2014. 6(21): p. 18938-18950.
29. Singh, R.N. and R. Awasthi, Graphene support for enhanced electrocatalytic activity of Pd for alcohol oxidation. *Catalysis Science & Technology*, 2011. 1(5): p. 778-783.
30. Liu, Y.-T., et al., Electrochemical activity and stability of core-shell Fe<sub>2</sub>O<sub>3</sub>/Pt nanoparticles for methanol oxidation. *Journal of Power Sources*, 2013. 243: p. 622-629.
31. Siwal, S., et al., Single step synthesis of a polymer supported palladium composite: a potential anode catalyst for the application of methanol oxidation. *RSC Advances*, 2016. 6: p. 47212-47219.
32. Jana, N.R., T.K. Sau, and T. Pal, Growing Small Silver Particle as Redox Catalyst. *The Journal of Physical Chemistry B*, 1999. 103(1): p. 115-121.

33. Mallick, K., M. Witcomb, and M. Scurrall, Silver nanoparticle catalysed redox reaction: An electron relay effect. *Materials Chemistry and Physics*, 2006. 97(2–3): p. 283-287.
34. Choudhary, M., et al., Polymerization Assisted Reduction Reaction: A Sequential Electron–Proton Transfer Reaction Catalyzed by Gold Nanoparticle. *The Journal of Physical Chemistry C*, 2013. 117(44): p. 23009-23016.



## CHAPTER 6 CONCLUSION AND PERSPECTIVES

---

### 6.1 Summary of Findings and Conclusion

This work has demonstrated the successful synthesis of metal nanoparticles-polymer based nanocomposite by using the “*in situ* polymerization and composite formation” (IPCF) technique. It has been found that the synthesized nanocomposite shows good electrocatalytic activity for the electro-oxidation of alcohols fuel cell.

Polymer supported ionic palladium has been synthesized using a single step, IPCF route from the corresponding monomer and metal salt precursors. During the reaction, the *in situ* formation from ionic palladium to palladium nanoparticles has been noticed and this plays a major role for the significant improvement of the oxidation process. In another study, polymer supported palladium nanoparticles has been synthesized using an IPCF method, where potassium tetrachloropalladate was used as a precursor of palladium nanoparticles synthesis. The synthesized material was successfully used as an electro catalysts for the methanol oxidation in alkaline media.

This study progressively clear that metal nanoparticles-polymer based catalyst is a promising nanocomposite system for electro-oxidation of direct alcohol fuel cell. The simple preparation method as well as the stability and the recyclability performance indicates that material have potential in methanol fuel cell application. In conclusion from this thesis it can be summarize that the developed polymer based material have promising properties for fuel cell application.

### 6.2 Recommendations for Future Work

In concern with the work considering from this thesis is that IPCF technique is very promising methods for the synthesis of metal nanoparticle and polymer nanocomposite

---

system for the intact interaction between both entities and their respective application in methanol fuel cell application.

Furthermore, the synthesized polymer based earth-abundant material (EAM) doped palladium catalysts for the harvesting of hydrogen energy. This study excites the demand for research to invent an advanced Pd-based low-cost catalyst for the technical execution of direct fuel cells (DFCs). Other types of carbon based materials such as graphitic carbon nitride, and graphene can be explored as nanocomposites by using IPCF technique. This proposed approach can be extended to the electro-oxidation of methanol, ethanol and formic acid along with other carbon chain. It will be plausible to take this work at another level by the synthesis of bimetallic nonmaterial's and application in the fuel cell. Since the technique is currently at initial stage, it can only be used to study methanol oxidation in alkaline media. In addition, we can deal with the different analytes in different media as well. The inability of simultaneously electro-oxidation of multiple analytes in same time at same platform (i.e. same electrolyte). This will further enhance its utility in cognitive research.



UNIVERSITY  
OF  
JOHANNESBURG